TNO innovation for life

Welds at plate ends and corners – a literature review

Hot spot stress & effective notch stress compared with fatigue tests

TNO Public › TNO 2025 R12616
24 November 2025

Mobility & Built Environment
www.tno.nl
+31 88 866 20 00

TNO 2025 R12616 – 24 November 2025

Welds at plate ends and corners - a literature review

Hot spot stress & effective notch stress compared with fatigue tests

Author(s)	Dr.ing. H.M. Slot

Classification report	TNO Public
Title	TNO Public
Report text	TNO Public
Number of pages	87 (excl. front and back cover)
Number of appendices	2
Sponsor	Rijkswaterstaat
Programme name	Vervanging & Renovatie 2024/2025
Project name	V&R Korte lassen
Project number	060.64314

Contents

1 Introduction

Welds at plate ends and corners in geometrically stress concentrated areas often occur in welded steel bridges and other steel structures such as ships. Often occurring details are mouse holes and loaded attachments. These details create complex stress situations and consequently challenging fatigue assessments. These assessments can be done by different assessment methods, such as the hot spot stress methods Type “a” or “b” and effective notch stress method. Applications of these methods are frequently shown and compared in literature, but studies showing reliable comparisons with fatigue test results from different sources are scarce.

In the framework of the “*Vervanging & Renovatie*” (V&R) project of Rijkswaterstaat, a project has started to select or develop a fatigue assessment method for these welds at plate ends.

Fillet welds are often applied in these types of structures for economic reasons. Consequently, assessment of the weld root and weld toe should be performed. Within this V&R project, a finite element (FE) study of different specimen types with varying stress concentrations at the plate end has been performed in 2023. A reliable assessment method based on Fricke’s averaged stress in the weld could be derived for assessing the weld root. However, no satisfying method based on hot spot stresses or effective notch stresses could be selected or derived for the weld toe. Further details of this study can be found in TNO report “*Fatigue assessment for weld roots and toes of weld ends*” [1].

This report presents a literature review of fatigue tests with specimens containing welds at plate ends, and the assessments methods that have been used. The goal of the study is to determine whether or not the prediction of the fatigue strength with the assessment methods corresponds to the fatigue strength following from tests with failure at the weld toe at plate ends. This allows for checking whether the methods are conservative, too conservative, or unsafe, and for determining which method results in the smallest scatter for the ratio predicted fatigue strength / tested fatigue strength.

Fatigue test specimens which have been stress-relieved by a heat treatment are considered most valuable, as it will be demonstrated that as-welded specimens containing plate ends tested with constant amplitude loading can show a *higher* fatigue life than the stress-relieved specimens. In as-welded specimens, *compressive* residual welding stresses develop at weld ends and these are often beneficial for fatigue. However, it depends on the local geometry and the welding sequence whether compressive or tensile residual stresses arise. These welding stresses can (partly) relax due to incidentally occurring high loads as found in practical situations with variable amplitude loading. These high loads or overloads result in a local exceedance of the yield stress and result in a reduction of the residual stresses. Consequently, the as-welded specimens tested under constant amplitude loading might provide a too optimistic result for practical situations. This is the reason to consider the stress relieved specimens as most valuable.

It should be emphasised that the focus in this study is on the fatigue strength of the weld toe at the attachment or plate end. Fatigue test results with failure initiated at the weld root or in the middle of the width of the attachment are interpretated as run-outs for the weld

toe at the attachment or plate end. These run-outs are only mentioned in the presented studies where they have added value, otherwise they are neglected.

Chapter 2 gives a summary of the used local fatigue assessment methods, such as the hot spot stress methods and the effective notch stress method. Chapter 3 gives an overview of the available literature with fatigue test results, the used assessment methods, and results. The chapter gives a short summary of the performed fatigue tests and FE analyses for all references. The derived hot spot stress concentration factors and effective notch stress concentration factors by the original sources have been used by TNO to re-assess the ratio predicted fatigue strength / tested fatigue strength. S-N curves have been derived and compared with the relevant FAT value for each specimen geometry and condition.
Chapter 4 combines all obtained datasets of fatigue test results in groups and uses this to determine global S-N curves. A discussion, conclusions and recommendations are given in Chapters 5 to 7, respectively.

2 Local fatigue approaches

The simplest method of a fatigue assessment is a global approach, such as the nominal stress method. This approach can only be used for more or less standardized welded joints for which detail categories (DC) or FAT values are given in the standards, such as NEN-EN 1993-1-9 [2] and Hobbacher (2016) [3].

For the more complex welded connections the structural hot spot stress method, and the effective notch stress method can be used, see Niemi, Fricke and Maddox (2018), "*Structural Hot spot Stress Approach to Fatigue Analysis of Welded Components, Designer's Guide*" [4] and Fricke (2012), *IIW Recommendations for Fatigue Assessments of Welded Structures by Notch Stress Analysis* [5].

In Chapter 2 of the TNO report "*Fatigue assessment for weld roots and toes of weld ends*" [1], these different stress calculation methods for welds using the FE method are described. In the next sections the essentials for the structural hot spot stress method and the effective notch stress method are summarized.

2.1 Structural hot spot stress approach

Based on Niemi., Fricke and Maddox, *Structural Hot spot Stress Approach to Fatigue Analysis of Welded Components, Designer's Guide*, 2nd Edition, IIW collection (2018), [4].

Structural hot spot stress locations can be divided in two types:

a) Type "a", the weld toe is located on a plate surface, see Figure 2.1, or.
b) Type "b", the weld toe is located on a plate edge, see Figure 2.2a to d.

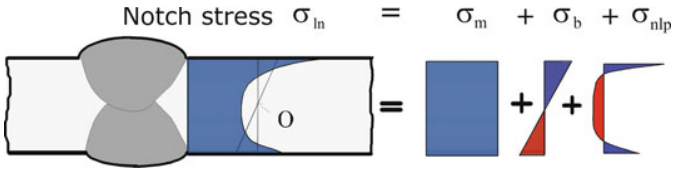

Figure 2.1 – A typical non-linear stress distribution across the plate thickness at a Type "a" hot spot [4].

In this method the structural hot spot stress σ_{hs} is calculated by extrapolation of the stresses to the weld toe of interest. Figure 2.3 shows some guidelines and extrapolation paths for Type "a" and "b", and the used distances for the extrapolations. For Type "a", these distances are all relative to the plate thickness (t). For Type "b", these distances are absolute, and with a fine mesh a quadratic extrapolation using the (nodal) stresses at 4, 8 and 12 mm can be applied.

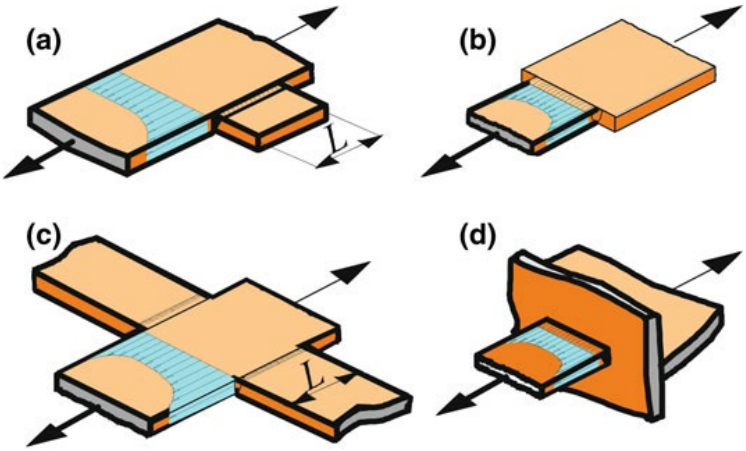

Figure 2.2a to d – Structural details Type “b” hot spots at plate edges [4].

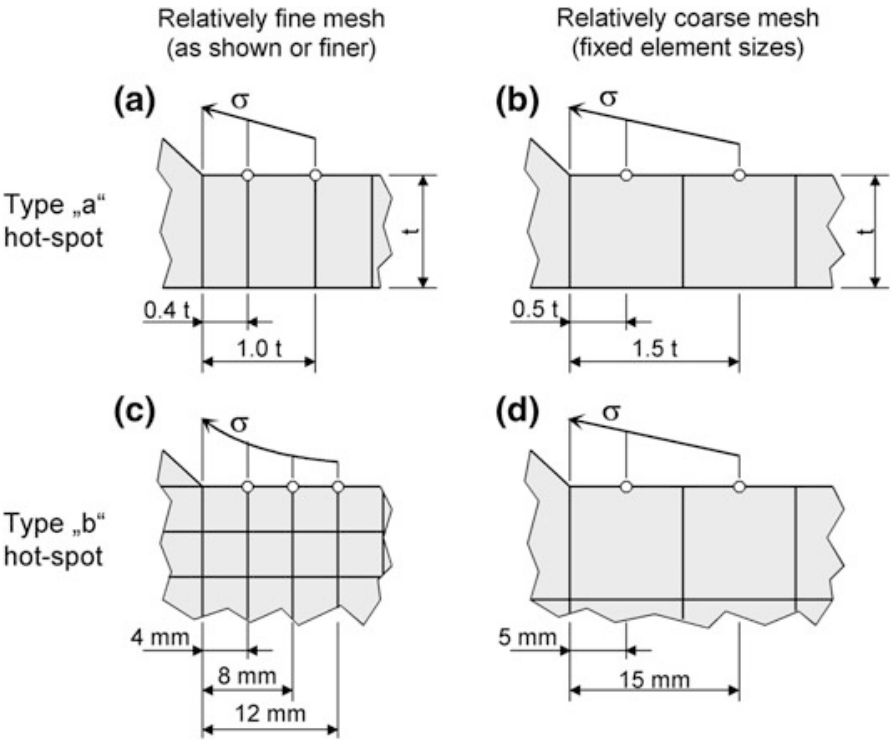

Figure 2.3 – Guideline on meshing and stress evaluation using surface stress extrapolation [4].

The structural stress concentration factor K_s is defined as:

$$K_s = \frac{\sigma_{hs}}{\sigma_{n,p}}$$

where $\sigma_{n,p}$ = the nominal axial net section stress in the loaded plate.

A linear-elastic material behaviour should be used in the FE models. As a result, the structural stress concentration factor (K_s) is independent of the applied stress range, and is thus specific for a certain specimen or structural detail. For each stress range level the hot spot stress range can be calculated with:

$$\Delta\sigma_{hs} = K_s \Delta\sigma_{n,p}$$

For the fatigue assessment of the weld toe using the structural hot spot stress method, Hobbacher [3] and Niemi et al. [4] recommend different FAT values for cruciform joints with load-carrying full penetration welds and load-carrying fillet welds, see Table 2.1. Table 2.2 summarises the properties of the recommended S-N curves.

Table 2.1 - Hot spot FAT values for cruciform steel joints with full penetration welds and fillet welds. Source: "*Table 6.1 Hot spot S-N curves for plates made of steel up to 25 mm thick*", [4]

No	Joint	Description	Quality	FAT_{St}
2	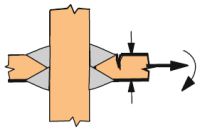	Cruciform or T-joint with full penetration K-butt welds	K-butt welds, no lamellar tearing	100
6	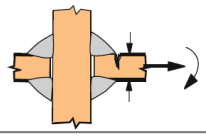	Cruciform joint with load-carrying fillet welds	Fillet weld(s) as-welded	90

Table 2.2 - Values for the parameters in the S-N curve for fatigue assessment of the weld toe with the hot spot stress method [4]

Parameter	Value
Slope of the S-N curve, m (-)	3.0
Number of cycles at FAT, N_C (cycles)	2.0×10^6
S-N curve for full penetration welds, FAT (MPa)	100
S-N curve for fillet welds, FAT (MPa)	90

2.2 Effective notch stress approach

Based on Fricke W., *IIW Recommendations for Fatigue Assessments of Welded Structures by Notch Stress Analysis*, IIW-2006-09 (2012), [5].

In this method, the effective notch stress σ_{en} is calculated with an FE model, for which a fictitious rounding of the weld toes and roots is modelled using a radius of 1 mm, see Figure 2.4.

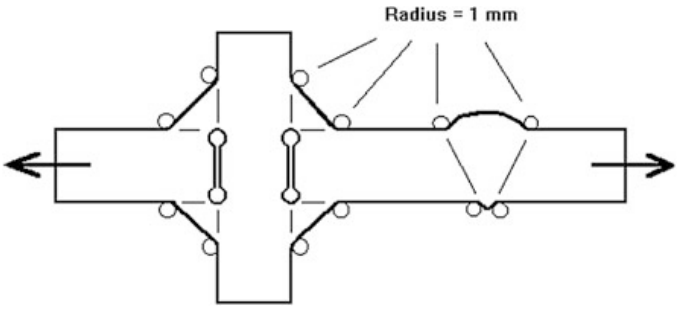

Figure 2.4 – Fictitious rounding of weld toes and roots [3], [5].

Similar to the hot spot stress method, the effective notch stress concentration factor K_{en} is defined as:

$$K_{en} = \frac{\sigma_{en}}{\sigma_{n,p}}$$

As linear-elastic material behaviour should be used in the FE model, this stress concentration factor (K_{en}) is also independent of the applied fatigue range, and is thus specific for a certain specimen or structural detail.

Fricke [5] recommends the parameters shown in Table 2.3 for the S-N curve of the effective notch stress (σ_{en}). The effective notch stress range can be calculated for each stress level as:

$$\Delta\sigma_{en} = K_{en}\Delta\sigma_{n,p}$$

Table 2.3 - Values for the parameters in the S-N curve for fatigue assessment with the effective notch stress method

Parameter	Value
Slope of the S-N curve, m (-)	3.0
Number of cycles at FAT, N_C (cycles)	2.0 x 10^6
Classification reference to S-N curve, FAT (MPa)	225

2.3 Fatigue detail category modifications

2.3.1 Plate thickness

The mentioned FAT values in the previous section are valid up to a wall thicknesses of 25 mm. The influence of larger plate thickness on the FAT value should be taken into account for the nominal stress method and hot spot stress Type “a”, see Hobbacher [3]. This plate thickness correction factor is not required in the case of assessments based on effective notch stress method and hot spot stress Type “b”.

2.3.2 Stress ratio

The presence of high tensile residual stresses has been included in the fatigue detail categories as given in the previous sub-sections. Based on consideration of the sum of the applied and the residual stresses, a fatigue enhancement factor $f(R)$ may be applied for effective stress ratios $R < 0.5$, see Hobbacher [3]. For stress relieved welded components, in which the effects of constraints or secondary stresses have been considered in the analysis, the following factor can be used to enhance the detail category (see Figure 2.5):

$$\begin{aligned} f(R) &= 1.6 && for\ R < -1 \\ f(R) &= -0.4R + 1.2 && for -1 \le R \le 0.5 \\ f(R) &= 1.0 && for\ R > 0.5 \end{aligned}$$

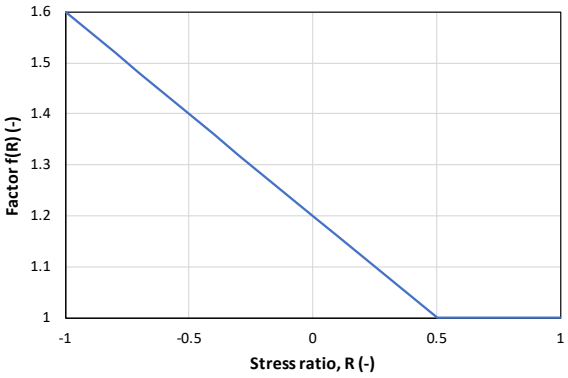

Figure 2.5 – Detail category enhancement factor as a function of stress ratio R.

This fatigue enhancement factor has been applied in the current study in the evaluation and assessment of fatigue tests of stress-relieved specimens. This enhancement factor $f(R)$ = 1.2 for tests performed with a stress ratio $R = 0$.

2.3.3 Misalignment

Misalignment in axially loaded joints leads to an increase of stress in the welded joint due to the occurrence of secondary bending stresses. Some allowance for misalignment is already included in the detail categories (DC) of classified structural details.

Tests aimed at the determination of detail categories of weldments should meet the requirements for quality level B given in NEN-EN-ISO 5817:2014, "*Welding - Fusion-welded joints in steel, nickel, titanium and their alloys (beam welding excluded) - Quality levels for imperfections*" [7]. This standard gives a maximum allowed linear misalignment (e) between the plates of $e/t \leq 0.05$ (t = plate thickness) and a maximum allowed angular misalignment between the plates of $\varphi \leq 1°$ for quality level B.

A stress magnification factor $k_m = 1.45$ ($e/t = 0.15$) has already been covered in the detail categories (DC) of cruciform joints in the nominal stress approach, see EN 1993-1-9 [2]. For the structural hot spot stress and effective notch stress methods, Hobbacher [3] remarks that the given detail categories (see Table 3.3 in [3]) cover a stress magnification factor $k_m = 1.05$ for cruciform joints. Larger misalignments have to be considered explicitly in the determination of the hot spot or effective notch stress range using an effective stress magnification factor:

$$k_{m,eff} = \frac{k_{m,calculated}}{k_{m,already\ covered}}$$

Hobbacher [3] and Niemi et al. [4] give the following equations for the stress magnification factors at the weld toe for misalignments in cruciform joints in their recommendations:

1. Axial misalignment between flat plates of equal thickness under axial loading, see Figure 2.6a:

$$k_{m,e} = 1 + \lambda \frac{e}{2t}$$

λ = factor for restraint, with λ = 6 for unrestrained joints. This is an upper bound, valid for relatively long specimens, for shorter specimens λ < 6, this upper bound has been used.

2. Angular misalignment between flat plates of equal thickness under axial loading with fixed ends, see Figure 2.6b:

$$k_{m,\varphi} = 1 + 3\frac{l\varphi}{2t}$$

The reduction of angular misalignment due to the straightening of the joint under tensile loading is ignored with these equations, which is conservative. The equations for k_m can be refined when necessary, see Maddox [12] and Andrews [13].

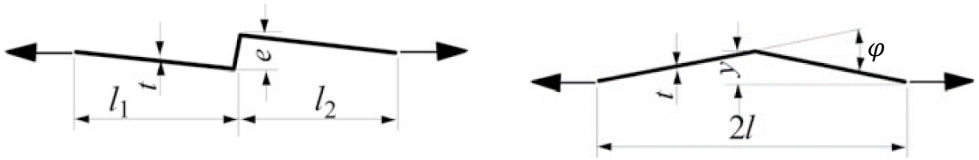

Figure 2.6a/b – Misalignments: a) eccentricity e and b) distortion angle φ, relative to the load lines.

Both stress magnification factors should be applied in joints containing both linear and angular misalignment:

$$k_m = 1 + \left(k_{m,e} - 1\right) + \left(k_{m,\varphi} - 1\right)$$

Combining these equations gives for the weld toe of cruciform joints:

$$k_{m,eff} = \frac{1 + 3\frac{e}{t} + 3\frac{l\varphi}{2t}}{1.05}$$

3 Literature

3.1 Doerk & Fricke

Doerk & Fricke (2004-2006) [8],[9],[10],[11],[12] have performed extensive research on fatigue strength assessments of fillet-welded attachment ends and fillet welds around stiffeners and bracket toes. This section summarizes their fatigue test results and their assessment with the hot spot stress method in relation to the attachment end weld toe. In addition to the performed assessments of these geometries by TNO [1] using FE models, this report evaluates the test results and FE models of the original source. The next sub-section presents the relevant results of the fatigue tests with fillet-welded attachment ends, both in as-welded and stress-relieved state. Sub-section 3.1.2 gives the assessment results of Doerk & Fricke, and Sub-section 3.1.3 summarises the assessment results of TNO for this geometry.

3.1.1 Fatigue test results

Figure 3.1 shows the fatigue specimen designed by Doerk & Fricke for fillet welds around an attachment end. Tests have been performed with plate thickness $t = 12$ mm and two throat sizes, namely $a = 4$ and 6 mm. Table 3.1 gives the mechanical material properties.

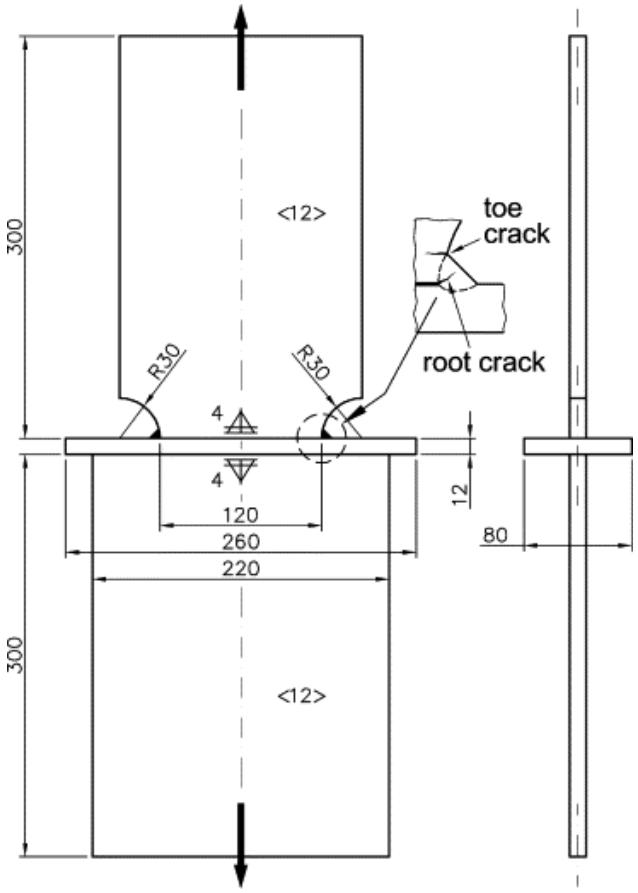

Figure 3.1 – Specimen dimensions. Fillet welds with throat sizes a = 4 mm and 6 mm have been tested.

Table 3.1 - Mechanical properties of used steel grade (thickness t = 12 mm)

Tensile strength R_m (MPa)	Yield strength R_e (MPa)	Elongation at fracture A_5 (%)
483	333	28

The fillet welds with a nominal throat size of $a = 4$ mm were made in one run and the fillet welds with a nominal throat size of $a = 6$ mm were made in three runs. Approximately 20 specimens and about 10 specimens were tested in the as-welded and stress-relieved condition, respectively, for each weld throat size. The stress relieve heat treatment was performed by heating up the specimen to 520 °C, maintaining this temperature for 3 hour and then gradually cooled down to room temperature.
The fatigue test conditions are:

- Apparatus: resonant pulsating machine.
- Constant amplitude loading.
- Frequency, $f = 30$ Hz.
- Environment: in air.
- Stress ratio, $R \approx 0$.
- Test termination: after crack length reached several centimetres.

Some of the specimens showed an axial misalignment. To study the effect of this, approximately 10 additional specimens were tested with an intended high misalignment of 4 mm. Figure 3.2a/b show the fatigue test results[1] of only those specimens that comply with the requirements in:

- EN 1993-1-9 [2], i.e. relative eccentricity $e/t \leq 0.15$, where e is the eccentricity and t the plate thickness, and;
- ISO 5817:2014 [7] Quality level B, i.e. a distortion angle $\varphi \leq 1°$.

A remarkable difference can be seen between the as-welded and the stress relieved specimens. The latter show on average a lower fatigue life, with crack initiation and growth from the weld toe at the weld end (plate edge), whereas all as-welded specimens show a longer fatigue life, with crack initiation and growth from the weld root. Both weld throat sizes, $a = 4$ mm and $a = 6$ mm, show this behaviour. Figure 3.2 provides the stress range in the net section of the plate ($\Delta\sigma_{n,p}$) even for the as-welded specimens, although stress range in the weld throat should normally be used. This has been done to show the run-out levels of the as-welded specimens for weld toe fatigue.

Figure 3.2 shows the S-N curves with a fixed reciprocal slope m = 3 and for a $p = 5\%$ lower prediction bound. The sample size (n) is included by using a random distribution for the residuals when n < 30 and using the Student's t-distribution for the eccentricity. This calculation procedure is summarized in Appendix A "*Statistical evaluation of fatigue data according to Eurocode 3*". Each S-N curve is now indicated with the stress range $\Delta\sigma_{n,p,C(m=3,p=5\%)}$ at N_C = 2 x 10^6 cycles, see Table 3.2.

[1] In this review the range of the nominal stress in the net section of the plate ($\Delta\sigma_{n,p}$) is also used for the as-welded specimens. This differs from the S-N curves given by Doerk & Fricke [8] to [12]; they use the nominal stress in the weld throat $\Delta\sigma_{n,w}$ for the as-welded specimens.

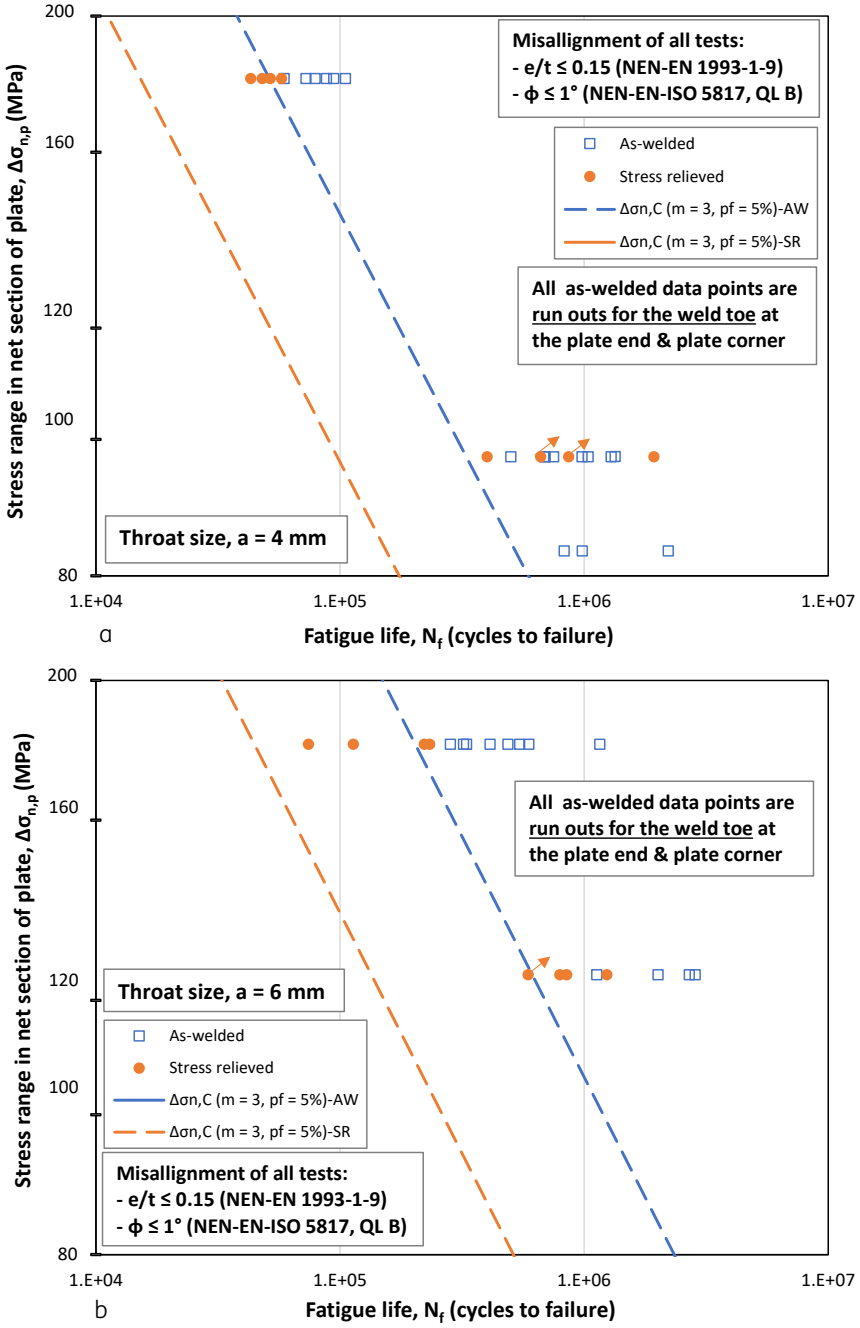

Figure 3.2a/b – Net stress range in the plate ($\Delta\sigma_{n,p}$) versus number of cycles to failure (N_f) for as-welded (AW) and stress-relieved (SR) specimens for Doerk & Fricke: a) weld throat size a = 4; b) weld throat size a = 6 mm. All displayed specimens comply with requirements in NEN EN 1993-1-9 [2], i.e. relative eccentricity $e/t \leq 0.15$ and NEN-EN-ISO 5817:2014 [7], Quality level B, i.e. a distortion angle $\varphi \leq 1°$. Note: all as-welded specimens are run-outs, thus the S-N curve is artificial and treats these data as failures.

Note that the $\Delta\sigma_{n,p,C(m=3,p=5\%)}$ values for the as-welded specimens with a = 4 and a = 6 mm deviate from the FAT values given by the original source. The values in Table 3.2 are based on the stress in the net section of the smallest attachment ($\Delta\sigma_{n,p}$), whereas the values given by the original source are based on the nominal stress in the weld throat ($\Delta\sigma_{n,w}$).

Further, note that the data for as-welded specimens in Figure 3.2a/b are run-outs. The individual data have probably a higher fatigue life at the plate edge and plate corner than indicated by the open dots. Nonetheless, the S-N curves $\Delta\sigma_{n,p,C\ (m=3,p=5\%)}$ for the as-welded specimens are determined as if there is no additional life, i.e., all data are failures. Note that this procedure is in disagreement with standards or best practice. It is just applied here to compare results between as-welded and stress relieved; it should not be applied in practical assessments or designs. The actual S-N curve might be lower than indicated, in case of a scatter larger than that of the run-outs, but it is likely higher, because of a higher number of cycles to failure for all specimens (higher mean). This is reflected by a "≥" symbol for resistance values in the tables presented hereafter, even though a small probability exists that the values are too high.

Table 3.2 provides all $\Delta\sigma_{n,p,C(m=3,p=5\%)}$ values based on the stress in the net section. The stress-relieved specimens with a weld throat size of $a = 4$ mm show a 33 % lower stress range and for $a = 6$ mm a 40 % lower stress range than for the as-welded specimens. The statistical evaluations of these data (not include in this report) show a standard deviation which is 70 % higher and a mean value which is 12 % lower for the weld throat size a = 4 mm for the stress-relieved specimens compared to the as-welded specimens. Thus, for this throat size, the difference in $\Delta\sigma_{n,p,C(m=3,p=5\%)}$ is mainly due to the substantially larger deviation. For a throat size $a = 6$ mm the mean value is about 28 % lower than for the as-welded specimens.

The scatter in the reported fatigue test results appear strongly correlated with the measured misalignments of the specimens. Hereafter, all specimens are analysed, including the specimens with a larger misalignment than allowed (see above). Figure 3.3 show the definitions and locations of measurement of the misalignments. All values are taken from Doerk [12].

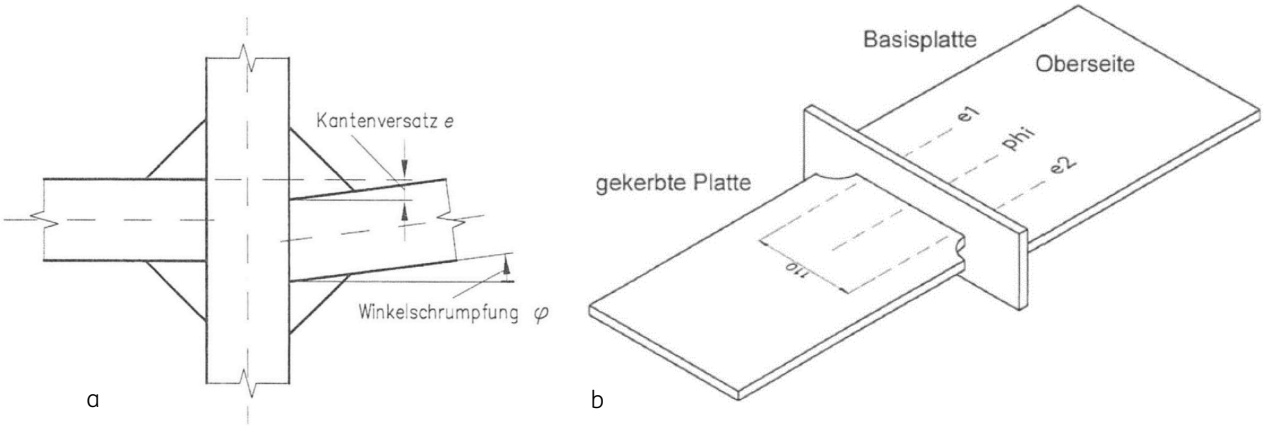

Figure 3.3a/b – Misalignments measured by the authors, a) eccentricity e and distortion angle φ, b) the locations on the specimen where this values have been measured [12].

Using the measured eccentricities and distortion angles [12] and the equations in section 2.3.3, TNO has analysed the influence of these on the stress concentration factors (SCF) for misalignment (k_m) at the weld toe. Figure 3.4 provides k_m versus the number of cycles to failure (N_f) for two stress ranges ($\Delta\sigma_{n,p}$). The specimens have eccentricities e/t up to 0.43 and distortion angles φ up to 4.2°. The figure shows a strong correlation between the measured misalignments and the fatigue life. A specimen with the maximum allowed eccentricity e/t = 0.15 and maximum allowed distortion angle φ = 1° has a SCF k_m = 2.1. Up

to this value this trend can already be recognised in Figure 3.4. The conclusion is that the observed scatter in the reported fatigue test results in Figure 3.2 are partially caused by specimen misalignments.

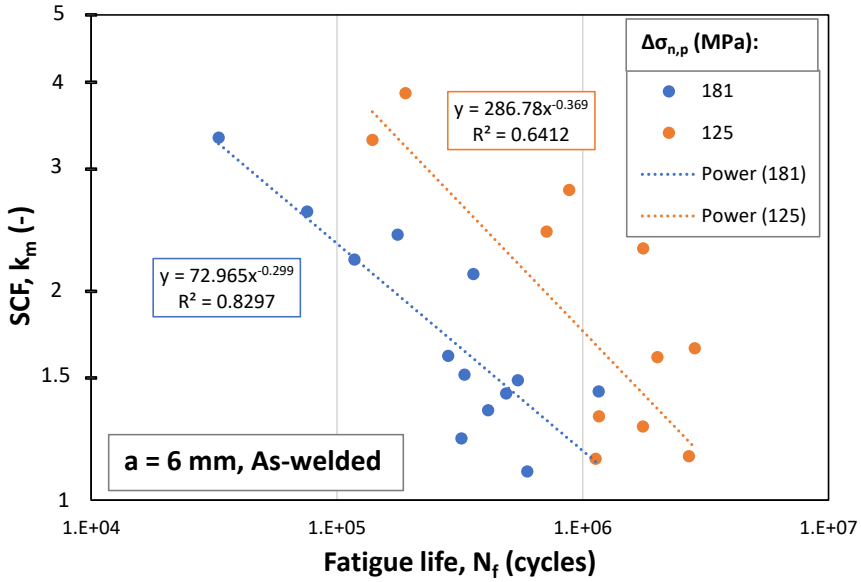

Figure 3.4 – The SCF due to misalignment (eccentricity and distortion angle), for two stress ranges in the plate ($\Delta\sigma_{n,p}$), versus number of cycles to failure (N_f) for as-welded specimens with weld throat size a = 6 mm.

Figures 3.5 shows all tested specimens, including the specimens that do not meet the requirements for the eccentricity and distortion angle. The stress ranges of the specimens that do not meet the misalignment requirements have been corrected by a SCF to the maximum allowed eccentricity when e/t > 0.15 or to the maximum allowed distortion angle when φ > 1° or to both maxima when both misalignments exceed these values. S-N curves with a fixed reciprocal slope m = 3.0 and a lower prediction bound $p = 5\%$ are also shown in Figures 3.5. Table 3.2 gives the resulting resistance $\Delta\sigma_{n,p,C(m=3,p_f=5\%)}$. The resistance increases with approximately 5% for specimens with a weld throat size $a = 6$ mm. Note again that run-outs are considered as failures for establishing the S-N curves. Figures 3.5 shows some of the corrected test results to be "over-corrected", especially at the higher stress ranges.

Table 3.2 - $\Delta\sigma_{n,p,C(m=3,p_f=5\%)}$ values for the as-welded and stress-relieved conditions, and both throat sizes

Condition	a (mm)	$\Delta\sigma_{n,p,C(m=3,p_f=5\%)}$ (MPa) $e/t \leq 0.15$ & $\varphi \leq 1°$	All specimens	Increase (%)
As-welded	4	≥53.2	≥52.4	-2
Stress-relieved	4	35.5	36.4	+3
As-welded	6	≥84.3	≥89.1	+6
Stress-relieved	6	50.9	53.4	+5

[1)] – Mean value for $N_C = 2 \cdot 10^6$ cycles and slope $m = 3.0$.

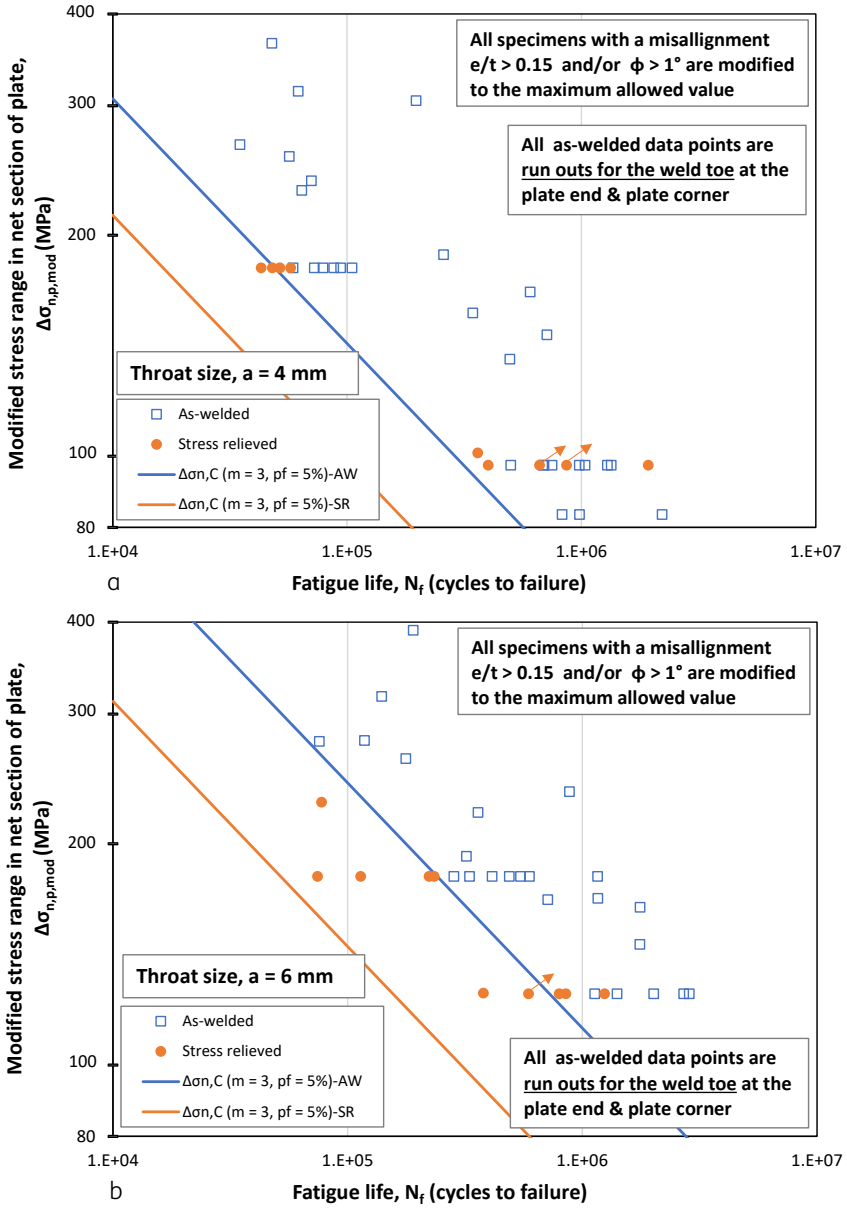

Figures 3.5a/b – Net stress range in the plate ($\Delta\sigma_{n,p}$) versus number of cycles (N_f) for as-welded (AW) and stress-relieved (SR) specimens: a) weld throat size a = 4 mm, b) weld throat size a = 6 mm. All specimens that do not comply with requirements: relative eccentricity $e/t \leq 0.15$ and distortion angle $\varphi \leq 1°$ are corrected with the SCF for this misalignment.

3.1.2 Assessment by Fricke & Doerk

Doerk [12] used the hot spot stress method for the assessment of the weld toe. In accordance with the recommendations of Niemi [4], the FE models contained a single element over the plate thickness, see Figure 3.6. Figure 3.7 shows the calculated stress distribution (average over the thickness) in the net section of the specimens for a weld throat size a = 4 mm (A1/B1) and a weld throat size of a = 6 mm (A2/B2), with a nominal net section stress in the smallest plate $\sigma_{n,p}$ = 69.4 MPa. For the weld throat size a = 4 mm (A1/B1) a maximum stress σ_{max} = 233 MPa and thus a SCF (= $\sigma_{max}/\sigma_{n,p}$) = 3.36 is found.

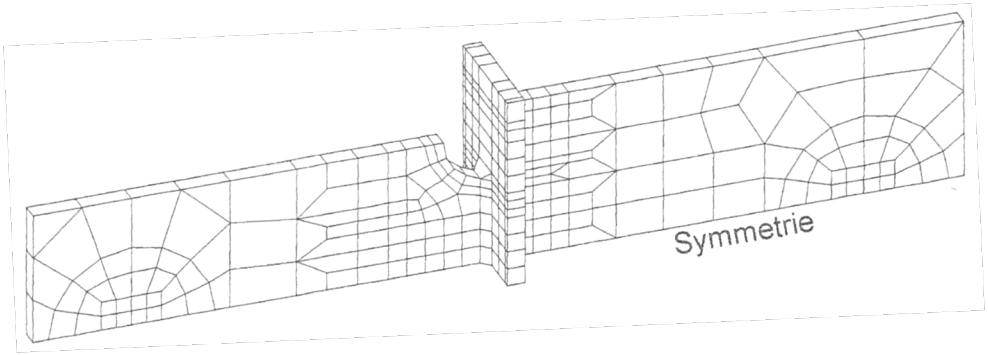

Figure 3.6 – FE model for the stress distribution and application of the hot spot stress method.

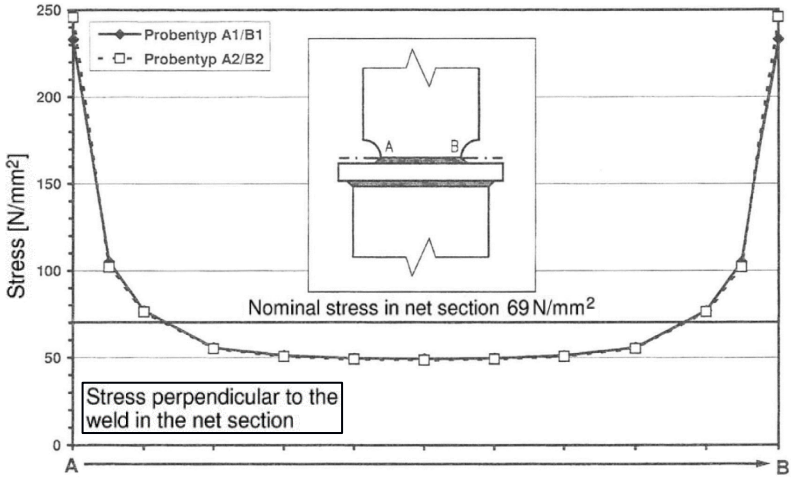

Figure 3.7 – The stress distribution (average over the thickness) in the net section of the specimens with weld throat sizes a = 4 mm (A1/B1) and a = 6 mm (A2/B2) for a nominal net section stress in the plate $\sigma_{n,p}$ = 69.4 MPa.

In agreement with the requirements given by Fricke & Bogdan (2001) [6], the hot spot stresses at the weld toe of the cut-outs were calculated by linear extrapolation of the tangential stresses at reference points 5 and 15 mm away from the weld toe. The structural stress concentration factors (K_s) have been calculated for specimens without misalignment (e/t = 0) and for specimens with eccentricity e = 4 mm (e/t = 4/12). Table 3.3 lists the structural SCF relative to the nominal net section stress. The same extrapolation path was used by TNO [1] as method D, see Figure 3.9.

Table 3.3 - Structural hot spot SCF for the weld toe at the attachment end

Structural hot spot stress at weld toe	Misalignment e/t (-)	Weld throat size (mm)	
		4	6
Structural SCF, K_s (= $\sigma_{hs}/\sigma_{n,p}$) (-)	0	2.60	2.55
	0.33 (4/12)	3.49	3.39

Figure 3.8 shows the test results as hot spot stress ranges ($\Delta\sigma_{hs}$) versus number of cycles to failure (N_f) for weld throat sizes of $a = 4$ and $a = 6$ mm, respectively. The figure also provides the hot spot S-N curves for $m = 3$ and $p = 5\%$ following from the tests (solid curves) and the hot spot FAT class according to Hobbacher [3] (dashed blue curve, FAT 90). The latter resistance is multiplied with a fatigue enhancement factor $f(R)$ = 1.2 for the stress-

relieved specimens (dashed orange curve, FAT 108). Table 3.4 gives the values of $\Delta\sigma_{hs,C\ (m=3,p_f=5\%)}$.

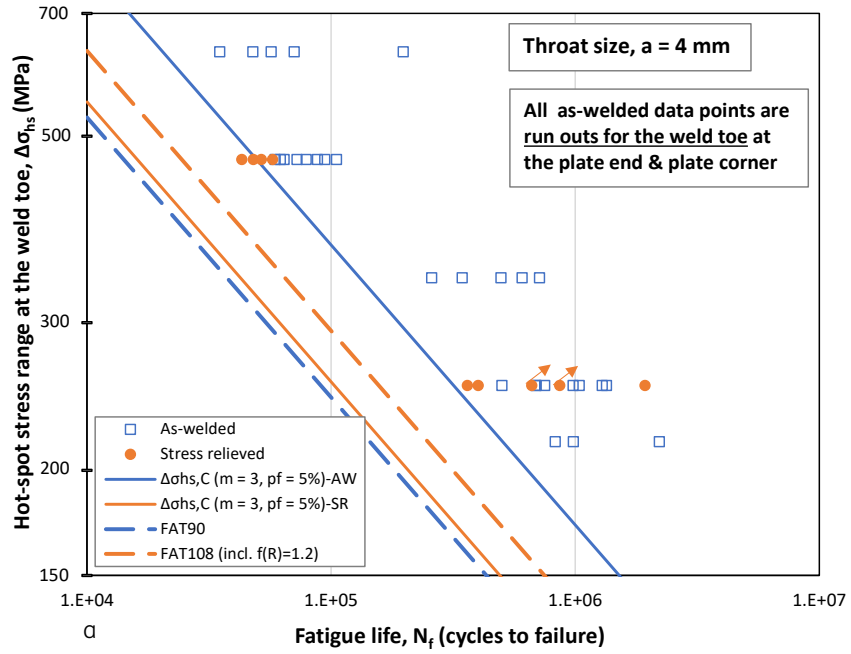

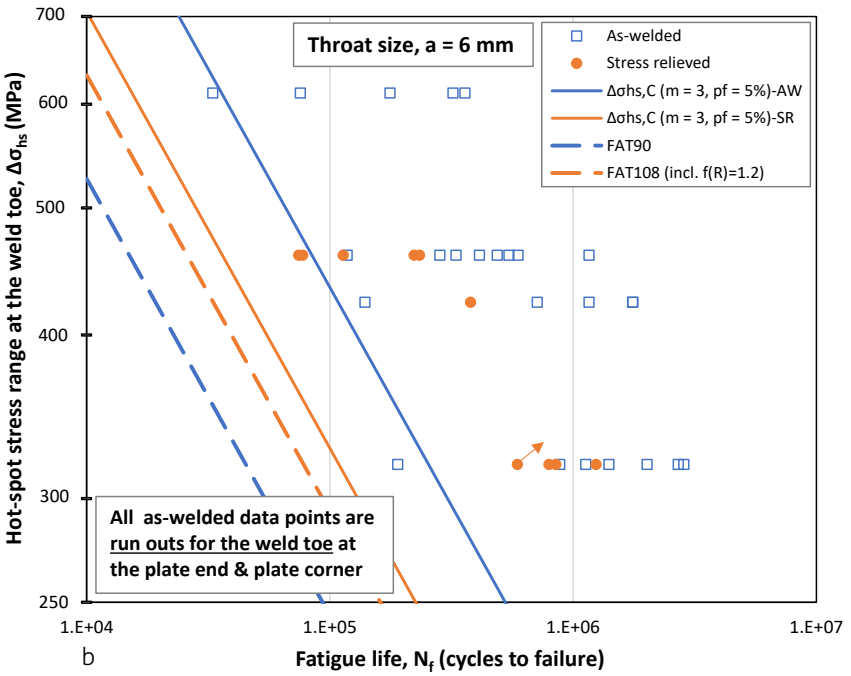

Figure 3.8a/b – The hot spot stress range ($\Delta\sigma_{hs}$) versus number of cycles to failure (N_f) for as-welded (AW) and stress-relieved (SR) specimens: (a) weld throat size a = 4; (b) weld throat size a = 6 mm. All specimens are shown, the structural hot spot SCF according to Table 3.3 have been used.

Table 3.4 – $\Delta\sigma_{hs,C(m=3,p_f=5\%)}$ values for the as-welded and stress-relieved conditions, and both throat sizes

Condition / size	$\Delta\sigma_{hs,C(m=3,p=5\%)}$ (MPa)		FAT (MPa)
Weld throat size, a (mm)	4	6	-
As-welded	≥137	≥160	90
Stress-relieved	94	121	108[2)]

[1)] – Mean value for $N_C = 2 \cdot 10^6$ cycles and slope $m = 3.0$.
[2)] – Includes $f(R) = 1.2$ for stress relieved welds.
[3)] – FAT 90 used by Doerk & Fricke [9] for the attachment end.

In Figure 3.8(a), for a throat size of 4 mm, the stress relieved data points are all above the FAT 108 S-N curve. The calculated S-N curves corresponding to $\Delta\sigma_{hs,C(m=3,p_f=5\%)}$ is lower than the FAT108 line due to the relatively large scatter of this dataset. The other three combinations, stress relieved with a throat size of 6 mm and the as-welded specimens with both throat sizes, all show an S-N curve corresponding to $\Delta\sigma_{hs,C(m=3,p_f=5\%)}$ that is higher than the applied FAT curve, see also the ratios between these S-N curves in Table 3.4. This means that, for the given conditions in these tests, an assessment with the hot spot stress method using these FAT values is conservative. However, other conditions, such as high tensile residual stresses and/or high stress ratios, are not covered by the presented test results.

Table 3.5 – $\Delta\sigma_{hs,C(m=3,p_f=5\%)}$ values for the as-welded and stress-relieved conditions, and both throat sizes

Condition / size	$\Delta\sigma_{hs,C(m=3,p_f=5\%)}/FAT$ (-)		$N_{hs,(m=3,p_f=5\%)}/N_C$ (-)	
Weld throat size, a (mm)	4	6	4	6
As-welded	≥1.52	≥1.78	≥3.5	≥5.6
Stress-relieved	0.87	1.12	0.7	1.4

3.1.3 Assessments by TNO

3.1.3.1 Hot spot stress method

TNO also used the hot spot stress method with FE models for the assessment of the weld toe of the specimen shown in Figure 3.1 (eccentricity e/t = 0), see report [1]. Figure 3.9 shows the four extrapolation paths A to D which have been applied. The extrapolation paths A and B are more or less free interpretations of the hot spot stress method, whereas the paths C and D are more in agreement with the initially proposed method of stress extrapolation along the surface. Path D in Figure 3.9 is nearly equal to the extrapolation path used by Doerk & Fricke. They used the average stress over the plate thickness and a linear extrapolation of the tangential stresses at reference points 5 and 15 mm from the weld toe, whereas TNO used the plate corner and the quadratic extrapolation (Type 'b' [4]). FE simulations have been performed for throat sizes a = 4 mm and a = 5 mm, as 5 mm was assumed to be more realistic for fillet welded plate ends in existing steel bridges than 6 mm. In addition to the specimens with a cut-out radius, specimens with a straight attachment end (infinite radius) were evaluated. Table 3.6 shows the hot spot SCF's (K_s) relative to the nominal net-section stress ($\sigma_{n,p}$). For path B, two methods have been applied, "B-surf" with the extrapolation path on the surface along the weld toe of the fillet weld, and "B-1mm" with the extrapolation path 1 mm below the surface of the weld toe of the fillet weld.

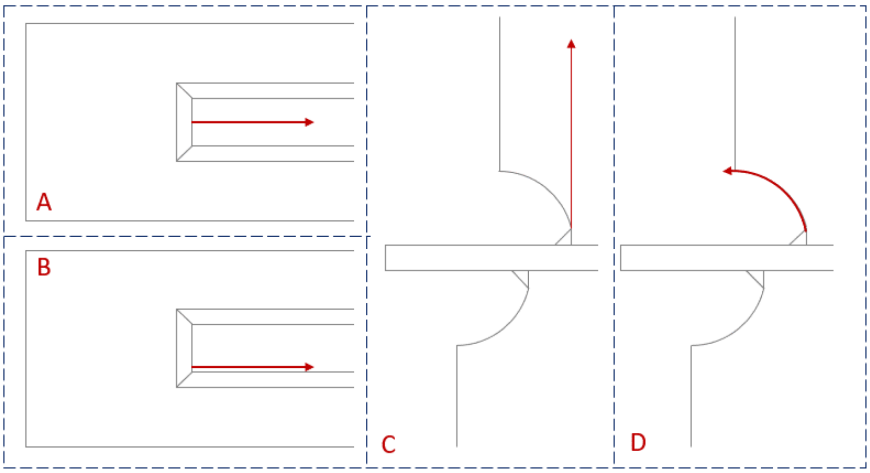

Figure 3.9 – Hot spot stress extrapolation paths A to D used by TNO [1]. (Paths C and D both along the plate surface.)

Table 3.6 – Hot spot SCF's for the five extrapolation paths, SCF's relative to the nominal net-section stress

Model nr.	a (mm)	R (mm)	Hot spot SCF, K_s (-) A	B-surf.	B-1mm	C	D
2	4	30	2.17	4.05	3.23	3.69	2.69
1	4	Infinite	1.81	3.23	2.56	3.24	3.24
5	5	30	2.32	4.06	3.14	3.23	2.75
4	5	Infinite	1.80	3.12	2.45	2.97	2.97

Application of this extrapolation path D and using the linear extrapolation with the same locations as Doerk & Fricke in the TNO FE model results:
- for a weld throat a = 4 mm in K_s = 2.62 (Doerk & Fricke found 2.60);
- for a weld throat a = 5 mm in K_s = 2.54 (Doerk & Fricke found K_s = 2.55 for a = 6 mm).

These hot spot SCF's (K_s) are shown in Figure 3.10a/b as a function of the weld throat size. The hot spot SCF's (K_s) calculated by Doerk & Fricke with the linear extrapolation method are also shown.

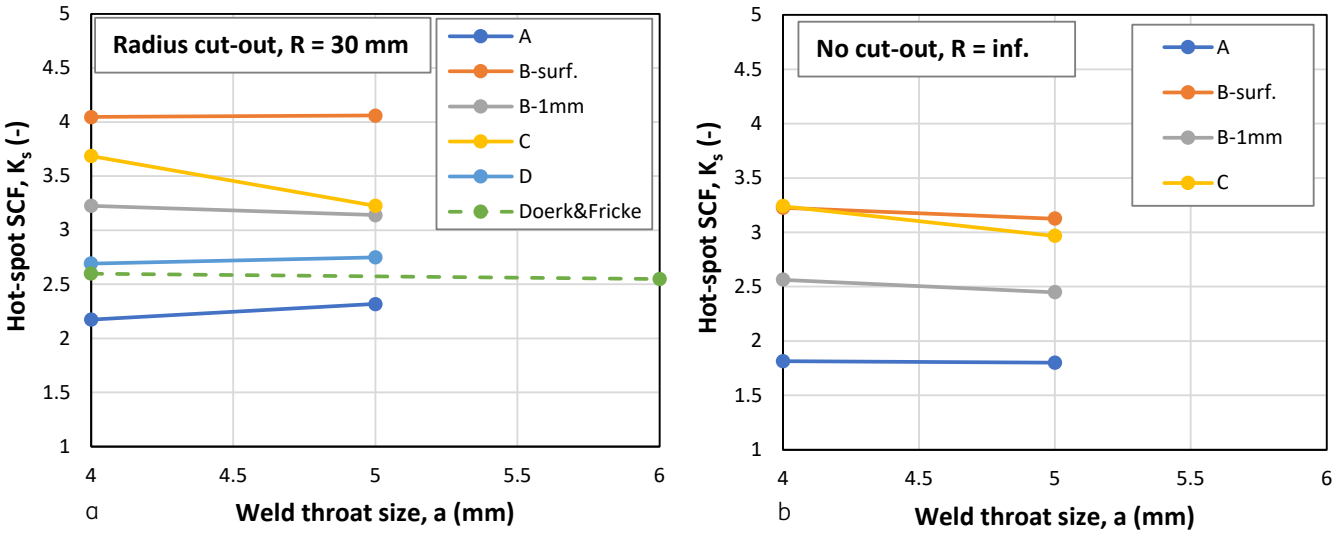

Figure 3.10a/b – The hot spot SCF's (K_s) for the paths as calculated by TNO and by Doerk & Fricke as a function of the throat size: a) for a cut-out radius of 30 mm, b) no cut-out (paths C and D are equal).

The hot spot SCF's (K_s) in Figure 3.10a/b show different levels, and also some variation in the slope as a function of the throat size. In Figure 3.10a the extrapolation paths "B-surf" and "C" seem to give relatively high hot spot SCF's (K_s), whereas extrapolation path "A" possibly under-estimates this hot spot SCF (K_s).

Figure 3.11 shows the hot spot stress ranges for the paths A, B-1mm, C and D versus fatigue life of the stress relieved specimens for a throat size of $a = 4$ mm (tests are not available for a throat size of $a = 5$ mm and hot spot stresses determined by TNO are not available for a throat size of $a = 6$ mm). According to Hobbacher [3] and Niemi et al. [4], valid hot spot stress ranges ($\Delta\sigma_{hs}$) should be smaller than two times the yield stress ($\Delta\sigma_{hs} < 2f_y$ with $f_y = R_e = 333$ MPa). For path B-1mm ($K_s = 4.05$), the fatigue tests with a nominal stress range $\Delta\sigma_{n,p}$ = 181 MPa result in hot spot stress ranges larger than 666 MPa and thus are not valid. Figure 3.12 show the hot spot stress ranges for the mentioned paths versus fatigue life of the as-welded specimens for a throat size of $a = 4$ mm. Table 3.7 shows the ratios of stress ranges and number of cycles for the S-N curve $\Delta\sigma_{hs,C(m=3,p_f=5\%)}$ relative to the applied FAT curve for a throat size of $a = 4$ mm.

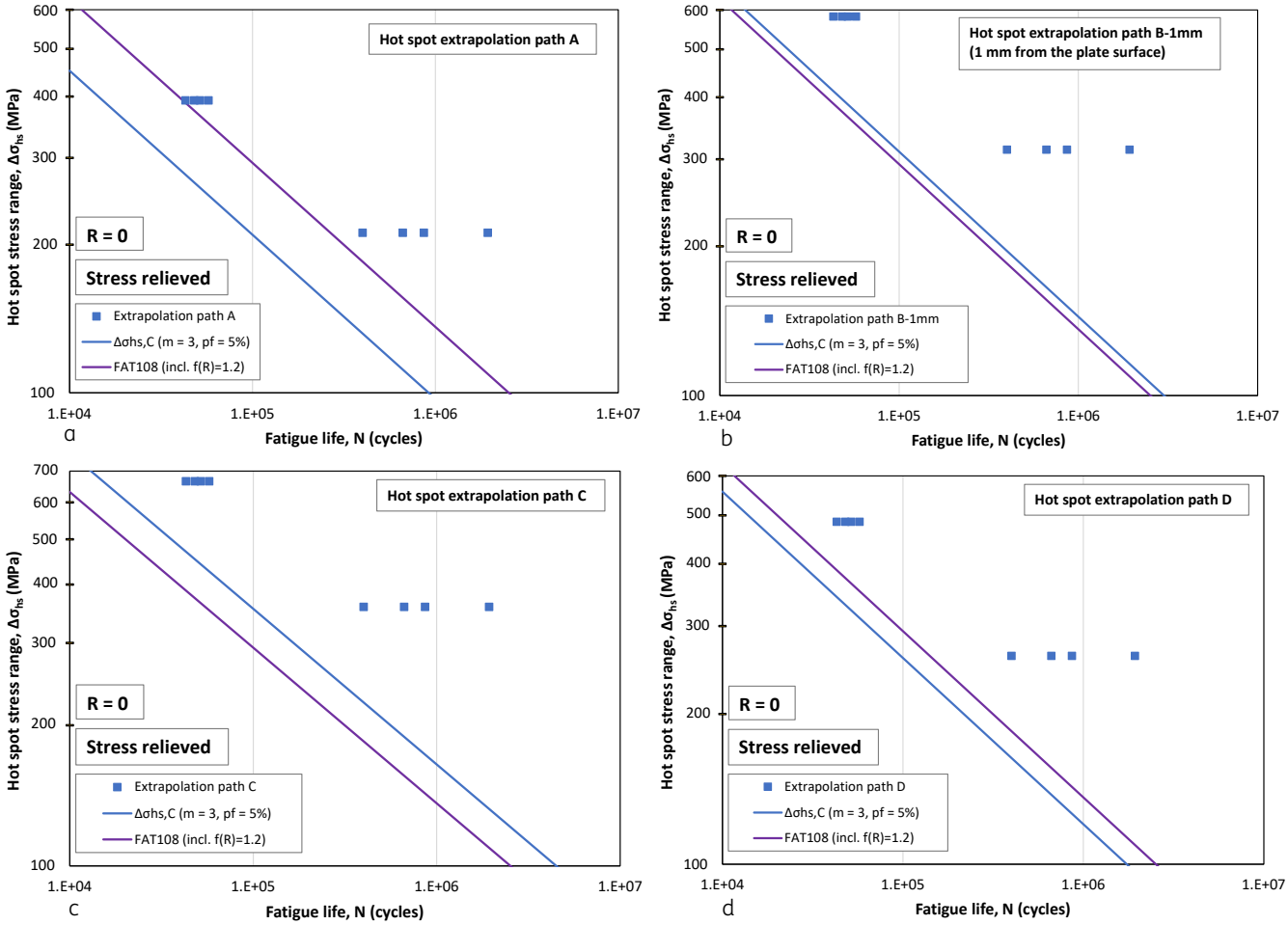

Figure 3.11a to d – Hot spot stress ranges as calculated by TNO as a function of fatigue life of the stress relieved specimens with a weld throat size of $a = 4$ mm tested by Doerk & Fricke [12].

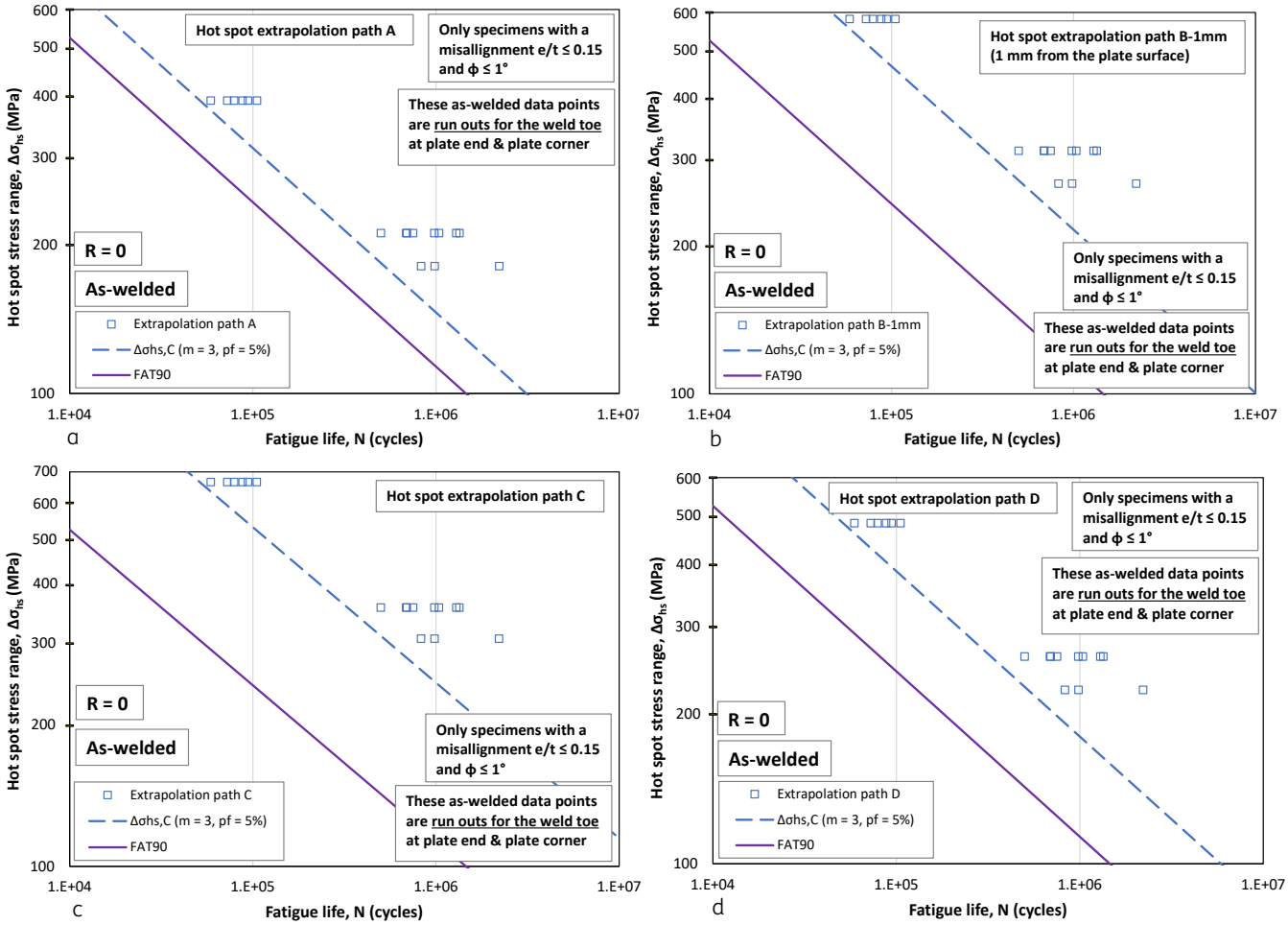

Figure 3.12a to d – Hot spot stress ranges calculated by TNO as a function of fatigue life of the as-welded specimens with a weld throat size of a = 4 mm tested by Doerk & Fricke [12].

Table 3.7 – Ratios of stress ranges and number of cycles for the S-N curve $\Delta\sigma_{hs,C(m=3,p_f=5\%)}$ relative to the FAT curve of Hobbacher [3] for the stress relieved and as-welded specimens with a throat size a = 4 mm

Condition	FAT	Weld throat size, $a = 4$ mm		
		Extrapolation path	$\Delta\sigma_{hs,C(m=3,p_f=5\%)}/FAT$ (-)	$N_{hs,C(m=3,p_f=5\%)}/N_C$ (-)
Stress-relieved	FAT 108 (incl. $f(R) = 1.2$)	A	0.71	0.4
		B-1mm	1.06	1.2
		C	1.21	1.8
		D	0.88	0.7
As-welded	FAT 90	A	≥1.29	≥2.1
		B-1mm	≥1.91	≥7.0
		C	≥2.18	≥10.4
		D	≥1.59	≥4.0

[1] For $m = 3$ and $N_C = 2 \cdot 10^6$.

Figure 3.11(a) and (d) (paths A and D, stress relieved) provide $\Delta\sigma_{hs,C(m=3,p_f=5\%)}$ S-N curves lower than FAT 108. All data are above the FAT curve for path A and D. Figure 3.11 (b) and (c) (paths B-1mm and C, stress relieved) show $\Delta\sigma_{hs,C(m=3,p_f=5\%)}$ S-N curves higher than the FAT

108 curve. Figure 3.12 (a-d) (all paths, as welded) show $\Delta\sigma_{hs,C(m=3,p_f=5\%)}$ S-N curves higher than the FAT 90 curve.

Table 3.7 provides ratios below unity for paths A and D applied to the stress relieved specimens. Hence, these paths are unconservative when combined with the FAT class of Hobbacher [3]. Paths B-1mm and C result in ratios of 1.06 and 1.21, respectively, and these are thus conservative.

3.1.3.2 Effective notch stress method

TNO-report [1] also provides results obtained with the effective notch stress method. Figure 3.13 shows the stresses in vertical direction (S22) in and around the weld toe. For this method the weld toes have been modelled with a radius of 1 mm. The corners in the horizontal plane of the plate have also been modelled with a radius of 1 mm. This radius should simulate the penetration during welding around this plate corner. However, this value is arbitrary and not supported by measurements or literature.

Figure 3.13 shows stress concentrations in the corners. It is unclear if these stresses are realistic. Figure 3.14 shows the effective notch SCF's (K_{EN}) over a quarter of the plate thickness, where location 0 is the corner of the plate. Results are given for two specimen configurations, one with a cut-out radius of 30 mm and one without a cut-out (infinite cut-out radius), for weld throat sizes a = 4 and 5 mm.

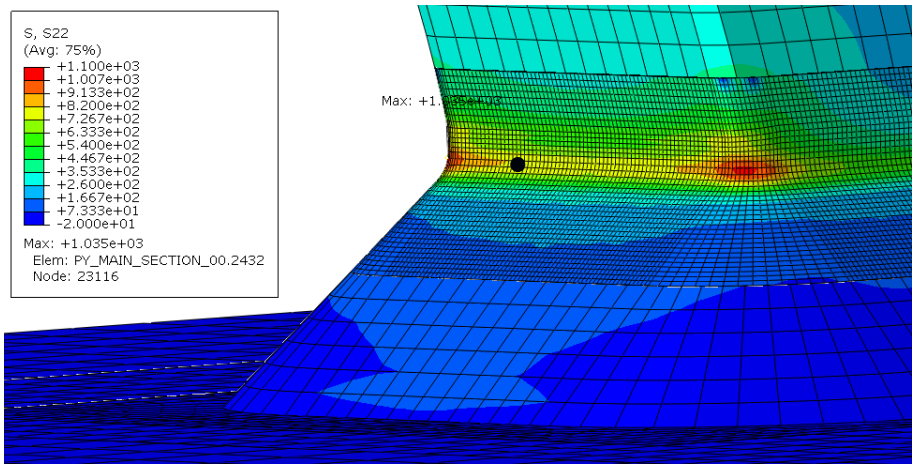

Figure 3.13 - Stresses in vertical direction (S22) in and around the weld toe as calculated with the EN-method. A radius of 1 mm has been modelled for the weld toes at the corners of the plate, and also in the horizontal plane. Black dot: stress at 1/4 of the plate thickness [1].

Figure 3.15 (a) and (b) show the effective notch stress ranges ($\Delta\sigma_{en}$) at a location of $1/4t$ = 3 mm from the corner and in the plate corner, respectively. The results are shown as a function of fatigue life of the stress-relieved specimens with throat $a = 4$ mm tested by Doerk & Fricke [12]. Figure 3.16 shows the same results for the as-welded specimens. All data in Figure 3.16 can be considered as run-outs.

The effective notch S-N curves for $m = 3, p_f = 5\%$ are added to the figures, as well as the standard FAT 225 curve for the as-welded specimens and FAT 225 x $f(R)$ = 270 for the stress relieved specimens.

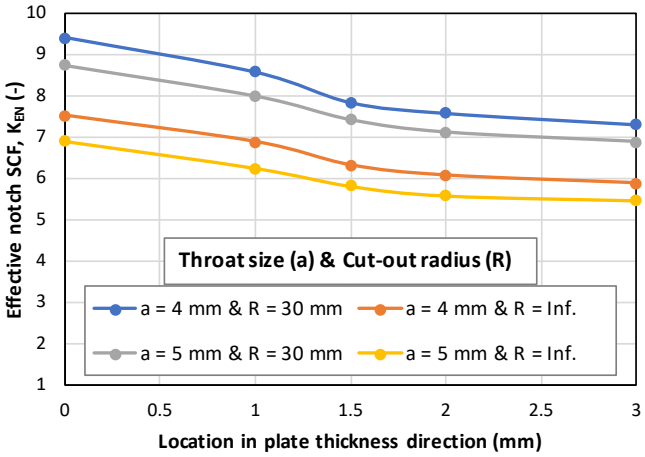

Figure 3.14 - The effective notch SCF's calculated by TNO as a function of the location along the weld toe in plate direction for two specimen configurations, namely, cut-out radii of 30 mm and infinity, using weld throat sizes of a = 4 and 5 mm.

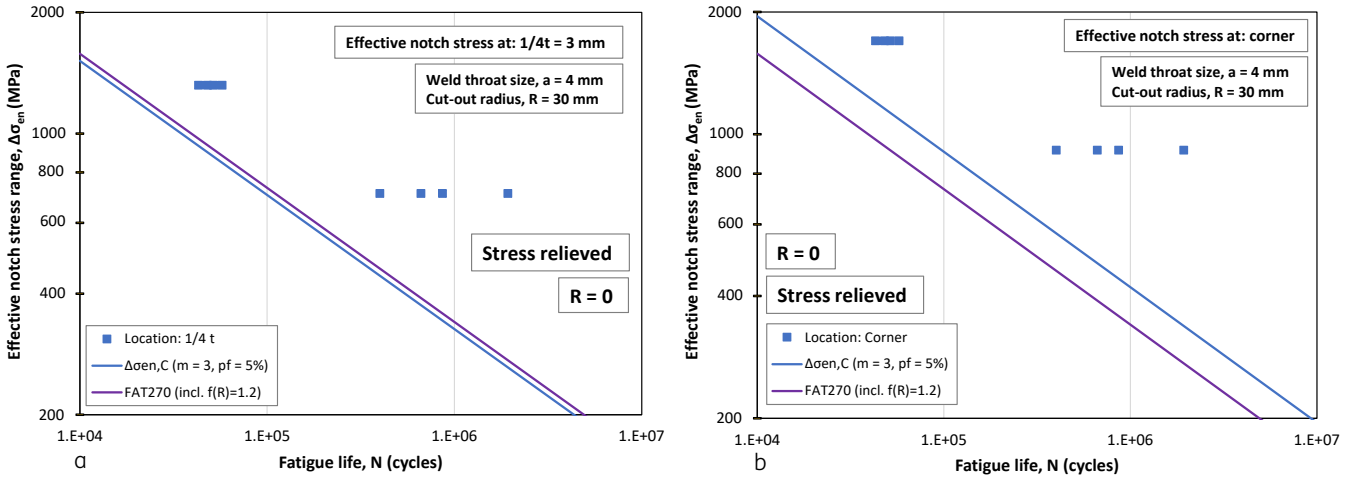

Figure 3.15a/b – Effective notch stress ranges calculated by TNO as a function of fatigue life of the stress relieved specimens tested by Doerk & Fricke [12].

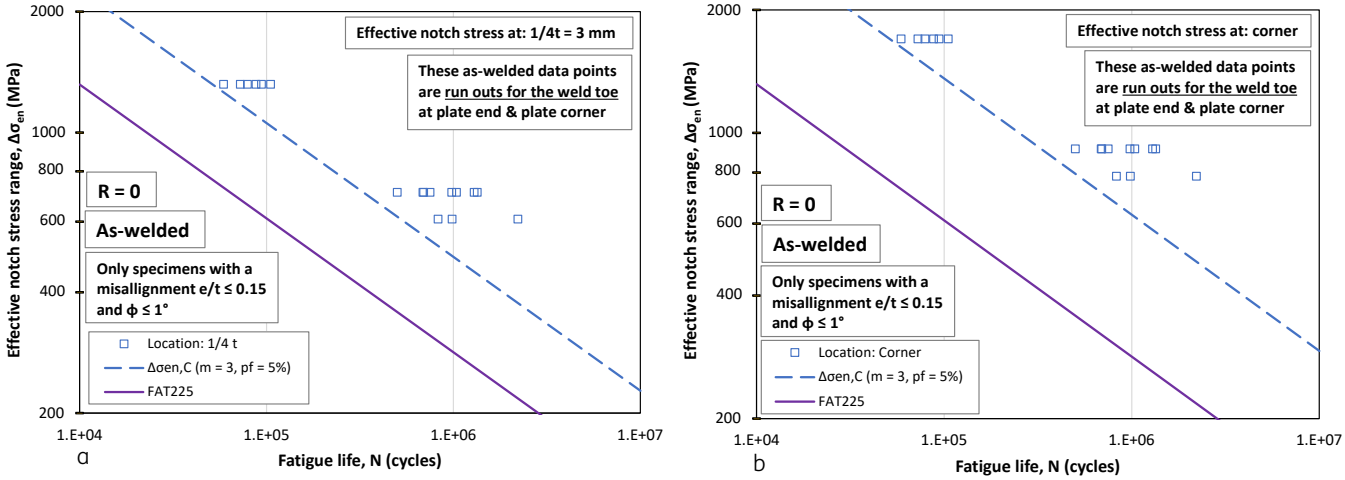

Figure 3.16a/b – Effective notch stress ranges calculated by TNO as a function of fatigue life of the as-welded specimens tested by Doerk & Fricke [12]. All data are run-outs.

In Figure 3.15a, for the stress relieved specimens at the location 1/4t = 3 mm, the data-points are all above the FAT 270 curve. Due to the relatively large deviation in this dataset the calculated $\Delta\sigma_{en,C(m=3,p_f=5\%)}$ S-N curves is lower than the FAT 270 curve. The other three combinations, stress relieved at the corner, and the as-welded specimens at both locations, all show a $\Delta\sigma_{en,C(m=3,p_f=5\%)}$ S-N curve higher than the FAT curve. Table 3.8 provides the ratios between $\Delta\sigma_{en,C(m=3,p_f=5\%)}$ and FAT class.

Table 3.8 – Stress ranges and number of cycles for $\Delta\sigma_{en,C(m=3,p_f=5\%)}$ relative to the FAT class for a throat size a = 4 mm

Condition	FAT	Weld throat size, a = 4 mm		
		Stress location	$\Delta\sigma_{en,C(m=3,p_f=5\%)}/FAT$ (-)	$N_{en,C(m=3,p_f=5\%)}/N_C$ (-)
Stress-relieved	FAT270 (incl. f(R)=1.2)	1/4t = 3 mm	0.96	0.9
		Corner	1.24	1.9
As-welded	FAT225	1/4t = 3 mm	≥1.73	≥2.23
		Corner	≥5.2	≥11.0

[1] $m = 3$ and $N_C = 2 \cdot 10^6$.

These results mean that, an assessment with the effective notch stress method using the applied FAT values will result in a conservative assessment for the conditions in these tests. However, other conditions with for instance high tensile residual stresses and/or high stress ratios are not covered by the presented tests.

3.2 Petershagen

Petershagen (2000) [16] has performed a test program with cruciform specimens with full penetration welds. Ship building steel grade D36 was used. The specimen dimensions and geometry are similar to those of Doerk & Fricke in Section 3.1. Petershagen's specimens contain a cut-out with a radius of 30 mm in both attached plates, see Figure 3.17. The specimens simulate a weld hole (rat hole) as often applied in ship structures. Specimens with plate thicknesses of 10 mm and 20 mm have been tested. Further, these specimens have been assessed with the structural hot spot stress method and effective notch stress method.

3.2.1 Fatigue tests

All specimens were tested in as-welded state. A stress ratio R = 0 and a test frequency of 30 Hz were used. The applied stresses were based on the net section of the attached plates.

Crack initiation occurred at the transitions to the rounded edges in all specimens, caused by the geometrical stress concentrations at these locations. However, the cracks appeared almost simultaneously at the plate edge and approximately in the middle of the specimens. The test results based on the nominal stress range in the net section are shown in Figure 3.18 for both plate thicknesses. The derived S-N curves ($\Delta\sigma_{n,C,m=3,p_f=5\%}$) are also shown. Table 3.9 provides the derived $\Delta\sigma_{n,C,m=3,p_f=5\%}$ values.

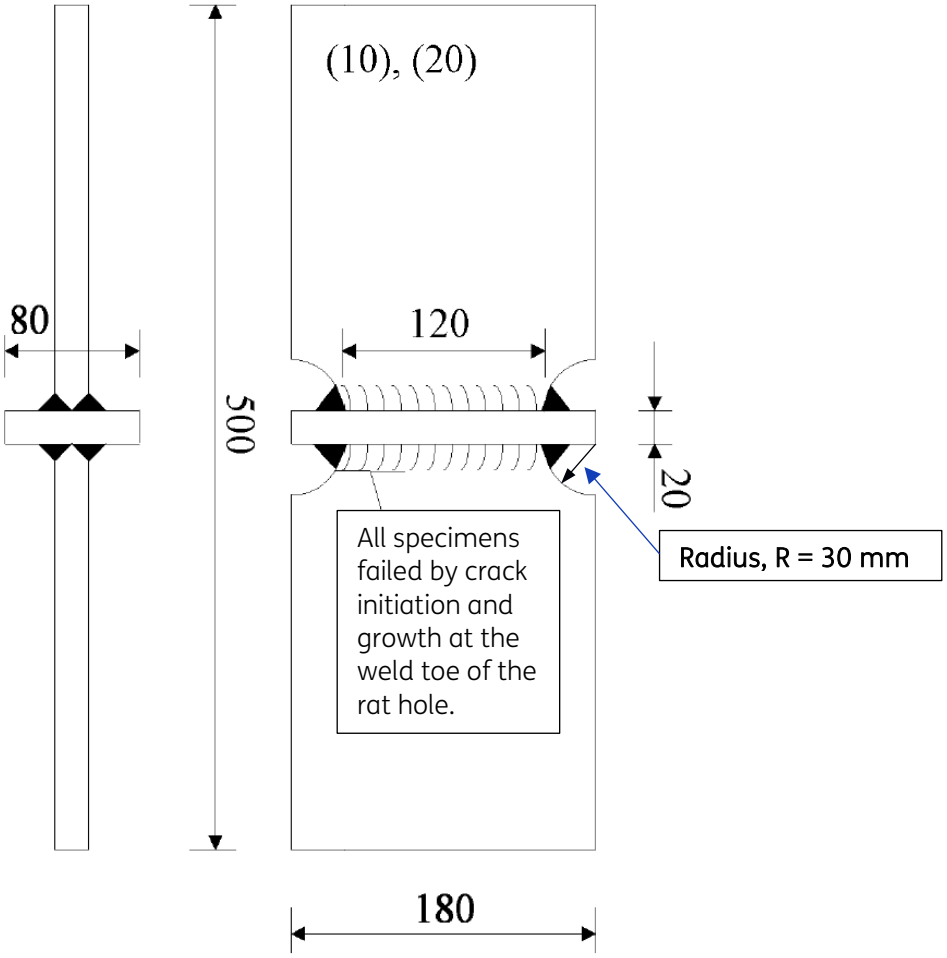

Figure 3.17 – Dimensions and geometries of the cruciform specimens with full penetration welds.

Table 3.9 – Derived $\Delta\sigma_{n,C,m=3,p_f=5\%}$ values for as-welded cruciform specimens with full penetration welds

Plate thickness t (mm)	Nominal stress $\Delta\sigma_{n,C,m=3,p_f=5\%}$ [1)] (MPa)
10	88
20	114

[1)] $m = 3$ and $N_C = 2 \cdot 10^6$.

The $\Delta\sigma_{n,C,m=3,p_f=5\%}$ value resulting from Petershagen's tests with plate thickness 10 mm and a full penetration weld, reported in Table 3.9 to be 88 MPa, is similar to that of Doerk and Fricke's as-welded specimens with a fillet weld of 6 mm, reported in Table 3.2 to be 84.3 MPa (specimens with e/t≤0.15 & ϕ≤1°) and 89.1 MPa (all specimens). The $\Delta\sigma_{n,C,m=3,p_f=5\%}$ values for the stress-relieved fillet-welded specimens with a throat size of 6 mm are much lower and vary between 50.9 and 53.4 MPa, respectively. Possible causes for the relatively high $\Delta\sigma_{n,C,m=3,p_f=5\%}$ values for the as-welded full penetration specimens by Petershagen, given by Fricke & Petershagen [15] [16], are: 1) relatively large weld toe radii at the plate edge, where values up to 3 mm were measured, 2) favourable compressive residual stresses at the plate edges. Indeed, compressive residual stresses at attachment ends were measured in a later study by Doerk & Fricke [11],[12].

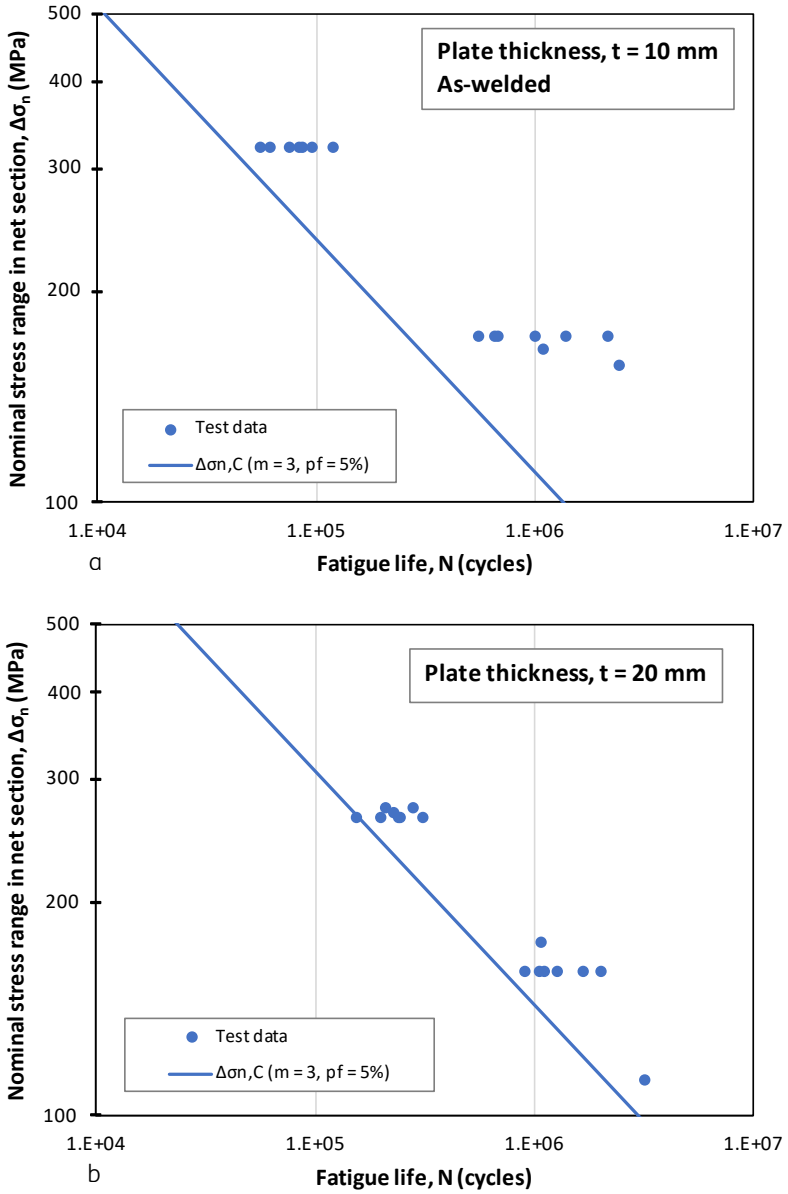

Figure 3.18a/b - S-N curve ($\Delta\sigma_{n,C,m=3,p_f=5\%}$) for the nominal stress range in the net section of the specimen for: a) a plate thickness of 10 mm, and; b) a plate thickness of 20 mm.

3.2.2 Assessment

3.2.2.1 Hot spot stress method

FE simulations were performed for both plate thicknesses and three different element sizes. Petershagen [16] used a quadratic extrapolation method with distances equal to the plate thickness for the hot spot stress at the weld toe, see Figure 3.19. Three different models (cases) with finite element sizes were used to determine the hot spot stress. The used element sizes are: $t \times t, t/4 \times t/4$, and $t/4$ to $t/16$. Figure 3.20 shows an example of a FE model of one quarter of the specimen with a plate thickness $t = 20$ mm and an element size $t/4 \times t/4$ (case 2) in the radius. Figure 3.21 shows a part of the FE model for a plate

thickness $t = 20$ mm and element sizes $t/4$ to $t/16$ in the radius (case 3). The red arrow in this figure indicates the hot spot extrapolation path in the direction of the weld toe.

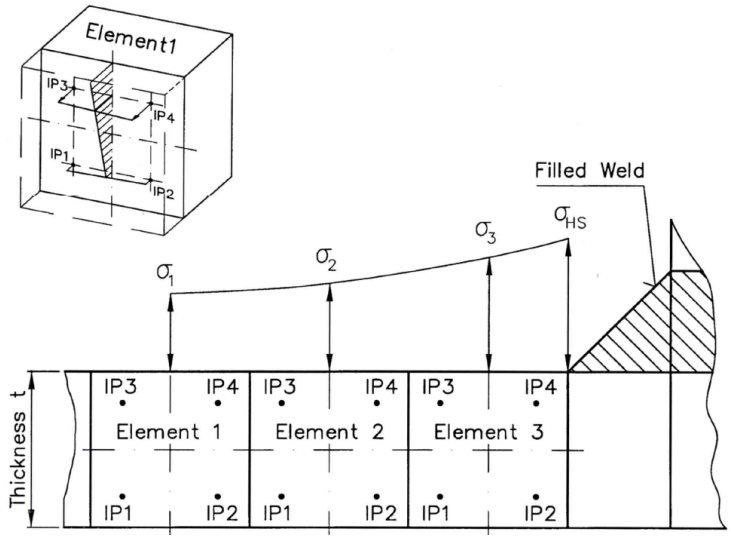

Figure 3.19 - Hot spot stress extrapolation procedure used by Petershagen (2000) [16].

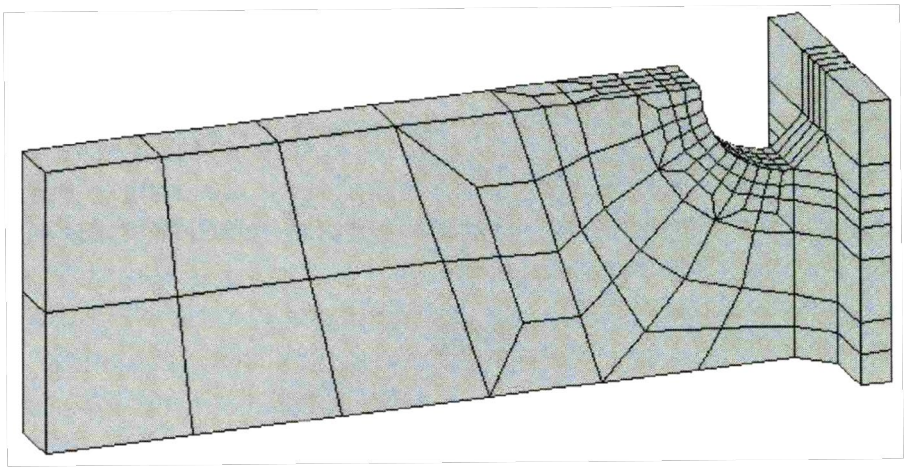

Figure 3.20 - FE model of one quarter of the specimen with a plate thickness t = 20 mm and element size $t/4 \times t/4$ (case 2) in the radius. The hot spot stress at the weld toe is calculated by applying the extrapolation procedure shown in Figure 3.19.

The used models are linear elastic and thus the calculated hot spot stresses can be expressed in structural hot spot stress concentration factors (SCF) K_s. Table 3.10 shows these SCF's for the three different element sizes and plate thicknesses, with reference to the nominal stress in the net section of the specimen.

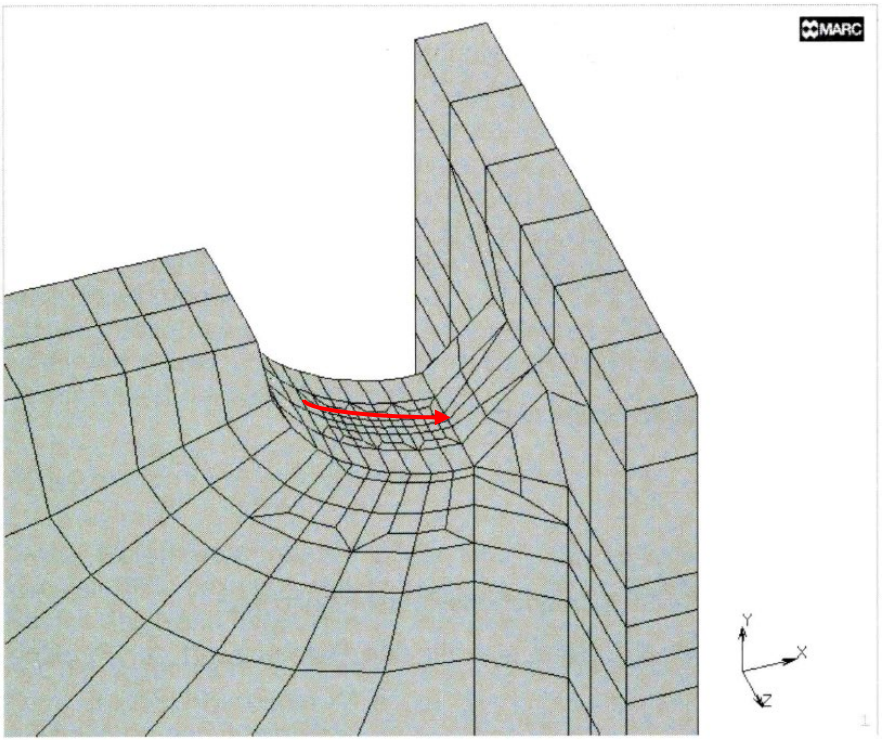

Figure 3.21 - Part of a FE model for a plate thickness t = 20 mm and element sizes of t/16 to t/4 in the radius (case 3). The hot spot extrapolation path in the direction of the weld toe is indicated (red arrow).

Table 3.10 – Derived hot spot stress factors K_s for both plate thicknesses and as a function of the used finite element size relative to the plate thickness

Case	Finite element size[1)]	SCF K_s (-) Thickness t (mm)	
		10	20
1	t x t	2.19	2.06
2	t/4 x t/4	**2.20**	**2.29**
3	t/4 & t/16	1.93	1.93

[1)] – t = plate thickness

Using the SCF the hot spot stress range $\Delta\sigma_{hs}$ of the performed fatigue tests can be calculated:

$$\Delta\sigma_{hs} = K_s \Delta\sigma_n$$

where $\Delta\sigma_n$ is the nominal net section stress. This also allows to determine the hot spot S-N curve for a fixed slope m = 3 and a prediction bound of 5% ($\Delta\sigma_{hs,C,m=3,p=5\%}$), see Table 3.9. Figure 3.22 gives the hot spot stress ranges versus the number of cycles to failure, including the $\Delta\sigma_{hs,C,m=3,p=5\%}$ S-N curve and the FAT 100 curve. The S-N curves in Figure 3.22, are substantially higher than the FAT 100 curve. Table 3.11 gives the ratios.

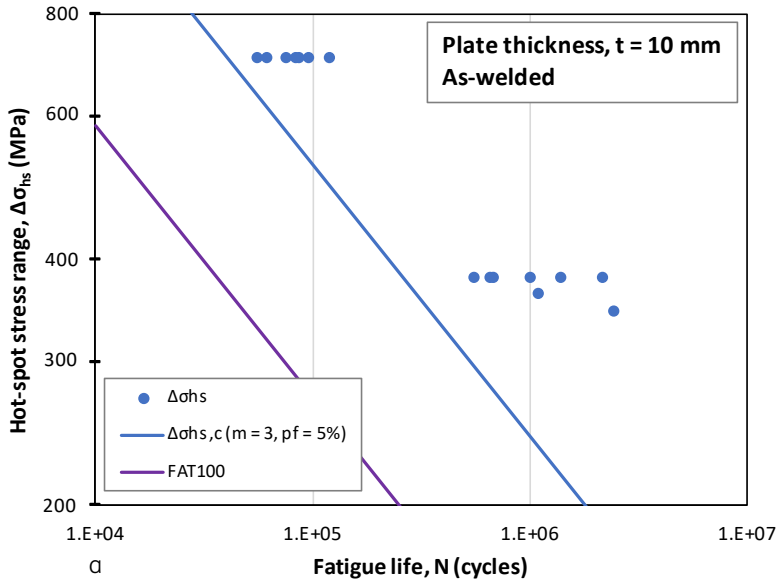

a

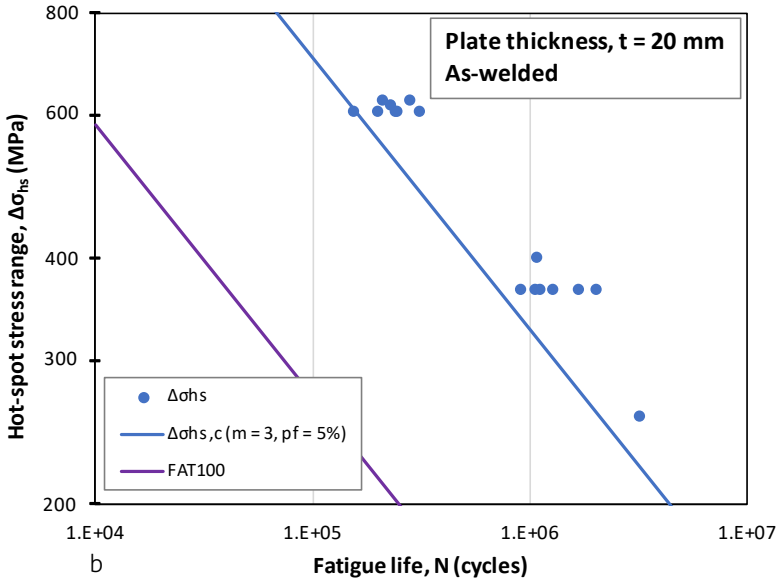

b

Figure 3.22a/b - Hot spot stress ranges of tests of Petershagen as a function of fatigue life, the $\Delta\sigma_{hs,C,m=3,p=5\%}$ S-N curve of these tests and the FAT 100 curve: (a) specimens with a plate thickness of 10 mm; (b) for specimens with a plate thickness of 20 mm.

Table 3.11 – Ratios of stress ranges at $N_C = 2 \times 10^6$ cycles, and corresponding number of cycles, for the S-N curve corresponding to a failure probability of 5% to FAT 100 curve

Plate thickness t (mm)	$\Delta\sigma_{hs,C,m=3,p=5\%}/FAT100$ (-)	$N_{hs,C,m=3,p=5\%}/N_{FAT100}$ (-)
10	1.93	7.2
20	2.61	17.7

The FAT class is hence very conservative for these specimens. However, note that these results are obtained for *as-welded* specimens with probably compressive welding stresses at the attachment ends and extremely smooth weld toe transitions (transition radius 3 mm).

3.2.2.2 Effective notch stress method

Figure 3.23 shows the FE mesh for a plate thickness of 10 mm with a radius of 1 mm applied at the weld toe. Half of the specimen was modelled. A nominal net section stress $\sigma_{n,p} = 100$ MPa was applied.

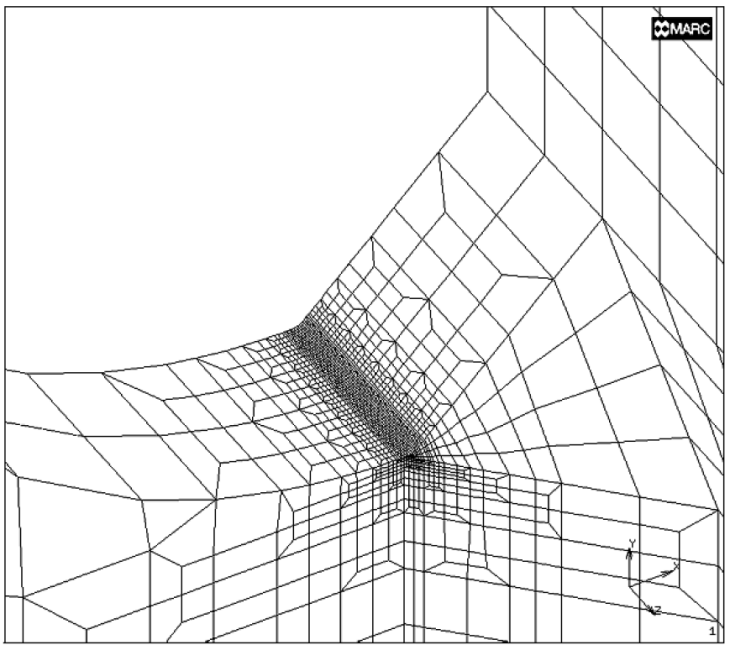

Figure 3.23 - FE model of the half specimen thickness for the effective notch stress calculation at the weld toe.

The effective notch concentration factors resulting from the FE analyses are $K_{en} = 3.68$ and $K_{en} = 4.03$ for the specimens with a plate thickness of 10 mm and 20 mm, respectively. The nominal stress in the net section is used as reference for this factor. Figure 3.24 shows the effective notch stress ranges of the performed tests, the S-N curve for a fixed slope m=3 and a 5% prediction bound ($\Delta\sigma_{en,C,m=3,p_f=5\%}$) and the FAT 225 curve. Table 3.12 gives the ratios between these curves.

The ratios for the effective notch stress method are about 25 % lower than the ratios found for the hot spot stress method, but still show large conservatism for these as-welded specimens with full penetration welds.

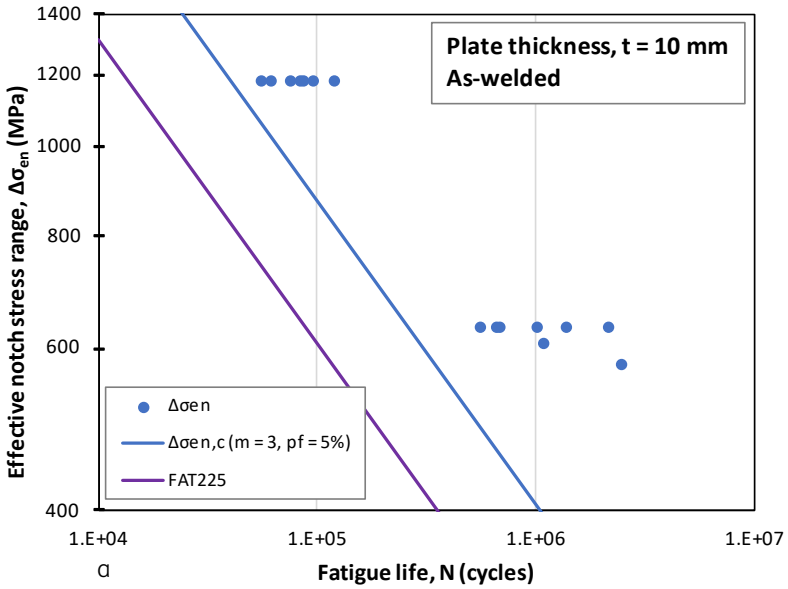

a

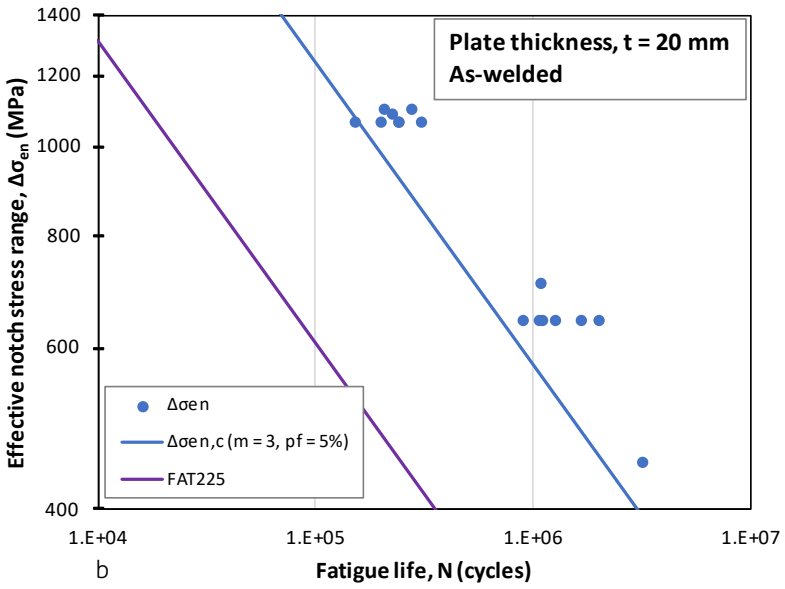

b

Figure 3.24a/b - Effective notch stress ranges of the performed tests, the S-N curve ($\Delta\sigma_{en,C,m=3,p_f=5\%}$) of these test results and the S-N curve for FAT225 as a function of fatigue life for: a) specimens with a plate thickness of 10 mm and b) for specimens with a plate thickness of 20 mm.

Table 3.12 – Ratios of stress ranges at $N_c = 2 \times 10^6$ cycles, and corresponding number of cycles, for the 5% prediction bound S-N curve and the FAT 225 curve

Plate thickness t (mm)	$\Delta\sigma_{en,C,m=3,p_f=5\%}/FAT225$ (-)	$N_{en,C,m=3,p_f=5\%}/N_C$ (-)
10	1.43	2.9
20	2.04	8.5

3.3 Fricke & Gao & Paetzold

Fricke & Gao & Paetzold (2017) [17] performed fatigue tests with as-welded and stress-relieved specimens without cut-out (fillet welds according to the authors, but actually full penetration welds), see Figure 3.25. The specimens have been assessed with the structural hot spot stress method and effective notch stress method. The subject of this study is the weld around a plate corner, which typically occurs at the ends of loaded stiffeners.

3.3.1 Fatigue tests

Steel grade S355J2 with a plate thickness of 20 mm was used for the specimens. Full penetration welds were applied. The plates were clamped during welding to avoid axial and angular misalignments, which were found to be negligible. Stress-relieving was performed at a temperature of 570 °C. Fatigue test conditions:

- Stress ratio $R = 0$.
- Frequency 30 Hz.

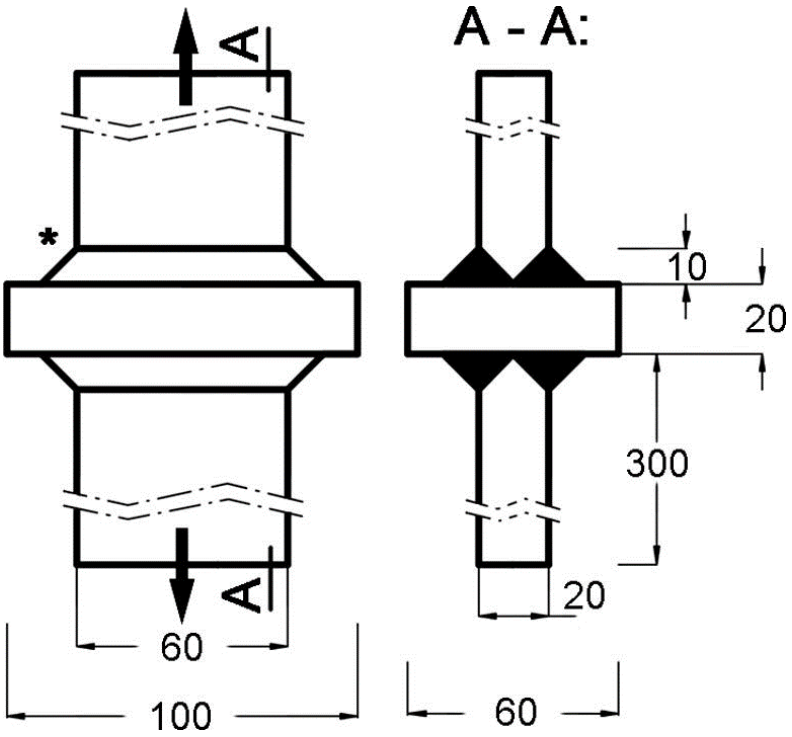

Figure 3.25 - Dimensions and geometries of the cruciform specimens with full penetration welds.

Figure 3.26 shows the test results and derived S-N curves of the as-welded and the stress-relieved specimens using the nominal (net section) stress. These S-N curves are derived for a fixed slope $m = 3$ and a prediction bound of 5% ($\Delta\sigma_{n,C,m=3,p=5\%}$). Table 3.13 provides the results.

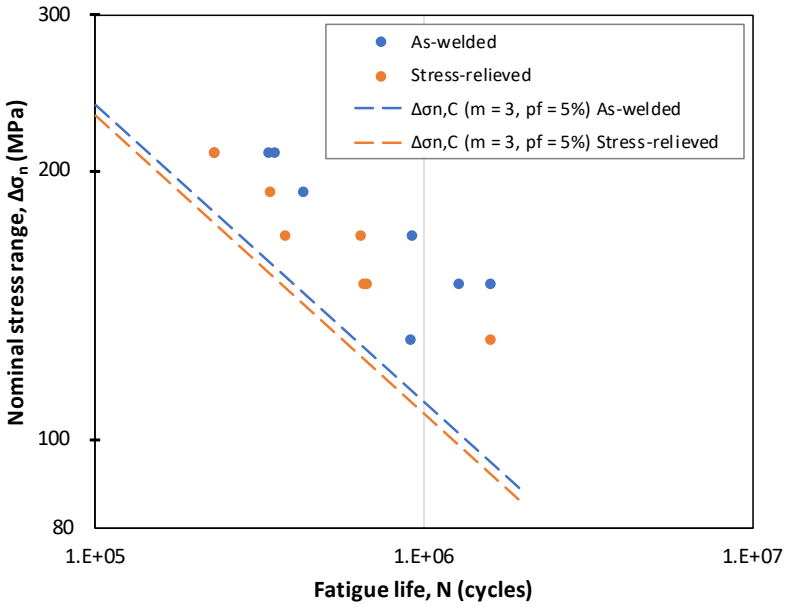

Figure 3.26 - Test results and S-N curves for the nominal (net section) stress for as-welded and stress-relieved specimens, without cut-outs and with full penetration welds. S-N curves for a fixed slope $m = 3$ and a prediction bound of 5%.

Table 3.13 – Results of the statistical evaluation of the tests with as-welded and stress-relieved specimens

Condition	Nominal stress $\Delta\sigma_{n,C,m=3,p_f=5\%}$ [1)] (MPa)
As-welded	87.7
Stress-relieved	85.1

[1)] $m = 3$ and $N_C = 2 \cdot 10^6$.

Figure 3.27 shows two examples of fracture surfaces of an as-welded specimen and a stress-relieved specimen. The arrow indicates the dominant crack growth direction; in the as-welded specimen from the long side and in the stress-relieved specimen from the attachment end. Although a clear distinction in crack initiation and growth direction follows from the tests [17], in practical situations also initiation at the plate corner is often observed and seems also be present in the fracture surface shown in Figure 3.27a.

Figure 3.26 shows that the as-welded specimens, which show crack initiation and growth at the weld toe at the long side (“plate surface”), see Figure 3.27a, show a longer fatigue life than the stress relieved specimens, which show crack initiation and growth at the weld toe at the attachment end (“plate edge”), see Figure 3.27b. Thus the obtained results for the as-welded specimens can all be interpreted as run-outs for the weld toe at the attachment end (“plate edge”).

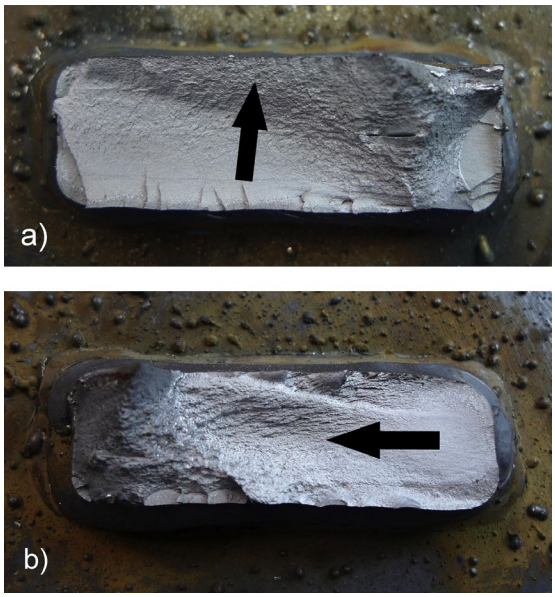

Figure 3.27a/b - Fracture surfaces of specimens in as-welded state (a) and stress-relieved (b); the arrow indicates the dominant crack propagation direction.

3.3.2 Assessments

3.3.2.1 Structural hot spot stress method

The authors of [17] calculated hot spot stresses at three locations, indicated by “plate edge”, “plate corner”, and “plate surface”. Figure 3.28 shows the locations and applied extrapolation paths. Extrapolation Type “a” (plate thickness dependent stress locations) was used for the plate corner and the plate surface and Type “b” (plate thickness independent stress locations) was used for the plate edge. The structural hot spot stresses were calculated using a nominal stress σ_n = 100 MPa. Table 3.14 shows the structural hot spot SCF’s (K_s) for the three extrapolation paths. A plate corner radius of 0.1 mm was applied in the FE model.

Using the hot spot SCF’s (K_s), the hot spot stress ranges of the tests are calculated for each extrapolation path. Figure 3.29 (a-c) and Figure 3.30 show these hot spot stress ranges for the as-welded and the stress relieved specimens, respectively, the latter only for the plate edge location. The FAT 100 curve is shown for the as-welded specimens in Figure 3.29 (a-c). This FAT class is multiplied with a fatigue enhancement factor $f(R)$ = 1.2 for the stress-relieved specimens (FAT 120) in Figure 3.30. The hot spot stress S-N curves for $m = 3, p = 5\%$ are also shown. Table 3.15 gives the $\Delta\sigma_{hs,C\ (m=3,p=5\%)}$ values.

The as-welded specimens did not initiate at the plate edge or plate corner but at the plate surface. The data in Figure 3.29(a) should therefore be interpreted as run-outs for the plate edge and plate corner of as-welded specimens. The hot spot stress S-N curve $\Delta\sigma_{hs,C\ (m=3,p_f=5\%)}$ when treating run-outs as failures is significantly higher than the FAT 100 curve, which indicates that the applied hot spot stress method for the locations plate edge and plate corner of as-welded specimens may be very conservative.

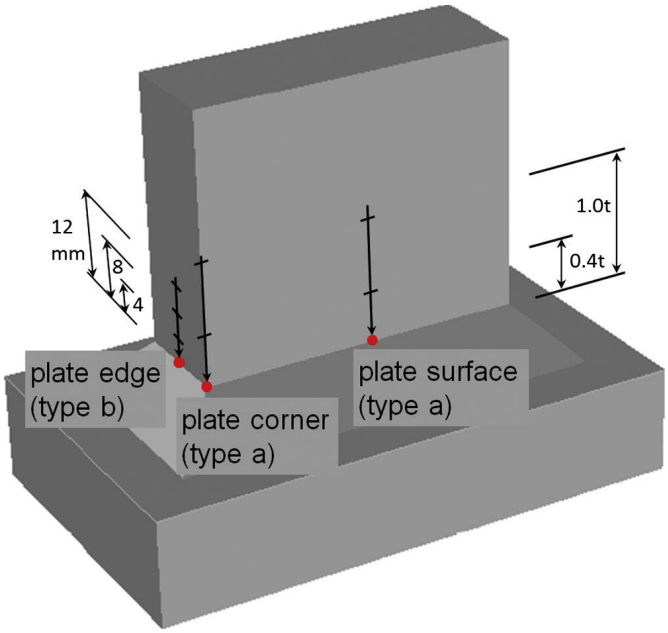

Figure 3.28 - Hot spot critical weld toes and the applied stress extrapolation paths.

Table 3.14 - Structural hot spot SCF's (K_s) for the three extrapolation paths in Figure 3.28

Hot spot stress assessment	Plate edge	corner[1)]	surface
Extrapolation type	b	a	a
Hot spot SCF, K_s (-)	1.21	1.10	0.95

[1)] A corner radius of 0.1 mm was used for the plate corner.

Table 3.15 – Hot spot stress S-N curves ($m = 3, p = 5\%$) for as-welded and stress-relieved specimens

Condition	Nominal $\Delta\sigma_{n,C\ (m=3,p_f=5\%)}$ (MPa)	$\Delta\sigma_{hs,C\ (m=3,p_f=5\%)}$[1)] edge (MPa)	corner (MPa)	surface (MPa)	Hot spot stress method FAT (MPa)
As-welded (AW)	87.7	≥105.7	≥96.5	**83.2**	100
Stress-relieved (SR)	85.1	**102.6**	≥93.6	≥80.8	120

[1)] – The values in bold are the location where the first crack initiations were observed.

None of the specimens, neither as-welded nor stress-relieved, initiated and failed at the plate corner. Thus, all test results, for both specimen conditions, can be interpreted as run-outs for the plate corner. All as-welded specimens initiated and failed at the plate surface, although the hot spot SCF at the plate corner was found to be about 16% higher than at the plate surface.

Figure 3.29(c) shows the hot spot stresses for the as-welded specimens at the plate surface. The $\Delta\sigma_{hs,C\ (m=3,p=5\%)}$ S-N curve is significantly lower than the FAT 100 curve, which indicates that the applied hot spot stress method for this location can be unconservative. Figure 3.30 shows the hot spot stresses for the stress-relieved specimens at the plate edge. The derived S-N curve $\Delta\sigma_{hs,C\ (m=3,p_f=5\%)}$ for this location is significantly lower than the FAT 120 curve, which indicates that the applied hot spot stress method for this location can be unconservative. The calculated hot spot stresses at the plate corner and plate surface of the stress-relieved specimens are lower than the stresses at the edge, based on the run-outs for these locations. Hence, no assessment can be given for this location.

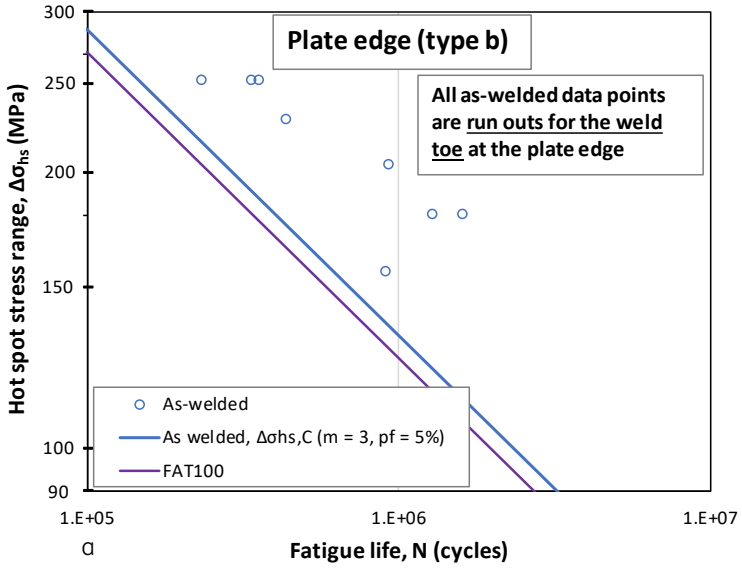

a

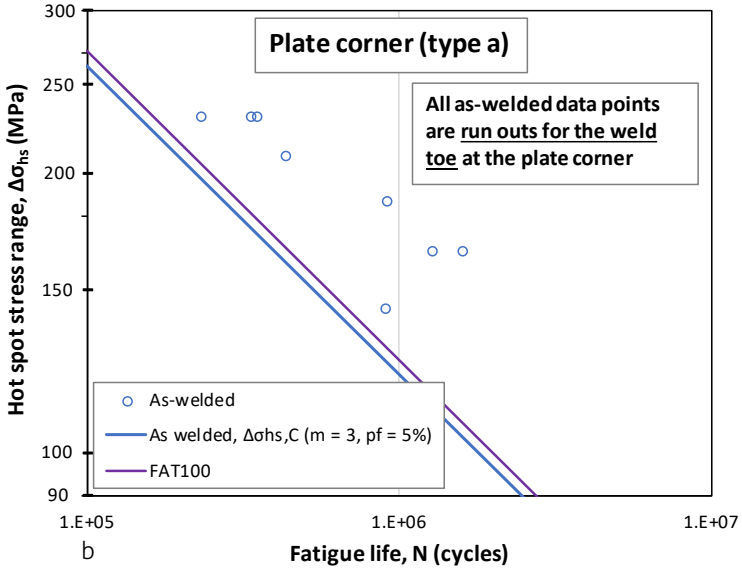

b

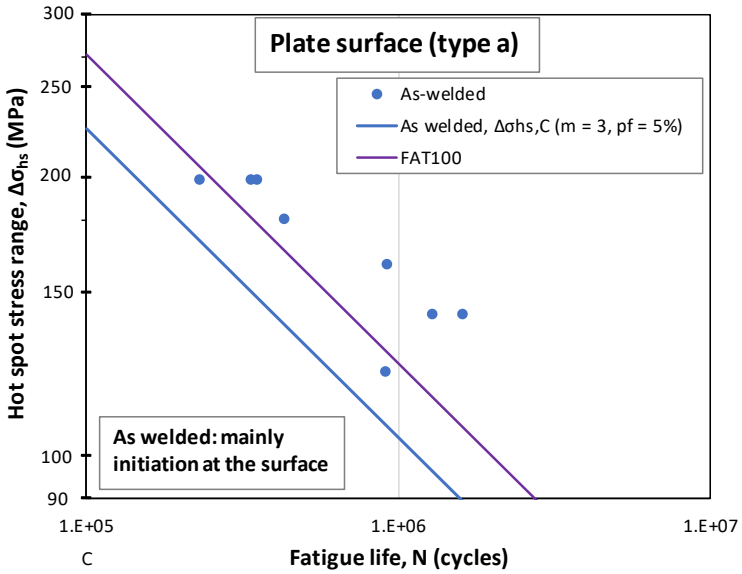

c

Figure 3.29a to c – Hot spot stress ranges for the three extrapolation paths of the as-welded specimens: a) plate edge; b) plate corner; c) plate surface. Test results in subfigure a) are run outs.

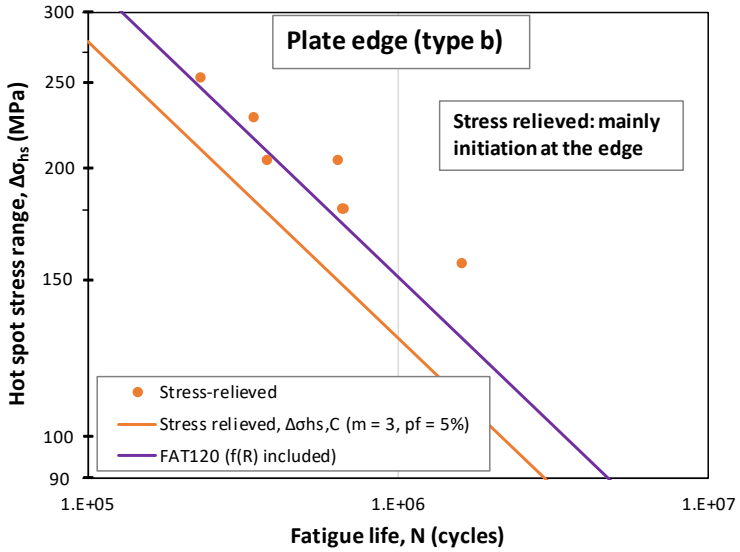

Figure 3.30 – Hot spot stress ranges for extrapolation path "plate edge" of the stress relieved specimens.

Table 3.16 shows the ratios relative to the applicable FAT curves. These ratios reflect the results shown in Figure 3.29 (a-c) and Figure 3.30.

Table 3.16 – Ratios of stress ranges and number of cycles for the S-N curves relative to the FAT curve for as-welded and stress-relieved specimens

Condition	FAT (MPa)	$\Delta\sigma_{hs,C,(m=3,p=5\%)}/FAT$ [1]			$N_{hs,C,(m=3,p=5\%)}/N_C$ [1]		
		edge (-)	corner (-)	surface (-)	edge (-)	corner (-)	surface (-)
As-welded (AW)	100	≥1.06	≥0.96	**0.83**	≥1.18	≥0.90	**0.58**
Stress-relieved (SR)	120	**0.85**	≥0.78	≥0.67	**0.62**	≥0.48	≥0.31

[1] $m = 3$ and $N_C = 2 \cdot 10^6$.

Three different locations were used to calculate the hot spot SCF's (K_s). Obviously, the values are the same for the as-welded and for the stress-relieved specimens. However, the authors indicate that the as-welded specimens mainly initiate at the plate surface, and stress-relieved specimen mainly initiate at the plate edge, see Figure 3.27. Consequently, for the stress-relieved specimens, the main initiation location coincides with the location with the highest hot spot SCF, $K_s = 1.21$, whereas for the as-welded specimens, the main initiation location coincides with the location with the lowest hot spot SCF, K_s = 0.95. The remarkable result for the as-welded specimens can be explained by the residual stresses, which are often compressive at weld ends and thus favour fatigue life at that location.

Table 3.16 shows that the "edge" extrapolation path gives a stress range ratio higher than one for the as welded specimens. For the "corner" location of the as-welded specimens the ratio is close to one and all datapoints are above the FAT100 line (Figure 3.29b).

3.3.2.2 Effective notch stress method

The effective notch stress method was also applied by the authors of [17] to calculate the notch stresses (σ_{en}) at the three attachment locations: plate edge, plate corner and plate surface. The applied nominal stress (σ_n) was 100 MPa. Figure 3.31 shows some of the FE results for a 1/4 part of the model. Figure a shows the distribution of the major principal stresses (S1); the three weld toe locations are indicated. Figure b shows the distribution of these principal stresses in the horizontal plane through the effective notches.

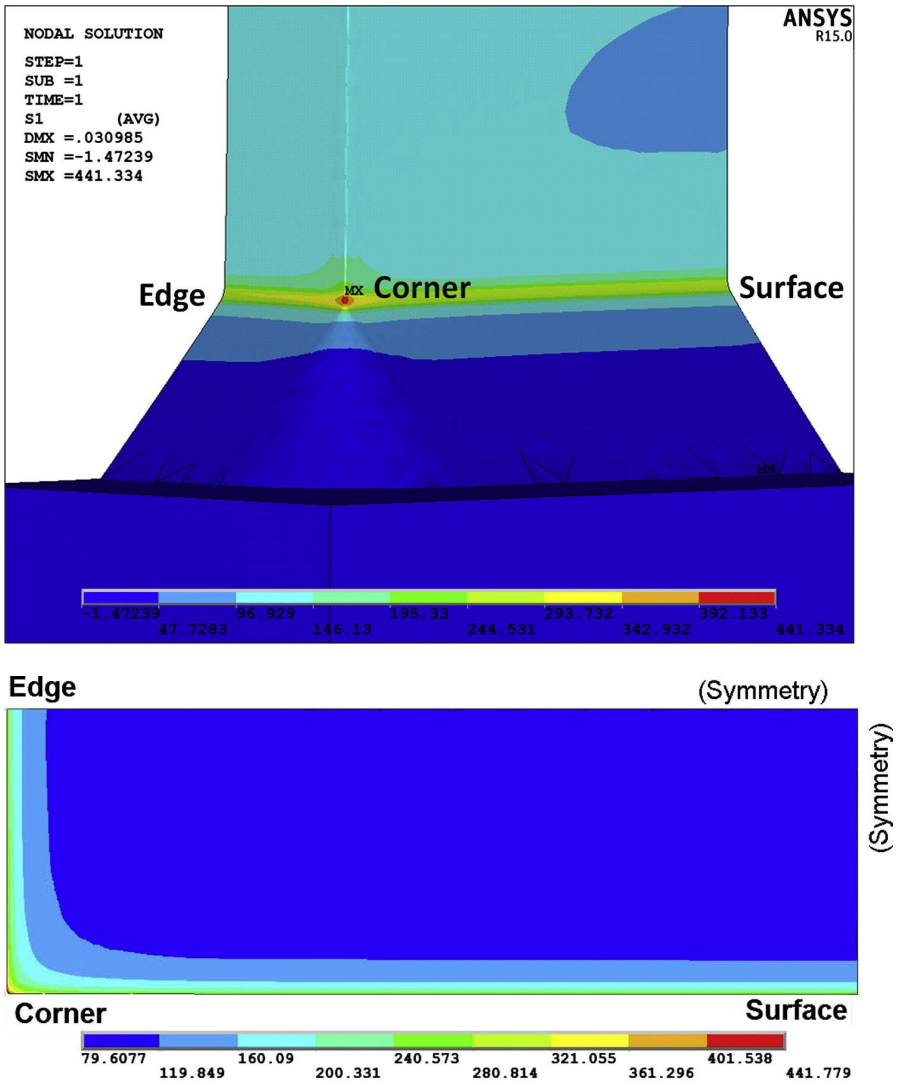

Figure 3.31 - FE results with the effective notch stress method for a 1/4 part of the FE model: (a) first principal stress with the three weld toe locations indicated; (b) distribution of these principal stress in the horizontal plane through the effective notches. A plate corner radius $r = 0.1$ mm was used.

Table 3.17 shows the effective notch SCF's (K_{en}) for the three locations indicated in Figure 3.31. A relatively high effective notch SCF, K_{en} = 4.4, was calculated for the plate corner for a sharp corner (radius of 0.1 mm). The application of a substantially larger corner radius of 3 mm results in a lower effective notch SCF, K_{en} = 3.4, which is still higher than K_{en} obtained for the plate edge and plate surface, see Figure 3.32.

Table 3.17 - Effective notch SCF's (K_{en}) for the three locations indicated in the Figure 3.31a/b

Effective notch stress assessment	Plate			
	edge	corner r = 0.1 mm	corner r = 3 mm	surface
Effective notch SCF, K_{en}	2.94	4.41	3.41	2.83

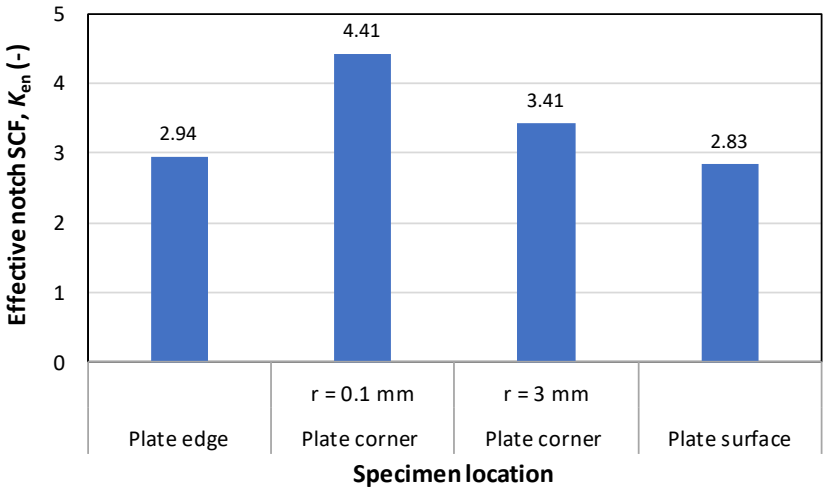

Figure 3.32 – Effective notch SCF's (K_{en}) for the three attachment locations, edge, corner and surface. For the corner calculations have been performed for two corner radius values.

The effective notch stress ranges for the three locations are calculated with these effective notch SCF's. Figure 3.33 (a-c) shows these stress ranges for the as-welded specimens. Figure 3.34 (a-b) shows the effective notch stress ranges for the plate edge and plate corner ($r = 3$ mm) of the stress-relieved specimens. The effective notch stress $\Delta\sigma_{en,C\ (m=3,p=5\%)}$ S-N curves, see Table 3.18, are also shown in these figures, together with the FAT 225 curve in Figure 3.33 (a-c) and the FAT 225 x $f(R)$ = FAT 270 curve for the stress-relieved specimens.

Table 3.18 – Effective notch stress S-N curves ($m = 3, p = 5\%$) for as-welded and stress-relieved specimens

Condition	Nominal $\Delta\sigma_{n,C\ (m=3,p_f=5\%)}$ (MPa)	$\Delta\sigma_{en,C\ (m=3,p=5\%)}$ [1)]			Effective notch stress method FAT (MPa)
		edge (MPa)	corner (MPa)	surface (MPa)	
As-welded (AW)	87.7	≥258	≥299	**248**	225
Stress-relieved (SR)	85.1	**250**	≥291	≥241	270

[1)] – The values in bold are the location where the first crack initiations were observed.

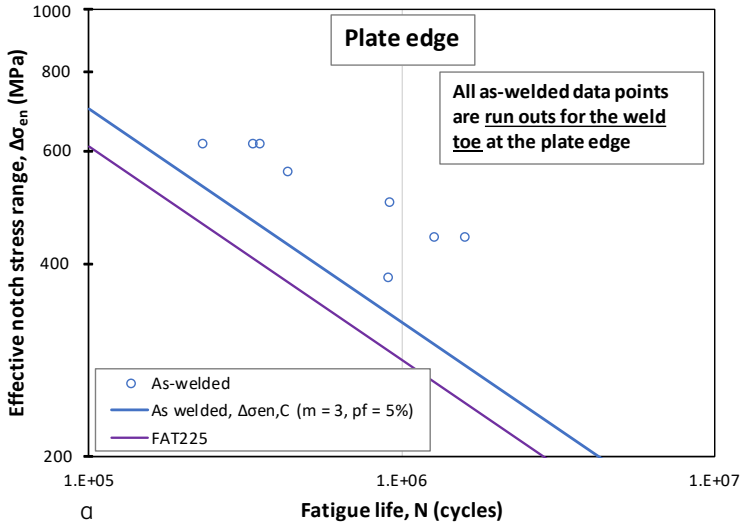

a

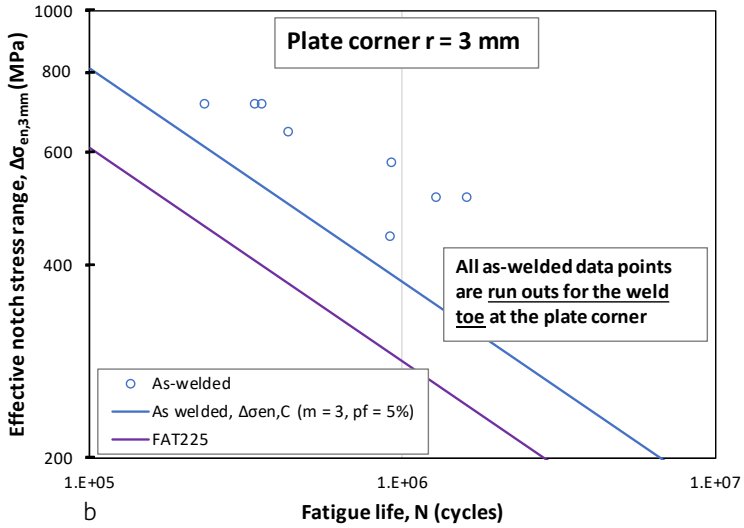

b

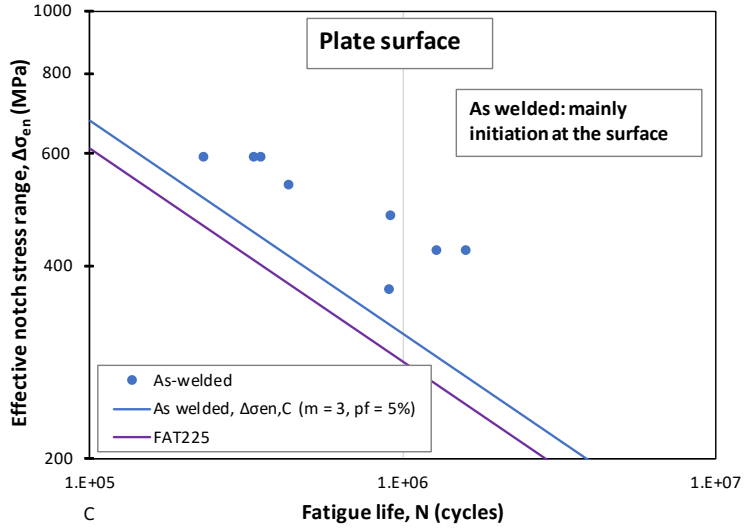

c

Figure 3.33a to c – Effective notch stress ranges for the as-welded specimens for the three locations: (a) edge; (b) corner (r = 3 mm); (c) surface. All data in figures (a) and (b) are run outs.

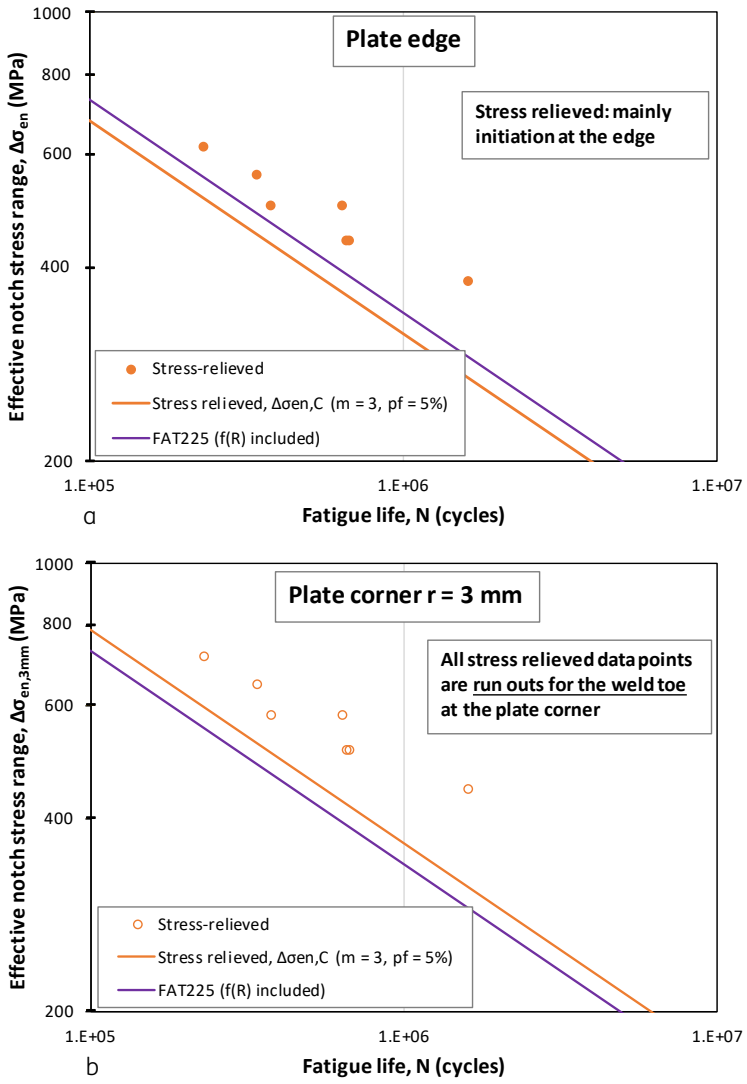

Figure 3.34a/b – Effective notch stress ranges for the stress relieved specimens for the two attachment locations: (a) edge; (b) corner (r = 3 mm). All data in figure (b) are run outs.

Although the highest effective notch SCF's (K_{en}) were found in the weld toe at the plate corner (K_{en} = 4.4 or 3.4 for a corner radius of 0.1 mm or 3 mm, respectively, versus 2.9 and 2.8 for the plate edge and plate surface, respectively) fatigue cracks did not appear at the plate corners, but at the plate surface for the as-welded specimens and at the plate edge for stress relieved specimens. According to Fricke & Gao & Paetzold [17] this can be caused by the small spot with high stress at the plate corner, see Figure 3.31 (a-b). In their publication the authors give an extended analysis, statistical size effect, of the size of the most highly stressed volume depending on the chosen plate corner radius. They present a possible approach how to deal with this size effect in an assessment, however, currently this approach does not yield satisfying results. Consequently, it is not included in the results shown in Figure 3.33 (b) and 3.34 (b). Table 3.19 shows the ratios relative to applicable FAT curves.

The ratios in Table 3.19 show values higher than unity for the three specimen locations in the as-welded specimens and thus the FAT class might be conservative. For the stress-

relieved specimens an assessment with the effective notch stress method and the standardised FAT class may be conservative only for the plate corner with radius $r = 3$ mm. It is unconservative and deemed unconservative, respectively, for the plate edge and the plate surface.

Table 3.19 – Ratios of stress ranges and number of cycles for the $p = 5\%$ S-N curve relative to the FAT curve for as-welded and stress-relieved specimens

Condition	FAT (MPa)	$\Delta\sigma_{en,C,(m=3,p_f=5\%)}/FAT$ [1)]			$N_{en,(m=3,p_f=5\%)}/N_C$ [1)]		
		edge (-)	corner [2)] (-)	surface (-)	edge (-)	corner [2)] (-)	surface (-)
As-welded (AW)	225	≥1.15	≥1.33	**1.10**	≥1.5	≥2.4	**1.3**
Stress-relieved (SR)	270	**0.93**	≥1.08	≥0.89	**0.8**	≥1.2	≥0.7

[1)] $m = 3$ and $N_C = 2 \cdot 10^6$.

[2)] Plate corner radius $r = 3$ mm.

3.4 Hanji et al.

Hanji et al. (2024) [18] performed fatigue tests with specimens composed of a T-bar with a welded attachment, see Figure 3.35. The width of the attachments varied between 80 and 160 mm and plate thickness varied between 6 and 25 mm.
The structural hot spot stress method and a notch stress method, using measured weld toe radii, were used by the authors to assess the plate edges.

3.4.1 Fatigue tests

A structural steel with a static strength of 400 MPa was used for the specimen attachments. The steel grade, or properties of the T-bar are not mentioned in [18]. Figure 3.35 gives the global specimen dimensions and fatigue test set-up. Table 3.20 shows the attachment thicknesses and widths of the specimens tested in this study. The table also shows the mean measured weld dimensions, weld toe properties and plate corner radii.

A stress ratio R= 0.05 and loading frequencies of 1.4 to 6.0 Hz were used. All specimens were tested in the as-welded condition.

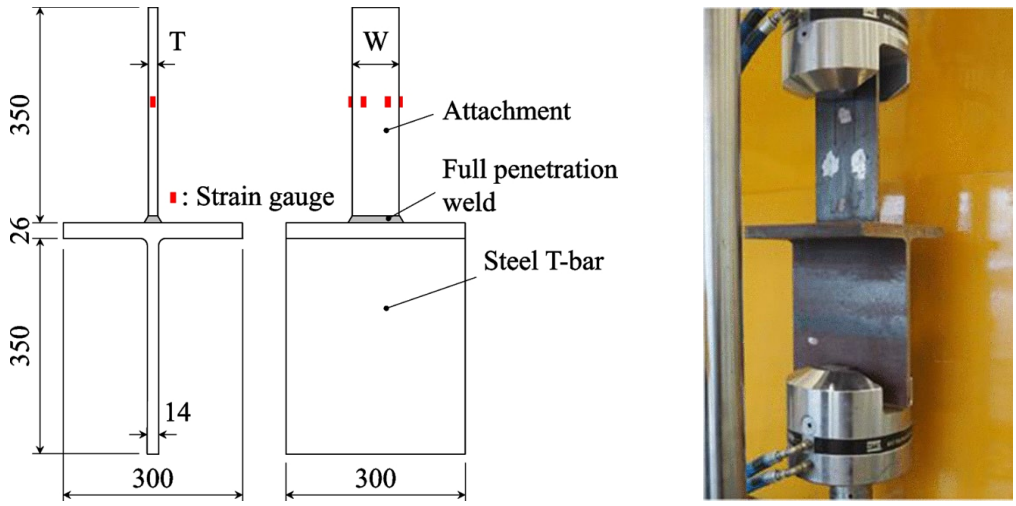

Figure 3.35 – Global specimen dimensions, see also Table 3.20, and fatigue test set-up.

Table 3.20 - Specimen name, attachment dimensions and weld dimensions

Specimen name	Attachment		Weld leg length		Weld toe		Corner
	Width, W (mm)	Thickness, T (mm)	Attachment side (mm)	Steel T-bar side (mm)	radius (mm)	angle (°)	radius (mm)
W80T6	80	6	13.1	8.7	2.4	46.0	0.4
W80T12	80	12	14.8	8.4	1.6	40.3	0.3
W80T25	80	25	17.4	9.4	1.7	36.4	0.4
W120T12	120	12					
W160T6	160	6	11.9	9.2	1.6	41.8	0.4
W160T12	160	12	13.6	9.1	1.6	33.6	0.4

Figure 3.36 summarises all test results. The nominal stress range in the attachment ($\Delta\sigma_n$) and fatigue life (N_f) of the specimens are shown. The "W80T12[9]" specimens refer to tests with similar specimens performed by Saito et al. (2017) [19]. In Section 3.5 these fatigue tests of Saito et al. are further analysed. A single test, represented by an asterisk in the figure, failed at the steel T-bar. The arrows in the figure represent run-outs. For comparison, the FAT 56 to FAT 125 curves with slope $m = 3$ up to $N = 10^7$ cycles are also shown.

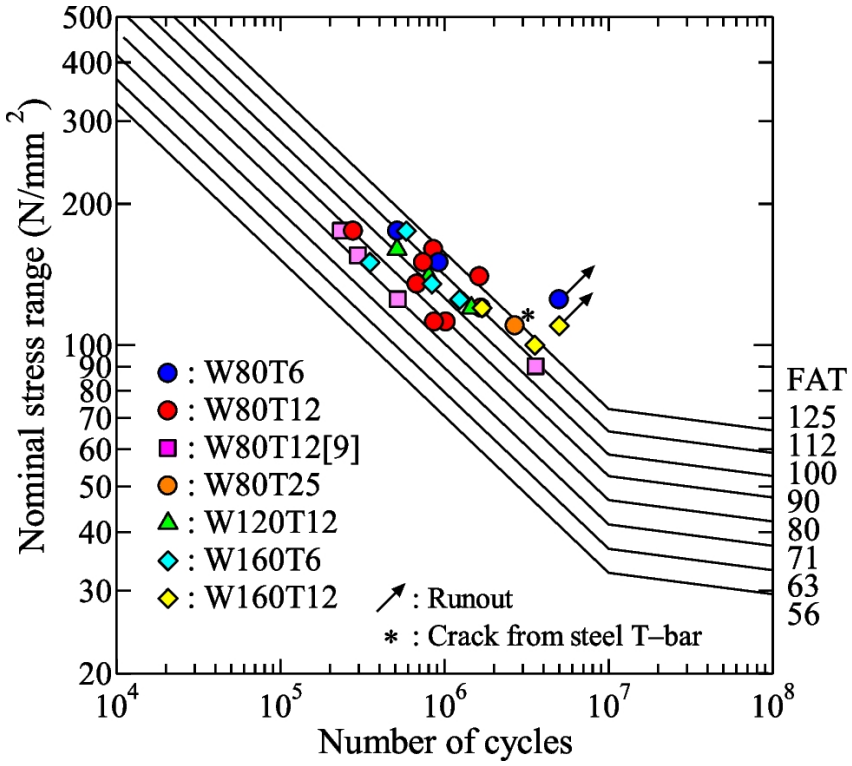

Figure 3.36 - Nominal stress range ($\Delta\sigma_n$) in the attachment and fatigue life (N_f) for all tested specimens. The "W80T12[9]" specimens refer to tests performed by Saito et al. (2017) [19].

Figure 3.37 shows the fracture surface of a specimen with an attachment plate thickness T= 12 mm and width W= 80 mm (W80T12). Crack initiation in this specimen is observed at both corners at one attachment end, see attachment end D in sub-figure (a) and the corner cracks indicated by the red arrows in sub-figure (b).

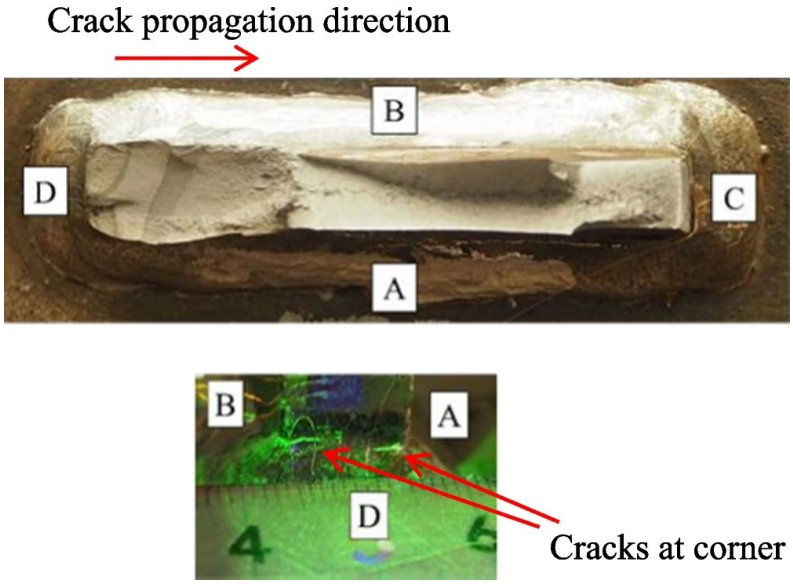

Figure 3.37 – Fracture surface of a specimen with an attachment plate thickness T= 12 mm and width W= 80 mm (W80T12). Initiation by corner cracks at one attachment side.

3.4.2 Assessments

Global and local FE models of the specimens were made to calculate the structural hot spot stresses at the plate corners. Figure 3.38 shows an example of the maximum principal stress distribution obtained by global and local FE models.

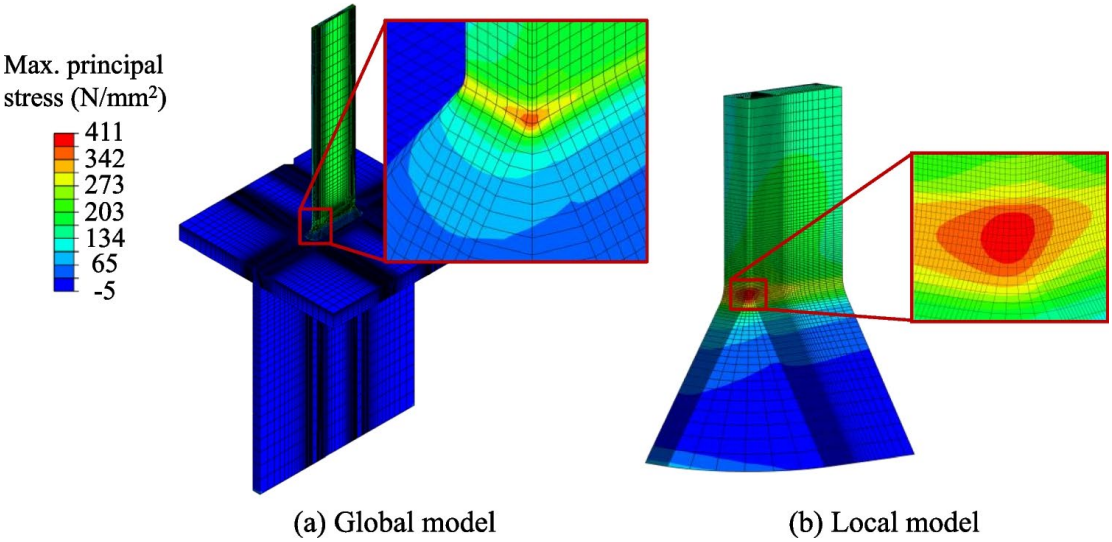

Figure 3.38 – An example of the maximum principal stress distribution obtained by global and local FE models of a specimen.

The plate corner of the attachment was modelled as rounded. The radius was taken as the average of some of the measured radii, see Table 3.20. Measured vales were used for the toe radius and weld flank angle. A slight specimen bending was observed of the attachment based on the strain measurements. Therefore, a small bending moment was applied to the model in addition to the axial load.

These FE analyses show that the highest stress concentration occurs at the weld toe of the attachment corner. This was observed for all specimens, regardless of the attachment width and thickness. This result is consistent with the crack initiation sites observed in the specimens.

3.4.2.1 Hot spot stress method

The highest stress ranges were identified on the cracked plate end of the attachment. The hot spot stresses were calculated by extrapolation along two paths:

1. centre of the plate thickness,
2. plate corner.

These stresses were calculated using the distances 4, 8, and 12 mm away from the weld toe (Type “b”) given in IIW [4].

Figure 3.39 (a-d) gives the hot spot SCF’s (K_s) as a function of attachment plate width and thickness for the specimen dimensions of Table 3.20. Sub-figures (a) and (b) show the results for the centre of the plate thickness, and (c) and (d) for the plate corner. The figures show that the hot spot stress at the plate corner is slightly higher than that at the centre of the plate. Further, the hot spot stresses increase with increasing attachment thickness and width.

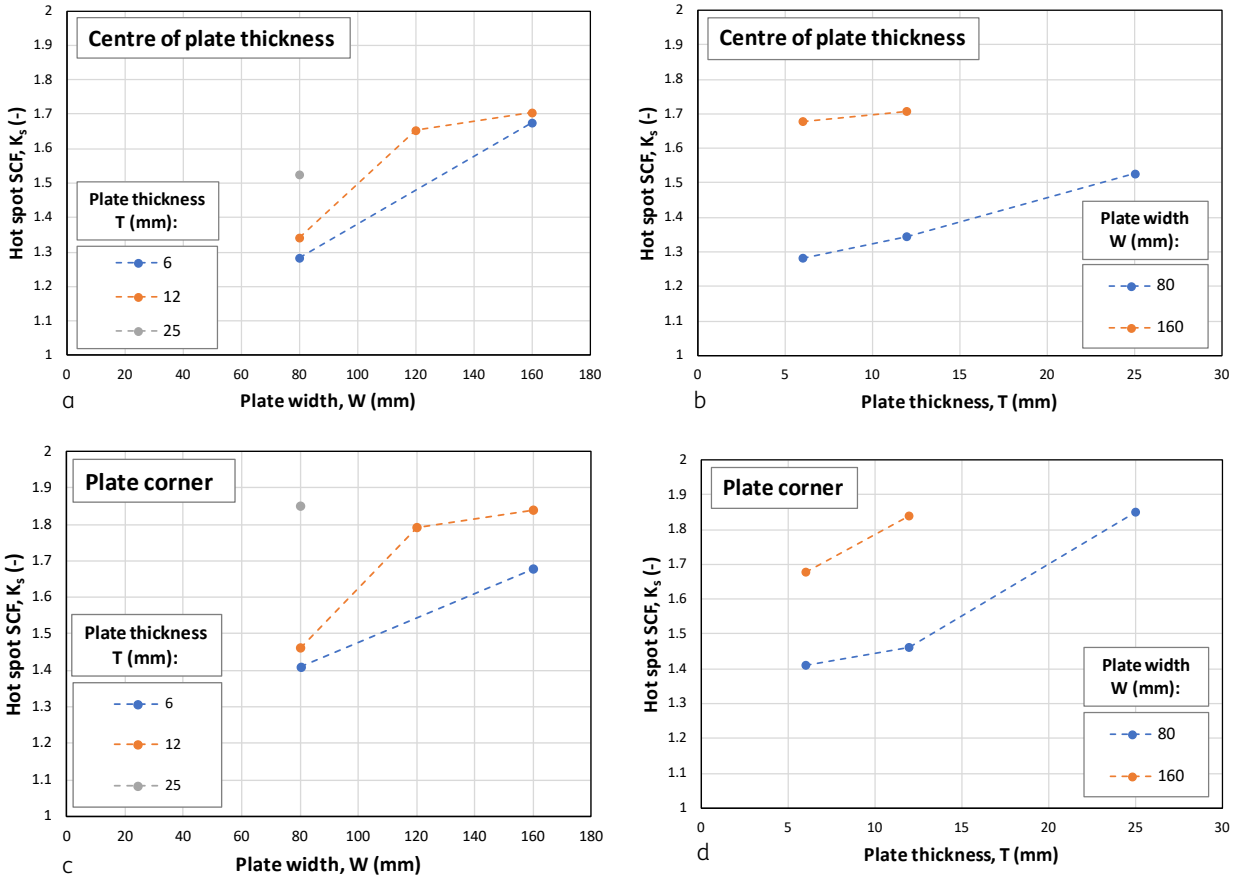

Figure 3.39a to d – Hot spot SCF’s (K_s) as a function of attachment plate width and thickness: (a) & (b) for the centre of the plate; (c) & (d) for the plate corner.

Figures 3.40 shows the hot spot stress ranges for the centre of the plate thickness (sub-figure a) and the plate corner (sub-figure b) versus fatigue life for all tested specimens. As, according to the authors, the cracks initiated at the corners, see Figure 3.37, sub-figure a shows for the centre of the plate thickness run-outs, and in sub-figure b for the plate corner failures. The $\Delta\sigma_{hs,C,(m=3,p=5\%)}$ S-N curve based on all tests and the FAT 100 curve are given.

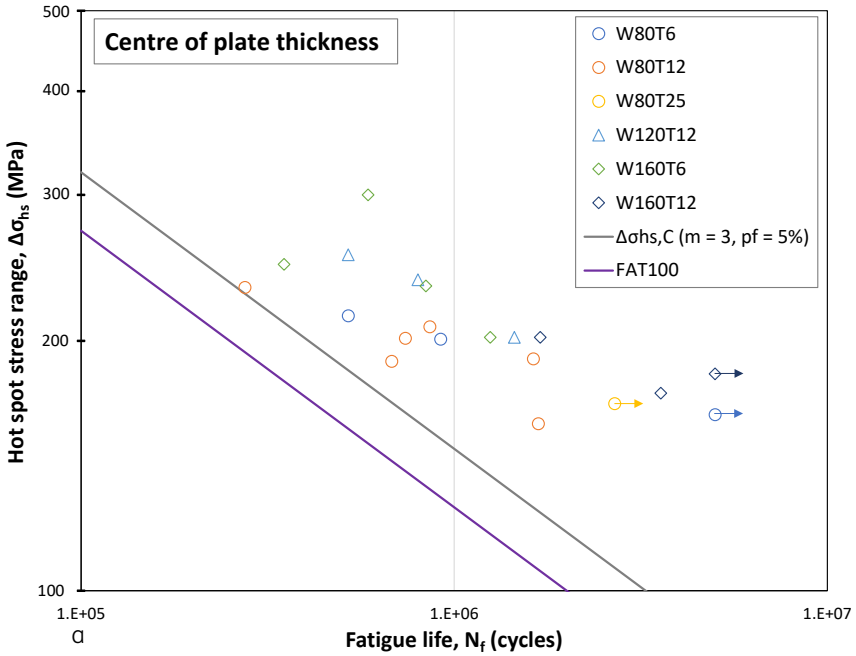

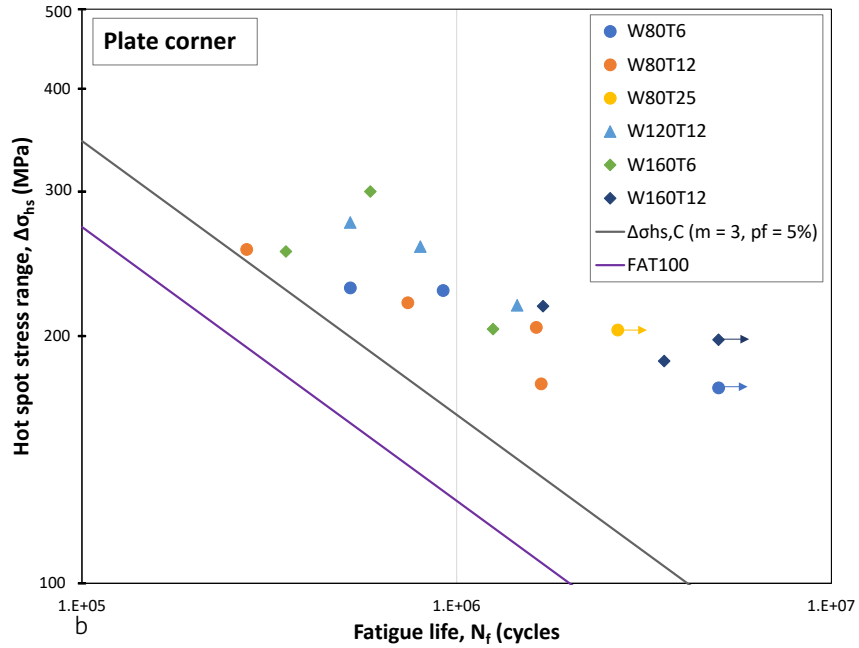

Figures 3.40a/b – Hot spot stress ranges for the centre of the plate (a) and the plate corner (b) as a function of fatigue life. The S-N curve of all tests ($m = 3$ & $p_f = 5\%$) and the FAT100 line are indicated.

Table 3.21 gives the ratios between $\Delta\sigma_{hs,C,(m=3,p=5\%)}$ and the FAT 100 class. These ratios reflect the results shown in the Figures 3.40a/b.

Table 3.21 – Ratios of stress ranges and number of cycles for the S-N curve relative to the FAT curve for all as-welded specimens

Condition	FAT (MPa)	$\Delta\sigma_{hs,C,(m=3,p_f=5\%)}/FAT$ [1)]		$N_{hs,(m=3,p_f=5\%)}/N_C$ [1)]	
		Centre of plate thickness (-)	Plate corner (-)	Centre of plate thickness (-)	Plate corner (-)
As-welded (AW)	100	≥1.18	1.27	≥1.63	2.06

1) - m = 3 and N_C = 2 x 10^6 cycles.

The ratios in Table 3.21 are higher than unity for both locations, centre of plate thickness and plate corner.

3.4.2.2 Notch stress method

The notch stress evaluation performed in [18] differs from the effective notch stress method because the real measured weld toe radius has been used, see measured values in Table 3.20, instead of the standardized effective radius of 1 mm, see Hobbacher [3] and Fricke [5]. The maximum principal stress at the weld toe was used as the notch stress. As shown in Figure 3.38 these maximum stresses were found on the plate corner. Figure 3.41 shows the notch SCF's (K_{ns}) at the plate corner as a function of attachment plate width and thickness.

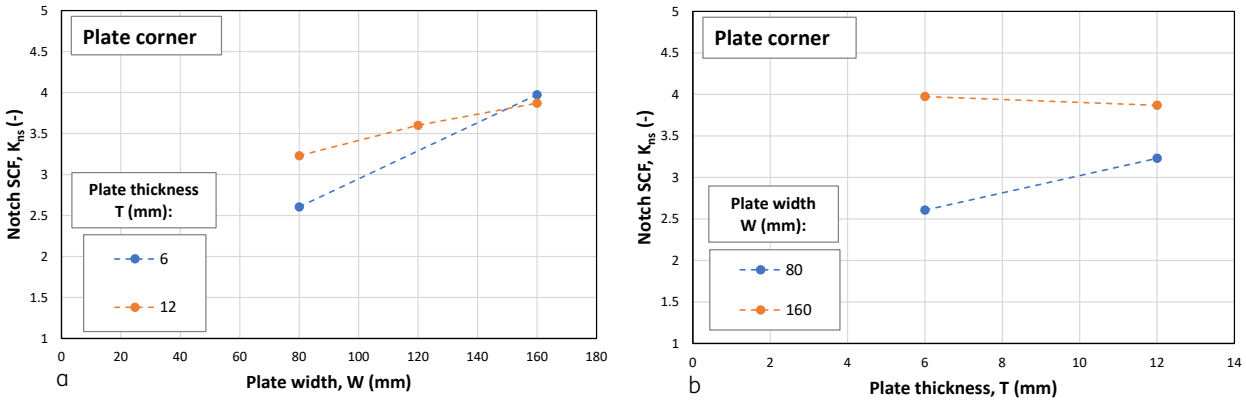

Figure 3.41a/b – The notch SCF's (K_{ns}) at the plate corner as a function of attachment plate width (a) and thickness (b).

Figure 3.42 shows the notch stress ranges based on measured weld toe radius for the plate corner versus the fatigue life of all tests. The $\Delta\sigma_{ns,C,(m=3,p=5\%)}$ S-N curve is also indicated. For reference, the FAT 225 curve is also given, although this curve should not be compared to the data because of the different notch radius for which it is calibrated.

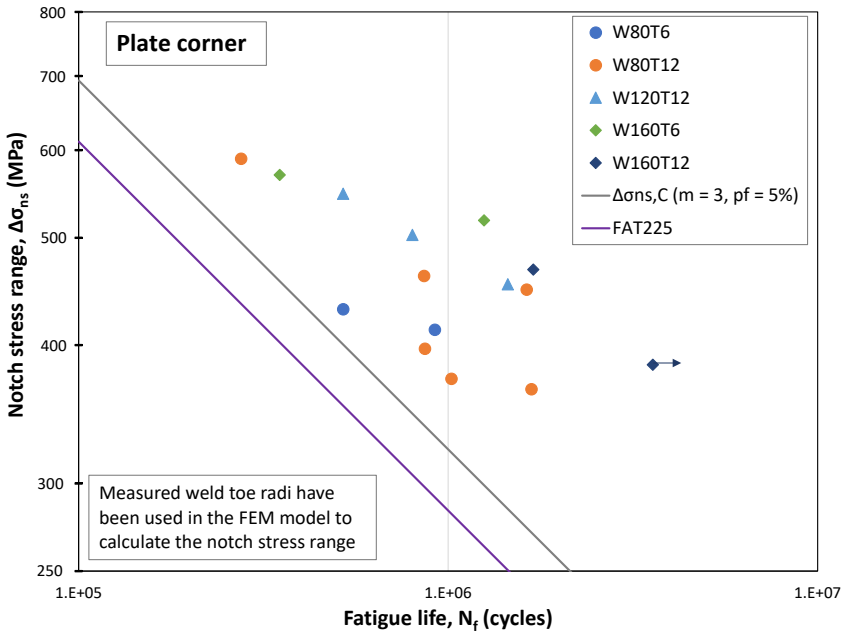

Figure 3.42 – Notch stress ranges (based on measured weld toe dimensions) for the plate corner versus fatigue life. The S-N curve of all tests $\Delta\sigma_{ns,C,(m=3,p_f=5\%)}$ and the FAT 225 curve are indicated.

Table 3.22 shows the ratio between notch stress resistance $\Delta\sigma_{ns,C,(m=3,p_f=5\%)}$ and FAT 225 class. Again, values are given for reference only, because of the different notch radii.

Table 3.22 – Ratios of stress ranges and number of cycles for the S-N curve relative to the FAT curve for the notch stresses at the plate corner

Condition	FAT (MPa)	$\Delta\sigma_{ns,C,(m=3,p_f=5\%)}/FAT$[1)] Plate corner (-)	$N_{ns,(m=3,p_f=5\%)}/N_C$[1)] Plate corner (-)
As-welded (AW)	225	1.14	1.46

[1)] $m = 3$ and $N_C = 2 \times 10^6$ cycles.

In this applied notch stress evaluation method measured weld toe radii of 1.6 to 2.4 mm were used. Although the results in Table 3.22 are larger than 1, it is unsure that the effective notch stress method with the application of a radius of 1 mm will also result in a conservative assessment method.

3.5 Saito et al.

Saito et al. [19] performed fatigue tests on cruciform specimens with full penetration welds, see Figure 3.43. An assessment using the hot spot stress method was applied. The applied steel grade was: SM490YA, with a yield stress, $R_e = 417$ MPa, a tensile strength, $R_m = 551$ MPa, and an elongation after fracture $A_5 = 22\%$. For the welds, a low temperature transformation welding material was applied. Weld properties: weld toe radius, $\rho = 1.14$ mm and a weld angle, $\theta = 140$ °. The side leg lengths were: attachment plate side, $L_1 = 14$ mm, main plate (middle plate) side, $L_2 = 13$ mm.

3.5.1 Fatigue tests

The fatigue tests were performed with a stress ratio $R = 0$. All specimens were in the as-welded condition. Figure 3.44 shows the nominal stress range in the attachment plate (1) as

versus fatigue life. The mean and 5% prediction bound S-N curves are also shown. Table 3.23 gives the fatigue resistance based on the nominal stress range.

Figure 3.45 shows a fracture surface of an as-welded specimen. Saito et al. observed crack initiation in all specimens at one of the attachment corners in plate (1), see Figure 3.43.

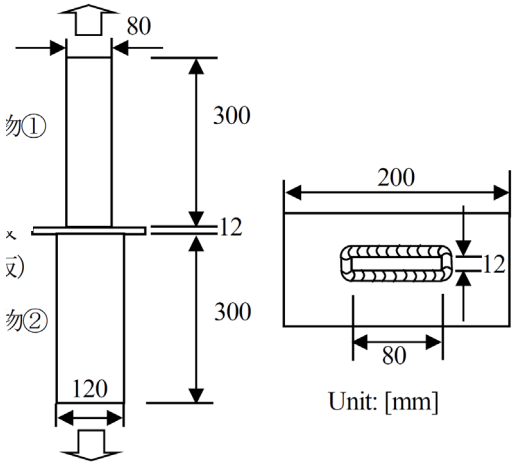

Figure 3.43 - Dimensions and geometries of the cruciform specimens with full penetration welds.

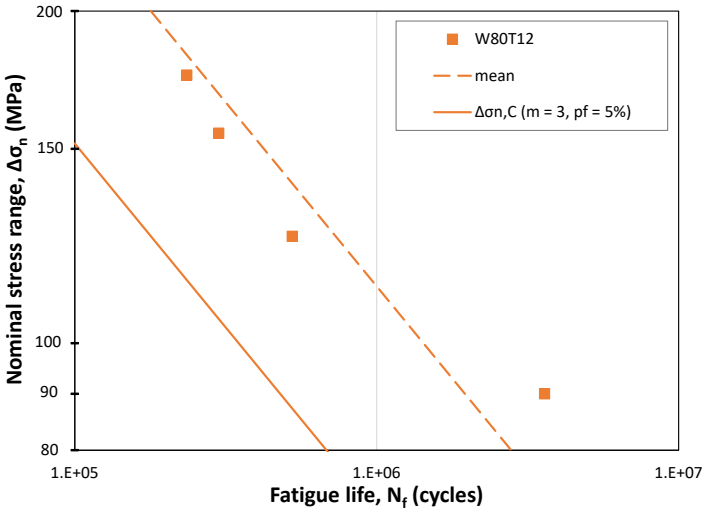

Figure 3.44 – Nominal stress range in the smallest attachment plate as a function of fatigue life.

Table 3.23 – Fatigue properties based on nominal stress in smallest attachment plate

Specimen name	W (mm)	T (mm)	$\Delta\sigma_{n,C}$ $(m=3)$ *mean* (MPa)	$p=5\%$ (MPa)
W80T12	80	12	89.4	55.9

W = 80 mm
T = 12 mm

Figure 3.45 – Fracture surface of an as-welded specimen, stress range 90 MPa, fatigue life 3.62 x 10^6 cycles.

3.5.2 Assessment

The hot spot stress calculations for the specimens tested by Saito et al. [19] have been performed by Hanji et al. [18] using Type "b". The SCF at the centre and corner of the plate are K_s = 1.63 and K_s = 1.80, respectively. Table 3.24 gives $\Delta\sigma_{hs,C\ (m=3,p=5\%)}$ for both locations.

Table 3.24 – Hot spot stress S-N curves ($m=3, p_f=5\%$) for the centre of plate thickness and plate corner

Condition	Nominal $\Delta\sigma_{n,C\ (m=3,p_f=5\%)}$ (MPa)	$\Delta\sigma_{hs,C\ (m=3,p_f=5\%)}$ [1)] Centre of thickness (MPa)	Corner (MPa)	Hot spot stress method FAT (MPa)
As-welded (AW)	55.9	≥90.9	**100.8**	100

[1)] – The value in bold is the location where the first crack initiations were observed.

Figure 3.46 shows the hot spot stress ranges calculated by Hanji et al. for the plate corner as a function of fatigue life determined by Saito et al, as well as the $\Delta\sigma_{hs,C,(m=3,p=5\%)}$ S-N curve and the FAT 100 curve. Table 3.25 gives the ratio between the hot spot stress resistance and FAT 100 for both locations.

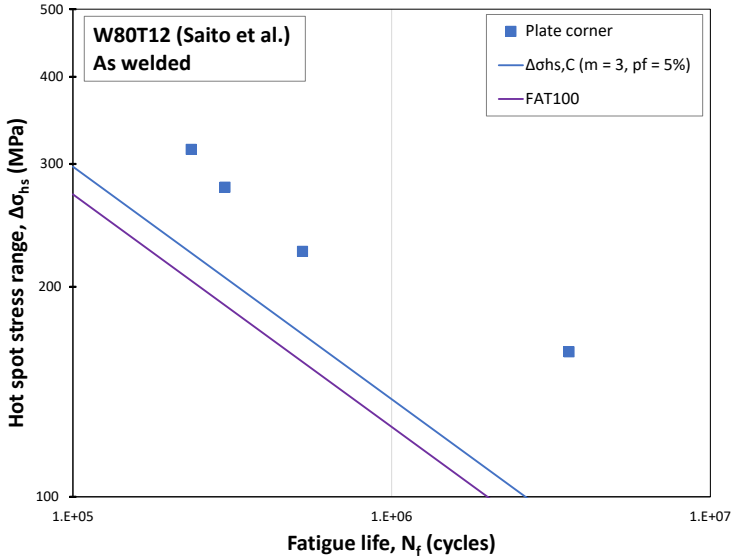

Figure 3.46 - Hot spot stress ranges for the plate corner as a function of fatigue life. The S-N curves for $\Delta\sigma_{hs,C,(m=3,p_f=5\%)}$ and the FAT100 line are indicated.

Table 3.25 – Ratios of stress ranges and number of cycles for the S-N curves relative to the FAT curve

Condition	FAT (MPa)	$\Delta\sigma_{ns,C,(m=3,p_f=5\%)}/FAT$[1]		$N_{ns,(m=3,p_f=5\%)}/N_C$[1]	
		Centre of thickness (-)	Plate corner (-)	Centre of thickness (-)	Plate corner (-)
As-welded (AW)	100	≥0.91	1.01	≥0.75	1.02

[1] $m = 3$ and $N_C = 2 \cdot 10^6$.

The ratios in Table 3.25 are for the centre of plate thickness somewhat below unity and for the plate corner a slightly larger than unity.

3.6 Shingai & Petershagen

3.6.1 Specimens & Fatigue tests

Shingai & Imamura [21] performed tests with cruciform joints. Figure 3.47 gives the specimen geometry and load direction. Note that a combined axial and bending load result at the location of stress concentration. The tests were aimed at representing the connection between the bottom longitudinal and web frame stiffeners of a tanker. Mild steel was used. Two fillet weld throat sizes were tested, a = 4.5 mm and a = 11.3 mm, see Table 3.26. The specimens were tested in as-welded condition. Petershagen [20] evaluated these tests. Based on the load line and the location of the net section area of the specimen in Figure 3.47, the ratio of maximum nominal bending stress and the maximum nominal axial tensile stress is 1.8 [20].

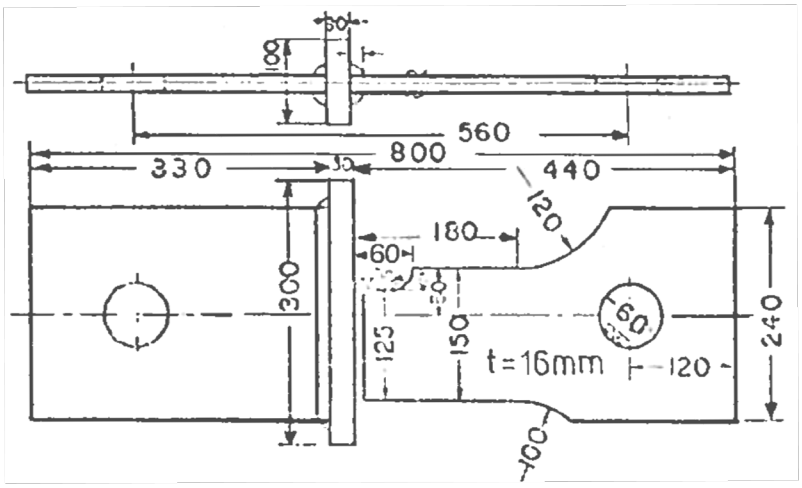

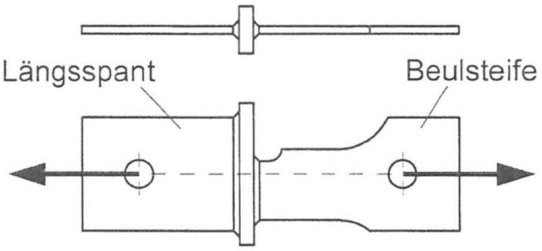

Figure 3.47 - Dimensions and geometries of the cruciform specimen with fillet welds, a) geometry, b) specimen loading.

Table 3.26 – Weld leg size (H) and throat size (a) of both specimens

Specimen code	H/t[1] (-)	H (mm)	a (mm)
S0.4	0.4	6.4	4.5
S1.0	1.0	16.0	11.3

[1] Plate thickness, t = 16 mm

The fatigue tests were performed with a stress ratio, R = 0. Figure 3.48 shows the nominal stress range (axial + bending stress) as a function of fatigue life (mean lines) for both fillet weld sizes. Individual data are not reported. Table 3.27 shows the values of the mean S-N

curves. Both reciprocal slopes of the fitted S-N curves are substantially higher than $m = 3$. This likely implies that these specimens, in addition to the crack propagation life, have a substantial crack initiation life.

Table 3.27 – Mean S-N curves for both fillet weld sizes. Source: Petershagen [20]

Specimen code	Throat size a (mm)	$\Delta\sigma_n$[1)] (MPa)	m[2)] (-)	Crack initiation & failure
S0.4	4.5	80	4.3	Weld root
S1.0	11.3	170	5.6	Weld toe

[1)] – at $N = 2$ million cycles,
[2)] – Reciprocal slope of S-N curve.

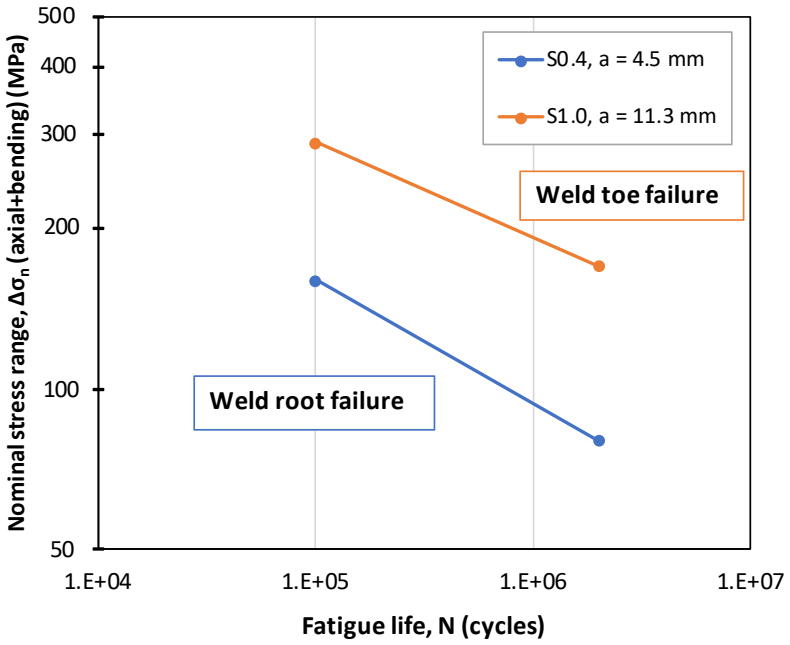

Figure 3.48 - Nominal stress ranges (axial + bending stress) as a function of fatigue life (mean lines) for both fillet weld sizes.

3.6.2 Assessment

structural stress method such as the hot spot or effective notch stress method are not reported in the original sources. Petershagen [20] evaluated the fatigue life of specimen type S1.0, which shows crack initiation at the weld toe, by fatigue crack growth simulations using stress intensity factors from FE simulation and integration of the Paris equation. Figure 3.49 shows the stress intensity factor SIF (K) for a through thickness crack as a function of crack length.

Although using a through thickness crack is conservative, Petershagen reported to have found a “reasonable agreement” between the test and simulation results. However, quantification of this agreement is not given.

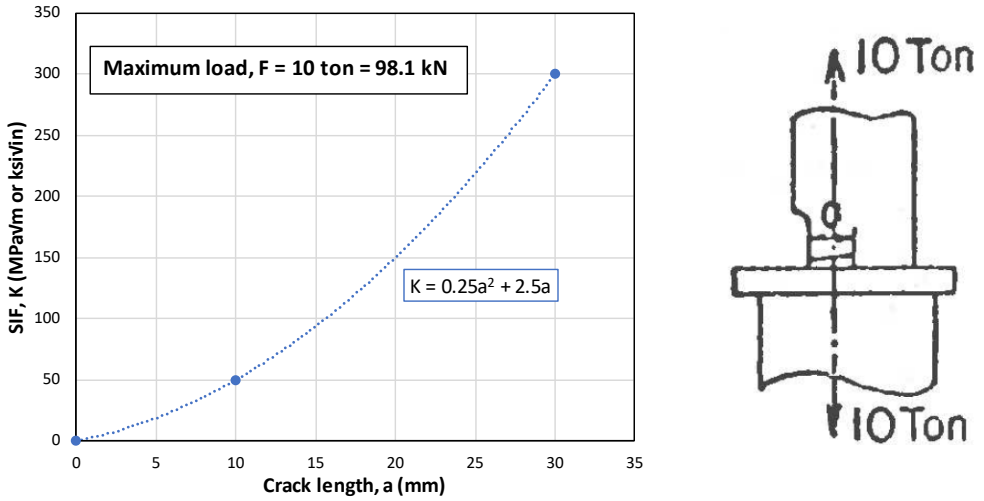

Figure 3.49 - SIF (K) as a function of crack length [20].

3.7 Eylmann & Paetzold

Eylmann & Paetzold [22] designed a three-point bending fatigue specimen with fillet welds around attachment ends, see Figure 3.50. Loading of the specimen results in bending stresses and shear stresses in the fillet welds around the attachments and at the attachment ends. Fatigue tests have been performed with throat sizes a = 4 and 6 mm and radii of R = 50 and 100 mm, see designation "R50" in Figure 3.50.

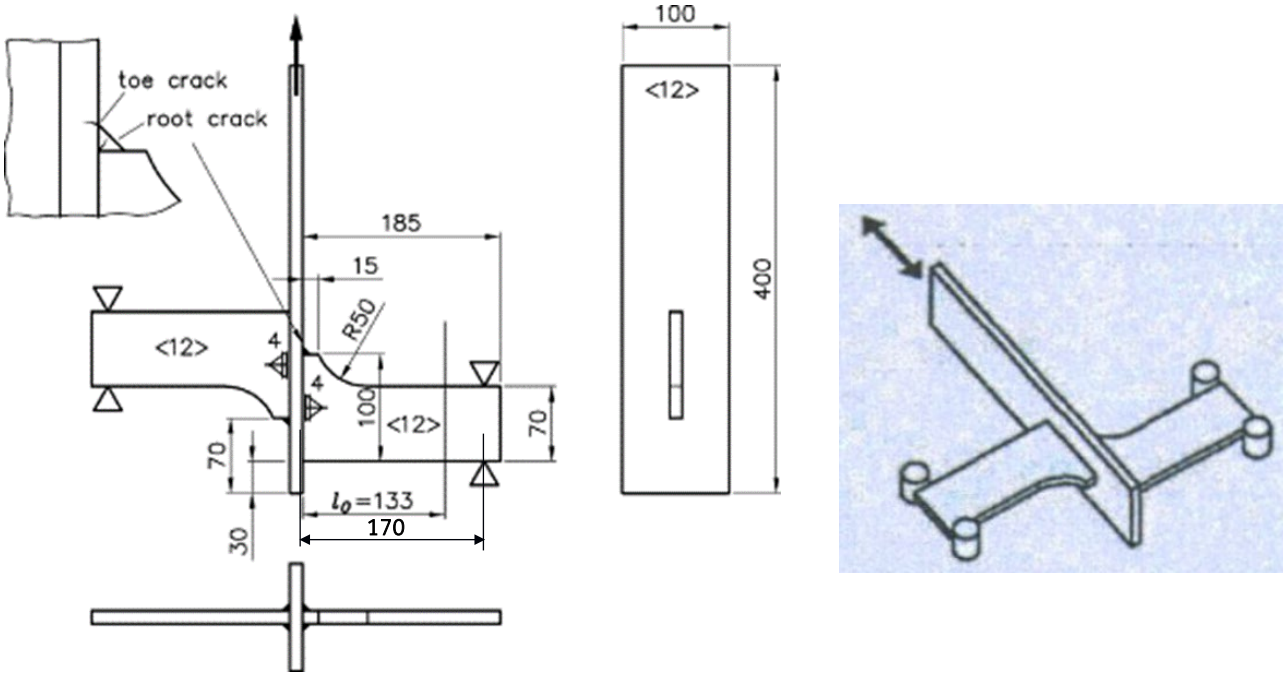

Figure 3.50 – Specimens used by Eylmann & Paetzold [22]. Fillet welds with throat sizes a = 4 and 6 mm and radii of 50 and 100 mm have been tested. Crack locations are indicated in inset.

Steel grade, mechanical properties and used welding specifications are not mentioned in reference [22]. However, the used plate thickness, weld throat sizes and period of production seem to agree with the specimens described in Section 3.1, as given by Doerk & Fricke [9],[12].

3.7.1 Fatigue test results

Table 3.28 gives the number of performed fatigue tests for each specimen geometry, condition, and applied stress ratio. The last column gives the number of specimens where failure initiated from the weld toe.

Table 3.28 – Number of performed fatigue tests and number of specimens showing weld toe failure for each specimen geometry, condition and applied stress ratio

Specimen model	Weld throat a (mm)	Plate radius r_p (mm)	Condition	Stress ratio R (-)	Number of Tests	Number of specimens with weld toe failure
A	4	50	As-welded	0	22	7
				0.5	8	0
			Stress-relieved	0	9	1
B	6	50	As-welded	0	13	6
				0.5	12	1
C	4	100	As-welded	0	10	5
D	6	100	As-welded	0	9	9

The fatigue test conditions are:

- Apparatus: resonance pulsating machine.
- Constant amplitude loading.
- Frequency, f = 30 Hz.
- Environment: in air.
- Stress ratio, $R \approx 0$ and 0.5.
- Test termination: after crack length reached several centimetres.

Figure 3.51 (a-d) gives the nominal stress range in the plate ($\Delta\sigma_{n,p}$) versus number of cycles to failure (N_f) for specimens A, B, C and D, respectively. For specimen model A the stress-relieved specimen is also shown.

The intention of these figures is to determine fatigue life and the S-N curve of the weld toe on the vertical plate at the attachment end. As in this test program most specimens failed by a root crack at the attachment end, especially for the throat size $a = 4$ mm, these tests are designated as “run outs” for the weld toe. These “run outs” are indicated with open symbols in Figure 3.51 (only the relevant data are shown). The $\Delta\sigma_{n,p,C,(m=3,p=5\%)}$ S-N curves for the as-welded condition are also added to the figures. The results of the specimens A and B are added to sub-figures (c) and (d) for comparison. Table 3.29 shows the $\Delta\sigma_{n,p,C,(m=3,p_f=5\%)}$ values at N_C = 2 x 10^6 cycles for each specimen model and condition.

Figure 3.51 (a) and (b) show only a small difference in mean $\Delta\sigma_{n,p,C,}$ between the weld throat sizes a = 4 mm and a = 6 mm. However, the specimens with a throat size of 4 mm show a larger standard deviation resulting in a lower resistance $\Delta\sigma_{n,p,C,(m=3,p=5\%)}$. Modifying the attachment radius from R_p = 50 mm (models A and B) to R_p = 100 mm (models C and D) slightly increases the fatigue life for both throat sizes, see Figure 3.51(c) and (d).

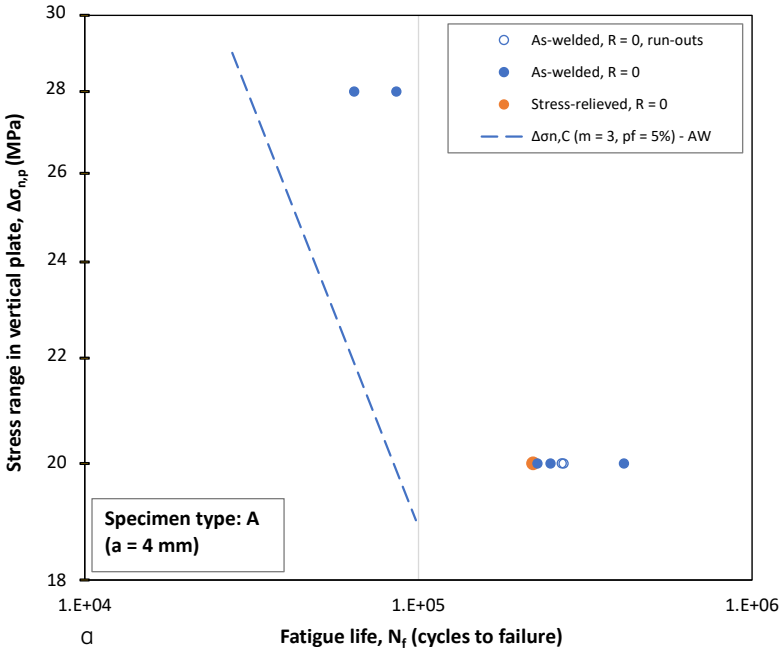
30
28
26
24
22
20
18
1.E+04
1.E+05
1.E+06
Stress range in vertical plate, Δσn,p (MPa)
Fatigue life, Nf (cycles to failure)
As-welded, R = 0, run-outs
As-welded, R = 0
Stress-relieved, R = 0
Δσn,C (m = 3, pf = 5%) - AW
Specimen type: A
(a = 4 mm)

a

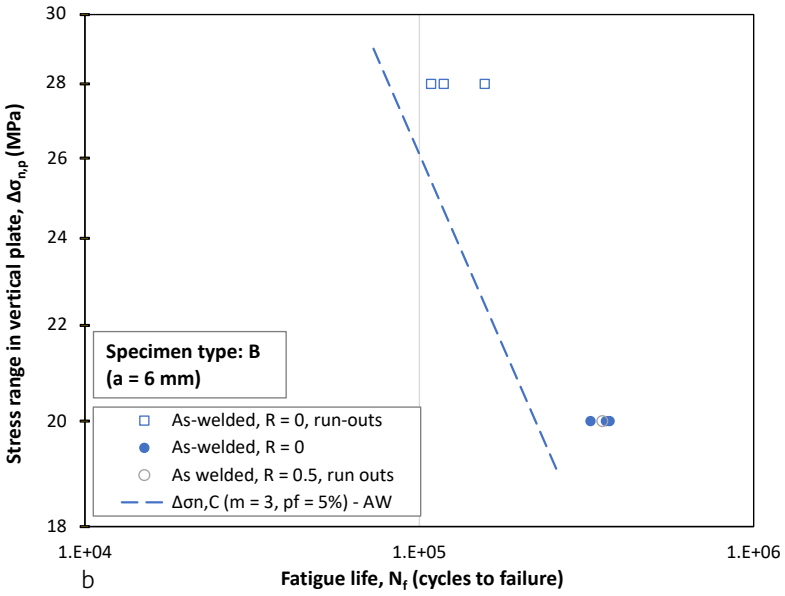
30
28
26
24
22
20
18
1.E+04
1.E+05
1.E+06
Stress range in vertical plate, Δσn,p (MPa)
Fatigue life, Nf (cycles to failure)
Specimen type: B
(a = 6 mm)
As-welded, R = 0, run-outs
As-welded, R = 0
As welded, R = 0.5, run outs
Δσn,C (m = 3, pf = 5%) - AW

b

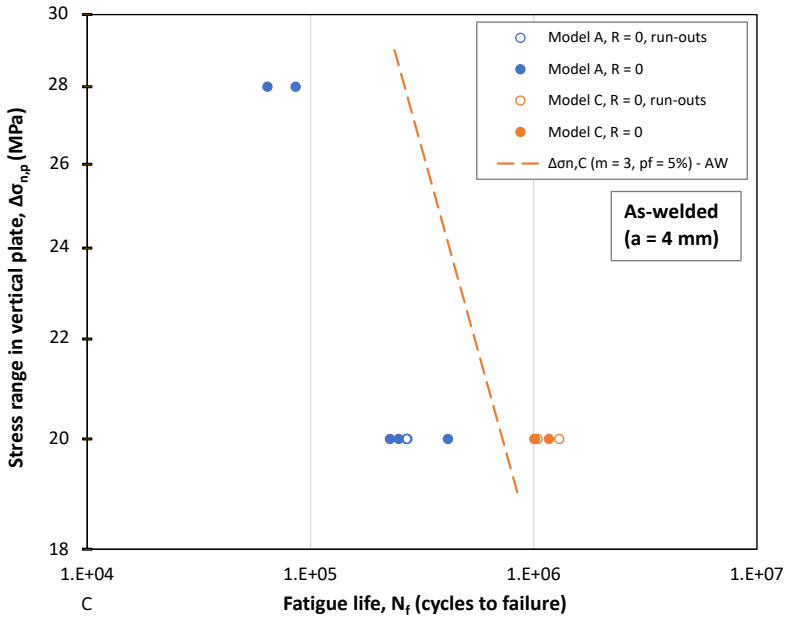

c

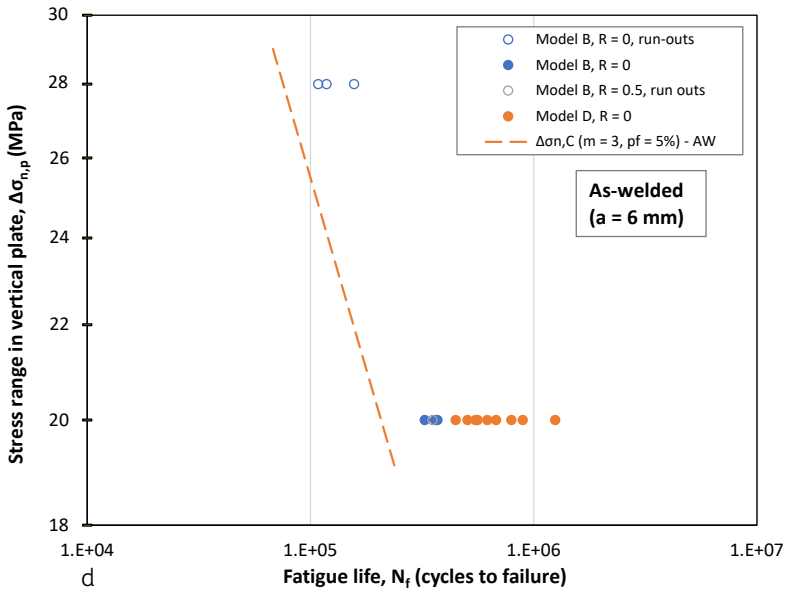

d

Figure 3.51a to d – Nominal stress range in the plate ($\Delta\sigma_{n,p}$) versus number of cycles to failure (N_f) for specimen models A, B, C and D (subfigures (a-d). Each figure shows the $\Delta\sigma_{n,p,C,(m=3,p_f=5\%)}$ S-N curve.

Table 3.29 – The nominal stress range in the vertical plate (using $m = 3, p_f = 5\%$) at 2 million cycles for each specimen geometry and condition

Specimen model	Weld throat a (mm)	Plate radius r_p (mm)	Condition	Stress ratio R (-)	$\Delta\sigma_{n,p,C,(m=3,p_f=5\%)}$ [1)] (MPa)
A	4	50	As-welded	0, 0.5	7.0
B	6	50	As-welded	0, 0.5	9.6
C	4	100	As-welded	0	14.3
D	6	100	As-welded	0	9.4

[1)] - Reciprocal slope m = 3 and N_C = 2 x 10^6 cycles.

Eylmann & Paetzold [22] reported that in their fatigue tests weld failures predominantly occurred, i.e., the cracks formed at the root of the fillet weld and grew from the inside outwards. If the test was run long enough, a crack appears as in Figure 3.52. Figure 3.53 shows cross sections on the symmetry plane of the weld toe. A typical weld root crack is visible in specimen A, as well as additional cracks at the two weld toes in the shown specimens B and D. It is clearly visible that both failure modes, namely weld toe cracking and weld root cracking, occurred in the specimens B and D, which both have a larger weld throat height of a = 6 mm. Figure 3.53 also shows some different fillet weld shapes. With the increase in weld throat height from a = 4 to 6 mm, the weld shapes tend toward the S-shape shown. These weld shape differences were not captured by the structural hot spot stress concept. In the FE models the ideal shape has been assumed.

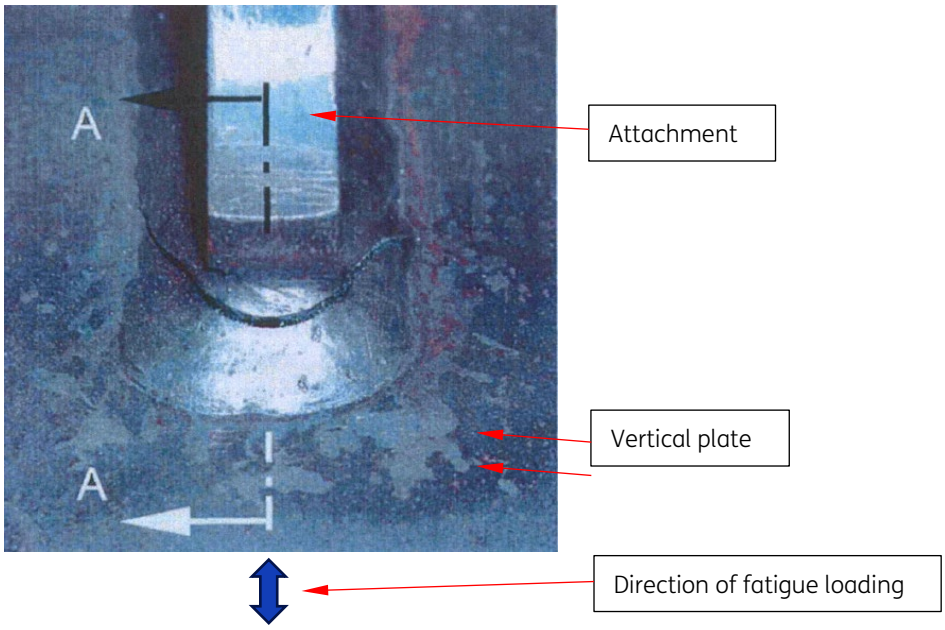

Figure 3.52 – Weld fractures predominantly occurred by crack initiation at the root of the fillet weld and grew from the inside outward.

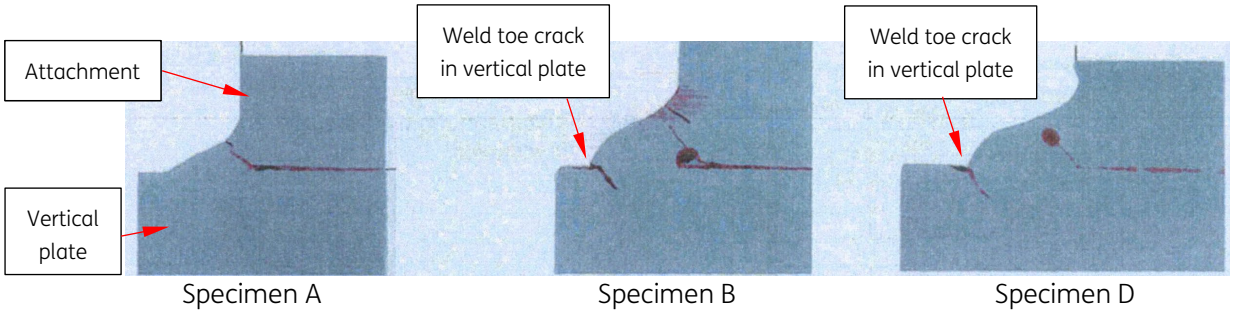

Figure 3.53 – Cross sections on the symmetry plane of the weld toe. A typical internal crack is visible in specimen A, as well as additional cracks at the two weld toes (specimens B and D).

3.7.2 Assessments

3.7.2.1 Stress analysis

Structural hot spot stresses at the weld toe on the vertical plate have been calculated using the FE method. The analyses were performed with a relatively coarse mesh, using one element over the plate thickness of 12 mm, see Figure 3.54. For these analyses, a nominal stress in the vertical plate of σ_n = 41.7 MPa (specimen load of 50 kN) was used. The FE model in Figure 3.54(a) shows the first principal stress and deformed state of the whole specimen, and Figure 3.54(b) shows a detail of the model with the first principal stress in and around the attachment end.

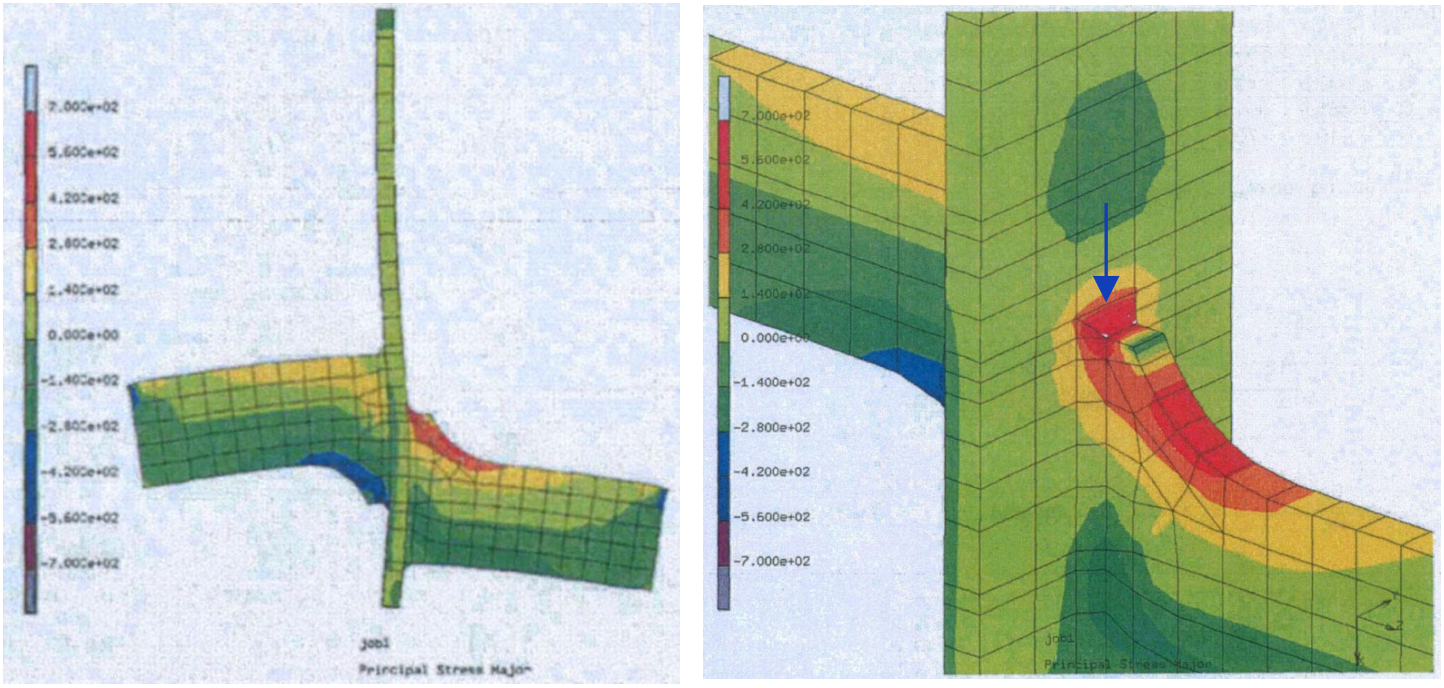

Figure 3.54 - FE analysis results with first principal stresses and deformed state under a tensile loading of 41.7 MPa in the vertical plate: (a) whole specimen, b) detail showing the weld around the plate end. The blue arrow indicates the direction of the hot spot extrapolation path Type “a” applied by Eylmann & Paetzold [22].

3.7.2.2 Hot spot stress method

The Eylmann & Paetzold [22] applied extrapolation path Type “a” to calculate the hot spot stresses at the weld toe. The blue arrow in Figure 3.54(b) indicates the direction of the hot spot extrapolation path. Table 3.30 shows the results of these hot spot stress extrapolations.

Table 3.30 - Results of the hot spot stress calculations for the weld toe. The used extrapolation path is indicated in Figure 3.54b. The nominal stress in the vertical plate σ_n = 41.7 MPa

Specimen model	Weld throat a (mm)	Plate radius r_p (mm)	Stress (MPa) $1.5t$	$0.5t$	σ_{hs}	K_s
A	4	50	46.9	192.2	265	6.4
B	6	50	46.1	164.4	224	5.4
C	4	100	46.4	176.1	241	5.8
D	6	100	46.4	151.9	205	4.9

The hot spot stress ranges were calculated for each specimen model geometry with these structural hot spot stress concentration factors (K_s). Figure 3.55 shows these hot spot stress ranges at the weld toe ($\Delta\sigma_{hs}$) versus number of cycles to failure (N_f) for all as-welded specimens, i.e. models A, B, C and D. (Only the as-welded specimens with failure at the weld toe in the vertical loaded plate are shown in Figure 3.55.) The $\Delta\sigma_{hs,C,(m=3,p_f=5\%)}$ S-N curve for all specimen models and the FAT90[2] line are indicated.

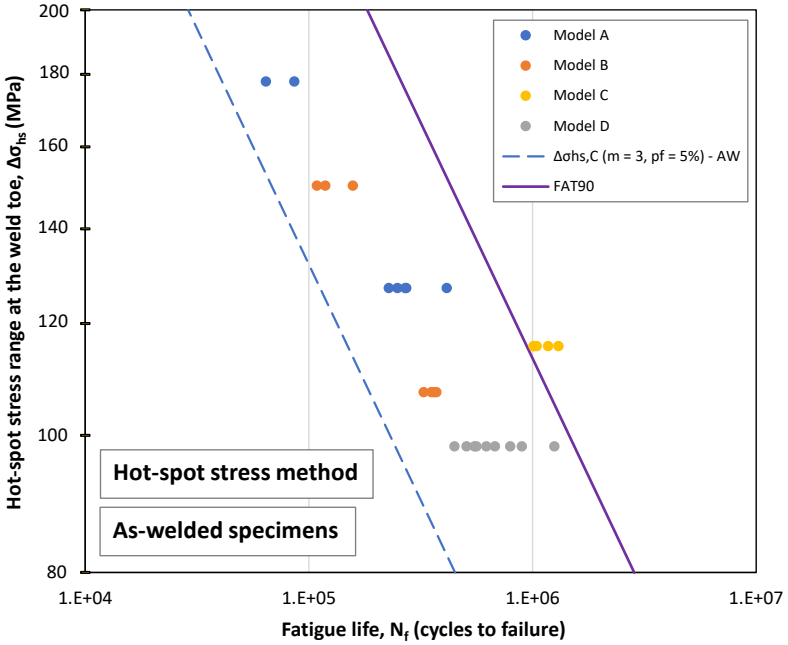

Figure 3.55 – The hot spot stress ranges at the weld toe ($\Delta\sigma_{hs}$) versus number of cycles to failure (N_f) for the weld toe, and the "run-outs", for the as-welded specimens, types A, B, C and D. The $\Delta\sigma_{hs,C,(m=3,p_f=5\%)}$ S-N curve and the FAT90 line are indicated.

Figure 3.55 shows that all test results with weld toe failure for the specimens A, B and D are substantially below the FAT 90 curve. Only specimens of type C (a = 4 mm, radius R_p = 100 mm) show a fatigue life all just above the FAT90 curve.

These tests were designed with a distance of 170 mm from the vertical plate to the roller supports at the attachment ends, see Figure 3.50. The FE analyses were performed assuming the this distance. However, due to "clamping issues", see explanation in Eylmann & Paetzold [22], the real support distances are argued to be about 133 mm, see "$l_0 = 133$" in Figure 3.50. For this reason, Doerk & Fricke [9] used a correction factor for the local stresses in the weld of 133/170. They seem to assume that this change has no influence on the stress distributions in the vertical plate as they did not apply a correction for the calculated hot spot stresses as given in Table 3.30.

The stress and cycle ratios between the two S-N curves in Figure 3.55 are given in Table 3.31.

[2] In reference [9] Fricke & Doerk used for the same specimen with fillet welds FAT100 for the weld toe. FAT90 is used in the current report, in agreement with Table 2.1.

Table 3.31 – Ratios of stress ranges and number of cycles for the S-N curve relative to the FAT curve

Condition	FAT (MPa)	$\Delta\sigma_{hs,C,(m=3,p_f=5\%)}/FAT$ [1)] (-)	$N_{hs,(m=3,p_f=5\%)}/N_C$ [1)] (-)
As-welded (AW)	90	0.54	0.16

1) - $m = 3$ and $N_C = 2 \times 10^6$ cycles.

The substantially lower value of $\Delta\sigma_{hs,C,(m=3,p=5\%)}$ than the FAT 90 class is astonishing. The current results suggest that application of the hot spot stress method (Type “a”) for the assessment of weld toes in loaded attachments can be very unconservative.

With regard to the results for these specimens of Eylmann & Paetzold [22], a good explanation seems to be that the crack at the weld root, which normally initiates first, accelerated the crack initiation and crack growth at the weld toe in the vertical plate, causing this weld toe to have a low fatigue life. A possible explanation for this phenomenon is that the crack at the weld root reduces the net section in the weld and results in a stress concentration increase at the weld toe in the vertical plate.

3.8 Summary

The obtained S-N curves relative to the FAT curves, as derived in the previous sub-sections for the different fatigue datasets, are summarized in two tables. Table 3.32 shows all relevant data assessed with the hot spot stress Type “a” and Type “b” (Type “a” when the used stress locations depend on the plate thickness and Type “b” when the used stress locations are plate thickness independent). Note that the tests of Doerk and Fricke are analysed with multiple extrapolation paths and by two institutions (University of Hamburg and TNO). Table 3.33 gives a summary of all relevant datasets assessed with the effective notch stress method.

Table 3.32 (hot spot stress method) shows $\Delta\sigma_{hs,C(m=3,p_f=5\%)}/FAT$ values lower than one for six datasets. In two of these cases, however, all data are above the FAT curve, which is designated here as acceptable given the relatively small sample size. The remaining four cases are unacceptable, and can result in unsafe situations. These values are for clarity given in red in the table. Two of these four datasets are assessed with Type “a”, both in as-welded condition, and two datasets are assessed with Type “b”, both in stress-relieved condition.

Table 3.33 (effective notch stress method) shows $\Delta\sigma_{en,C(m=3,p_f=5\%)}/FAT$ values lower than one for two datasets. In both cases the specimens are in stress-relieved condition. In both cases all data are above the FAT curve, designated here as acceptable given the relatively small sample size.

Table 3.32 – Summary of all relevant fatigue datasets assessed with the hot spot stress method. The $\Delta\sigma_{hs,C(m=3,p_f=5\%)}$ values relative to the applied FAT are shown

Reference	Condition	Plate thickness t (mm)	Weld throat size, a (mm)	FAT (MPa)	Extrapolation path	Type	$\Delta\sigma_{hs,C(m=3,p_f=5\%)}/FAT$ (-)	Remark
Doerk & Fricke [9]	As-welded	12	4	FAT90	D (1/2t)[2)]	B	≥1.52	
			6	FAT90	D (1/2t)	B	≥1.78	
	Stress-relieved	12	4	FAT108[1)]	D (1/2t)	B	0.87	All data above FAT curve
			6	FAT108[1)]	D (1/2t)	B	1.12	
TNO [1] & test results of Doerk & Fricke [9]	As-welded	12	4	FAT90	A	B	≥1.29	
			4		B-1mm	B	≥1.91	
			4		C	B	≥2.18	
			4		D	B	≥1.59	
	Stress-relieved	12	4	FAT108[1)]	A	B	0.71	All data above FAT curve
			4		B-1mm	B	1.06	
			4		C	B	1.21	
			4		D	B	0.88	All data above FAT curve
Petershagen [16]	As-welded	10	full pen.	FAT100		B	1.93	
		20				B	2.61	
Fricke & Gao & Paetzold [17]	As-welded	20	full pen.	FAT100	Plate edge	B	≥1.06	
					Corner	A	≥0.96	
					Plate surface	A	0.83	
	Stress-relieved	20	full pen.	FAT120[1)]	Plate edge	B	0.85	
Hanji et al. [18]	As-welded	6 to 25	full pen.	FAT100	1/2 t	B	1.18	
					Corner	B	1.27	
Saito et al. [19]	As-welded	12	full pen.	FAT100	Corner	B	1.01	
Eylmann & Paetzold [22]	As-welded	12	4 & 6	FAT90	Plate surface	A	0.54	

[1)] - Stress relieved - $f(R) = 1.2$ included in FAT value.

[2)] – As path D in Figure 3.9, but now with a linear extrapolation and at the middle of the plate thickness.

Table 3.33 – Summary of all relevant fatigue datasets assessed with the effective notch stress method. The $\Delta\sigma_{en,C(m=3,p_f=5\%)}$ values relative to the applied FAT are shown

Reference	Condition	Plate thickness t (mm)	Weld throat size, a (mm)	FAT	Stress location	$\Delta\sigma_{en,C(m=3,p_f=5\%)}/FAT$ (-)	Remark
TNO [1] & test results of Doerk & Fricke [9]	As-welded	12	4	FAT 225	$1/4t$ = 3 mm	≥1.73	
			4		Corner	≥5.2	
	Stress-relieved	12	4	FAT 270[1)]	$1/4t$ = 3 mm	0.96	All data above FAT curve
			4		Corner	1.24	
Petershagen [16]	As-welded	10	full pen.	FAT 225		1.43	
		20				2.04	
Fricke & Gao & Paetzold [17]	As-welded	20	full pen.	FAT 225	Plate edge	≥1.15	
					Corner	≥1.33	
					Plate surface	1.10	
	Stress-relieved	20	full pen.	FAT 270[1)]	Plate edge	0.93	All data above FAT curve
					Corner	≥1.08	
Hanji et al. [18]	As-welded	6 to 25	full pen.	FAT 225	$1/2\ t$	1.14	Used measured weld toe radii of 1.6 to 2.4 mm
					Corner	1.46	

[1)] - Stress relieved - $f(R) = 1.2$ included in FAT value.

4 Datasets combined

All datasets given in the previous sections are combined into groups in this chapter. 8 groups are distinguished for the hot spot stress method, depending on extrapolation type and FAT class. 2 groups are distinguished for the effective notch stress method, namely, as-welded and stress relieved.

The following groups are created:
1. Hot spot stress method:
   a) Extrapolation Type “b”:
      - Fillet welds,
        - As-welded (FAT90).
        - Stress-relieved (FAT107).
      - Full penetration welds,
        - As-welded (FAT100).
        - Stress-relieved (FAT120).
   b) Extrapolation Type “a”, (all studied plate thicknesses < 25 mm):
      - Fillet welds,
        - As-welded (FAT90).
      - Full penetration welds,
        - As-welded (FAT100).
        - Stress-relieved (FAT120).
2. Effective notch stress method:
   - As-welded (FAT225).
   - Stress relieved (FAT270).

An S-N curve $\Delta\sigma_{hs,C(m=3,p_f=5\%)}$ or $\Delta\sigma_{en,C(m=3,p_f=5\%)}$ is derived for each group. The next sections give the results.

4.1 Hot spot stress method

4.1.1 Extrapolation Type “b”

Figure 4.1 shows all hot spot stress ranges ($\Delta\sigma_{hs}$) versus number of cycles to failure (N_f) for the as-welded specimens with fillet welds evaluated with extrapolation Type “b”. All datapoints shown in this figure are run-outs, indicated with open dots. $\Delta\sigma_{hs,C(m=3,p_f=5\%)} \geq$ 133 MPa and thus substantially higher than FAT 90. Note that most tests are multiple analysed, with different stress paths and by different institutions. The figure provides all analyses, hence multiple dots represent one test specimen. Figure 4.2 shows the results for the stress-relieved specimens with fillet welds, which are also evaluated with extrapolation Type “b”. The same remark applies regarding the multiple analyses. All specimens in this figure represent fatigue failure at the attachment end. The $\Delta\sigma_{hs,C(m=3,p_f=5\%)}$ = 114 MPa and thus just above FAT 107, which includes the factor $f(R) = 1.2$ for stress relieved welds. Figure 4.3 shows all hot spot stress ranges ($\Delta\sigma_{hs}$) versus number of cycles to failure (N_f) for the as-welded specimens with full penetration welds evaluated with extrapolation Type “b”. Nearly all specimens in this figure failed at the attachment end (solid dots), only a few are

run-outs (open dots). Based on only the failed specimens results in a $\Delta\sigma_{hs,C(m=3,p_f=5\%)}$ = 119 MPa, which is significantly higher than FAT 100.

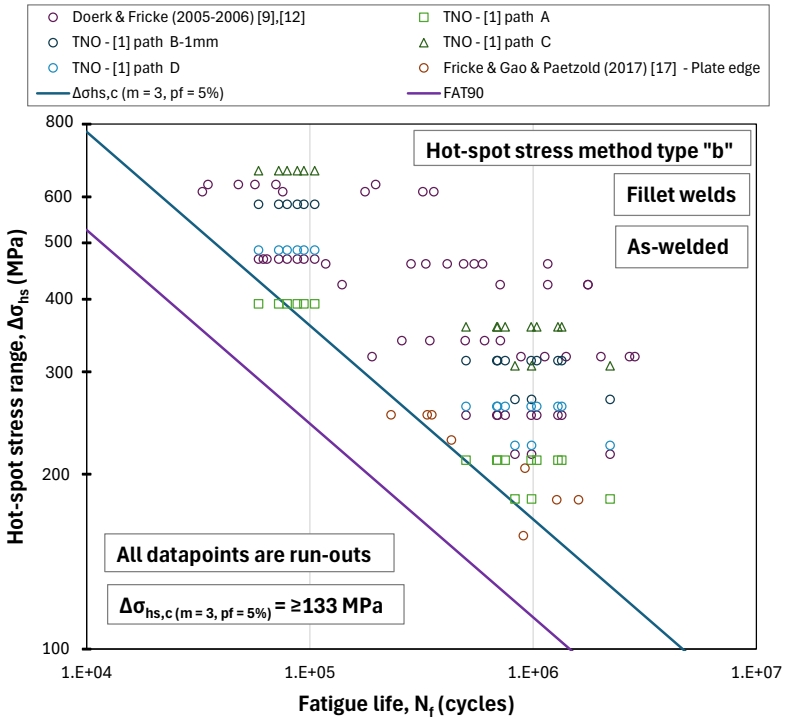

Figure 4.1 – Hot spot stress range ($\Delta\sigma_{hs}$) versus number of cycles to failure (N_f) for the as-welded specimens with fillet welds assessed with the hot spot stress Type “b”.

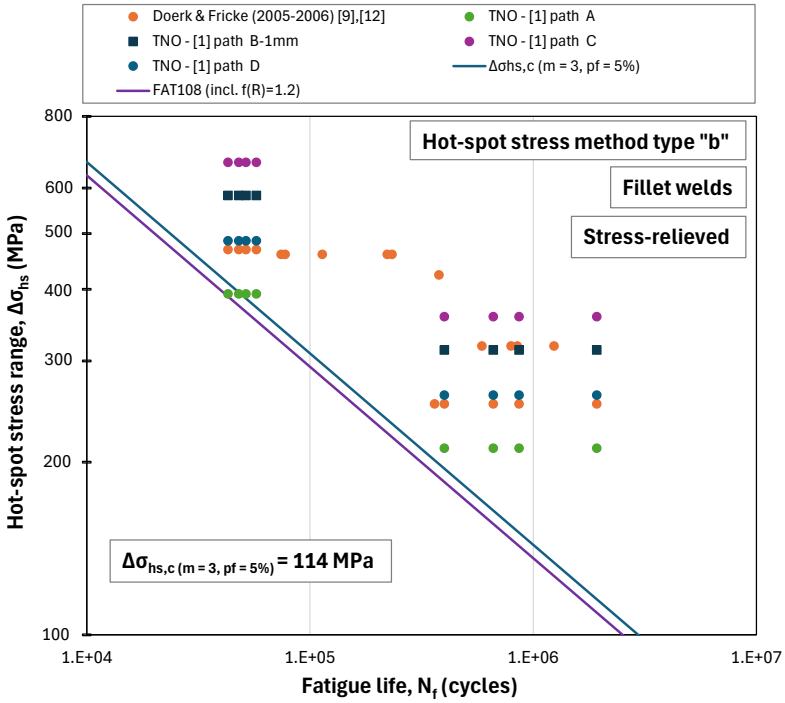

Figure 4.2 – Hot spot stress range ($\Delta\sigma_{hs}$) versus number of cycles to failure (N_f) for the stress relieved specimens with fillet welds assessed with the hot spot stress Type “b”.

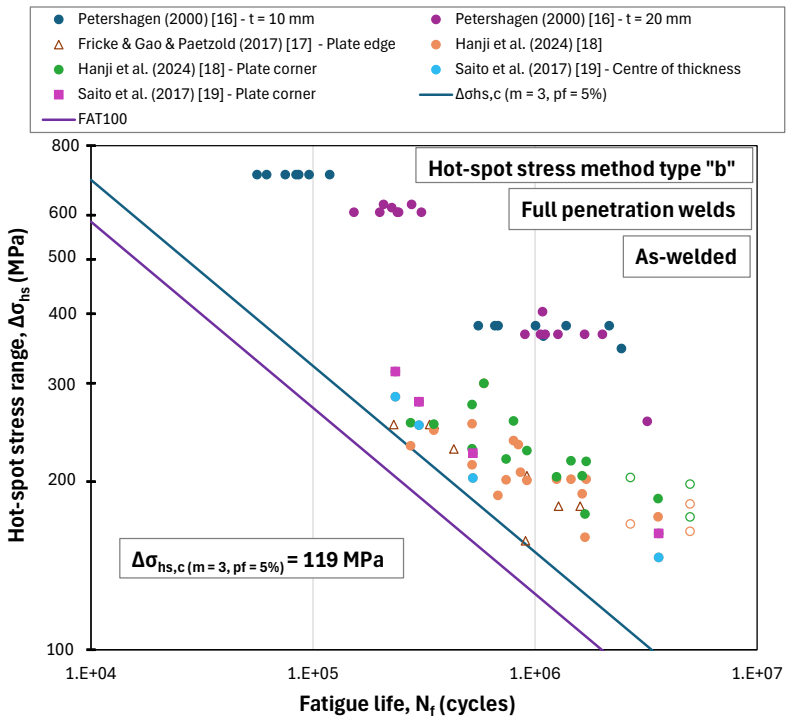

Figure 4.3 – Hot spot stress range ($\Delta\sigma_{hs}$) versus number of cycles to failure (N_f) for the as-welded specimens with full penetration welds assessed with the hot spot stress Type “b”.

Figure 4.4 shows the results for the stress-relieved specimens with full penetration welds evaluated with extrapolation Type “b”. All specimens of this small sample size showed fatigue failure at the attachment end. $\Delta\sigma_{hs,C(m=3,p_f=5\%)}$ = 103 MPa and thus *lower* than FAT 120.

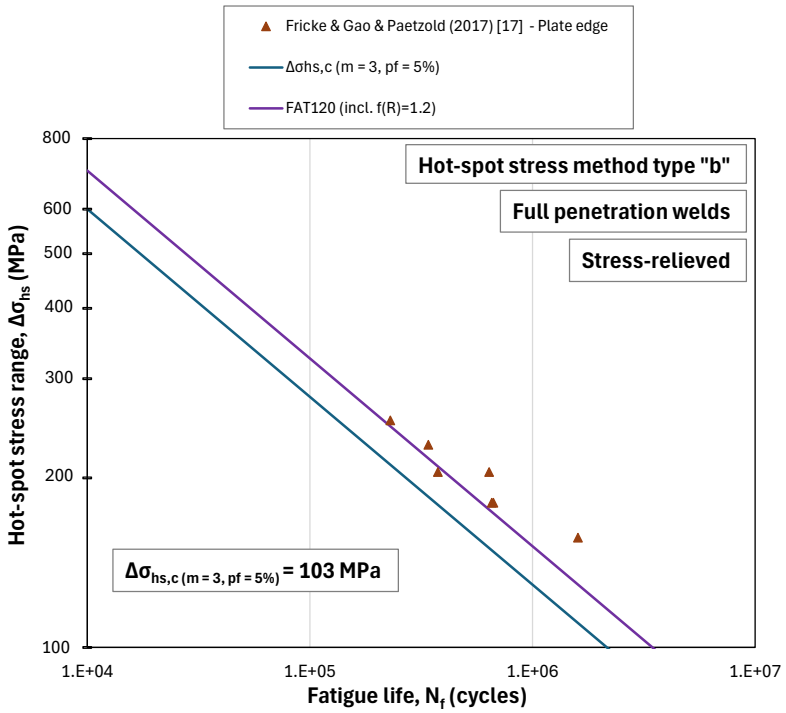

Figure 4.4 – Hot spot stress range ($\Delta\sigma_{hs}$) versus number of cycles to failure (N_f) for the stress relieved specimens with full penetration welds assessed with the hot spot stress Type “b”.

4.1.2 Extrapolation Type “a”

Figure 4.5 shows all hot spot stress ranges ($\Delta\sigma_{hs}$) versus number of cycles to failure (N_f) for the as-welded specimens with fillet welds evaluated with extrapolation Type “a”. All data shown in this figure are failures. $\Delta\sigma_{hs,C(m=3,p_f=5\%)} = 49$ MPa and thus substantially lower than FAT 90. Figure 4.6 shows the results for the as-welded specimens with full penetration welds evaluated with extrapolation Type “a”. 50% of the specimens in this figure are failures, the others are run-outs. $\Delta\sigma_{hs,C(m=3,p_f=5\%)} = 91$ MPa and thus lower than FAT 100. Figure 4.7 shows the results for the stress-relieved specimens with full penetration welds evaluated with extrapolation Type “a”. All specimens of this group are run-outs. $\Delta\sigma_{hs,C(m=3,p_f=5\%)} \geq 86$ MPa and thus lower than FAT 120. However, this latter dataset contains only run-outs.

Although these results obtained with extrapolation Type “a” are only partially related to the fatigue assessment of plate ends, they are of high relevance for practice. For the as-welded specimens with fillet welds the value obtained $\Delta\sigma_{hs,C(m=3,p_f=5\%)}$ = 49 MPa using extrapolation Type “a”, see Figure 4.5, is substantially lower than the $\Delta\sigma_{hs,C(m=3,p_f=5\%)}$ = 118 MPa for extrapolation Type “b” (and different specimens), see Figure 4.1. The remarkable data in Figure 4.5 are based on a single source [22] as summarized in Section 3.7.

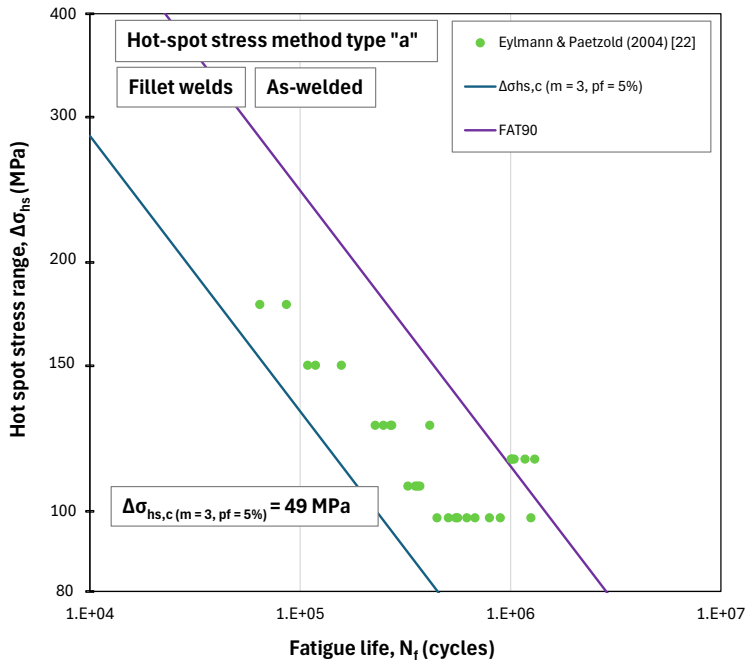

Figure 4.5 – Hot spot stress range ($\Delta\sigma_{hs}$) versus number of cycles to failure (N_f) for the as-welded specimens with fillet welds assessed with the hot spot stress Type “a”.

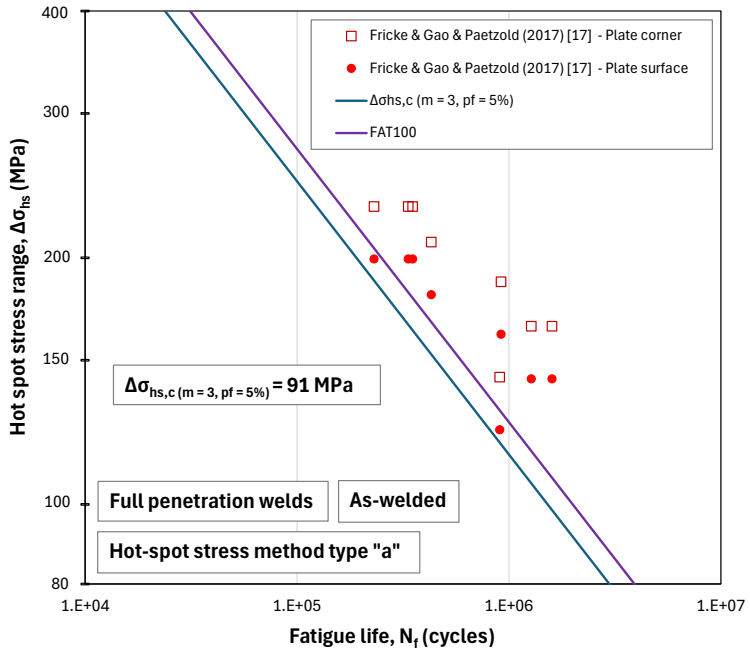

Figure 4.6 – Hot spot stress range ($\Delta\sigma_{hs}$) versus number of cycles to failure (N_f) for the as-welded specimens with full penetration welds assessed with the hot spot stress Type “a”.

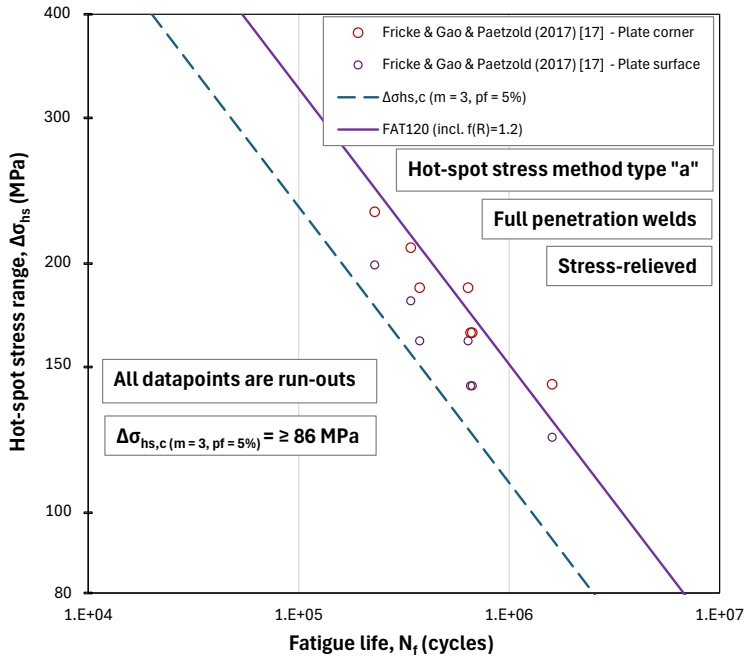

Figure 4.7 – Hot spot stress range ($\Delta\sigma_{hs}$) versus number of cycles to failure (N_f) for the stress relieved specimens with full penetration welds assessed with the hot spot stress Type “a”.

4.1.3 Summary

The derived S-N curves with the hot spot stress method, shown in the Figures 4.1 to 4.7, are summarized Table 4.1. The table provides the $\Delta\sigma_{hs,C(m=3,p_f=5\%)}$ values relative to the applied FAT class.

Table 4.1 – Summary of the derived S-N curves, based on all relevant datasets, for the hot spot stress method. The $\Delta\sigma_{hs,C(m=3,p_f=5\%)}$ values relative to the applied FAT are shown

Extrapolation Type	Weld type	Condition	Sample size n (-)	$\Delta\sigma_{hs,C(m=3,p_f=5\%)}$ (MPa)	FAT	$\frac{\Delta\sigma_{hs,C(m=3,p_f=5\%)}}{FAT}$ (-)	Remark
b	Fillet weld	As-welded	122	≥132.7	FAT90	≥1.47	All run-outs
b	Fillet weld	Stress-relieved	51	113.9	FAT107[1)]	1.05	
b	Full penetration weld	As-welded	92	118.8	FAT100	1.19	
b	Full penetration weld	Stress-relieved	7	102.6	FAT120[1)]	0.85	
a	Fillet weld	As-welded	28	48.7	FAT90	0.54	
a	Full penetration weld	As-welded	16	91.3	FAT100	0.91	
a	Full penetration weld	Stress-relieved	14	≥86.3	FAT120[1)]	≥0.72	All run-outs

[1)] - Stress relieved - f(R)=1.2 included in FAT value.

4.2 Effective notch stress method

Figure 4.8 shows the effective notch stress ranges ($\Delta\sigma_{en}$) versus number of cycles to failure (N_f) for the as-welded specimens. The figure shows all failures at the attachment end as closed dots and all run-out as open dots. A total number of 89 specimens is shown from which 39 failed and 50 are run-outs. Because of the deviating notch radius applied in Hanji et al. [18], these data are neither included in the figure, nor in the evaluation below.

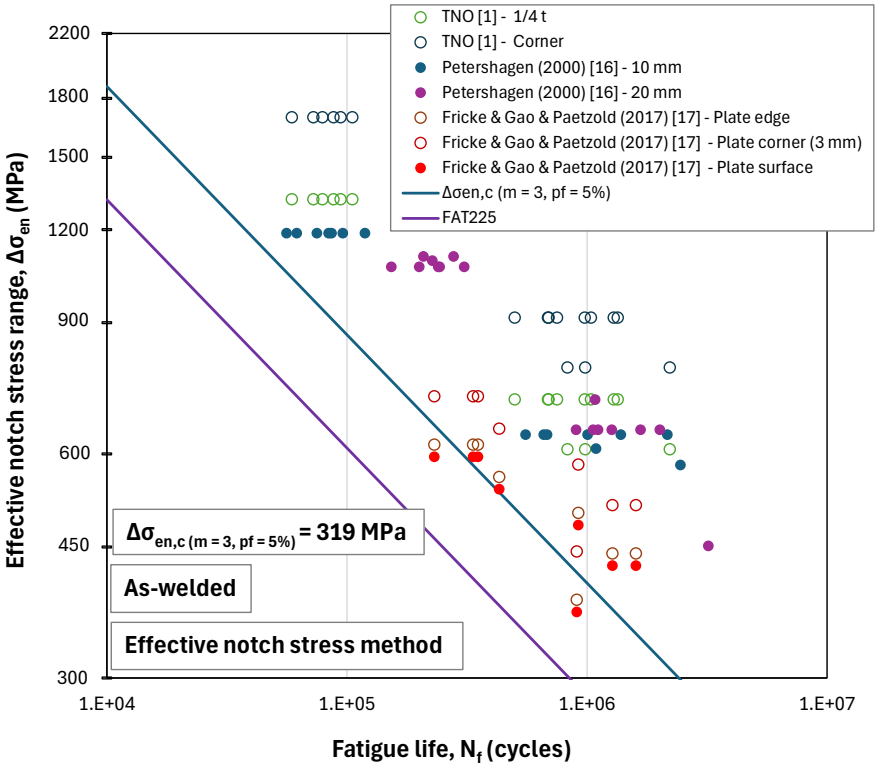

Figure 4.8 – Effective notch stress range ($\Delta\sigma_{en}$) versus number of cycles to failure (N_f) for the as-welded (AW) specimens.

Figure 4.9 shows the effective notch ranges ($\Delta\sigma_{en}$) versus number of cycles to failure (N_f) for the stress-relieved specimens. The figure shows a total number of 30 specimens from which 15 failed at the attachment end and 15 are run-outs.

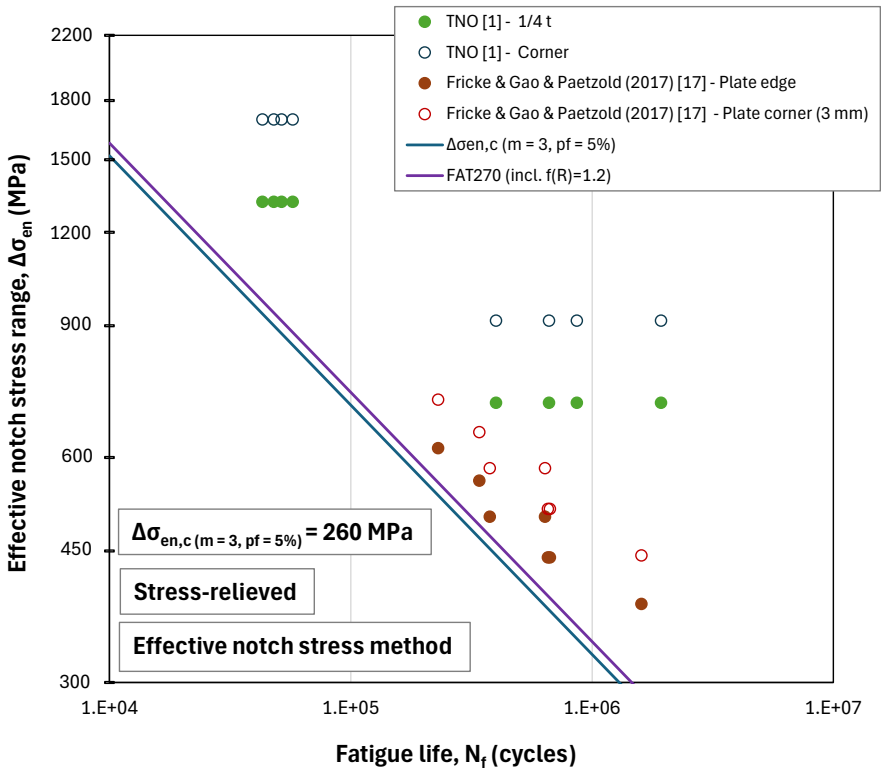

Figure 4.9 – Effective notch range ($\Delta\sigma_{en}$) versus number of cycles to failure (N_f) for the stress-relieved (SR) specimens.

A summary of the derived effective notch S-N curves is given in Table 4.2.

Table 4.2 – Summary of the derived S-N curves, based on all relevant datasets, for the effective notch stress method. The $\Delta\sigma_{en,C(m=3,p=5\%)}$ values relative to the applied FAT are shown

Condition	Sample size n (-)	$\Delta\sigma_{en,C(m=3,p_f=5\%)}$ (MPa)	FAT	$\Delta\sigma_{en,C(m=3,p=5\%)}/FAT$ (-)	Remark
As-welded	89	319	FAT225	1.42	
Stress-relieved	30	260	FAT270[1)]	0.96	All above FAT curve

[1)] - Stress relieved - $f(R) = 1.2$ included in FAT value.

The derived S-N curve in Figure 4.8, for the as-welded specimens, is with 42 % substantially higher that the FAT225 S-N curve. The resistance $\Delta\sigma_{en,C(m=3,p=5\%)}$ relative to FAT 270 is 0.96, i.e. nearly unity, for the stress-relieved specimens. All data are above the FAT270 S-N curve. Thus, the effective notch stress method gives safe results for the weld toe of the attachment ends included in this study. It should be noted, though, that the scatter of the data is extremely large.

5 Discussion

5.1 Reported finite element (FE) analyses

The hot spot stress method as well as the effective notch stress method should be based on accurate FE analyses. In the case of Eylmann & Paetzold (2004) [22] remarkable results have been found. They tested three-point bending specimen with fillet welds around the attachment ends, see Figure 3.50. The hot spot stress analyses and fatigue tests on all specimen models A to D combined, resulted in an astonishing low resistance $\Delta\sigma_{hs,C,(m=3,p=5\%)}$ compared to FAT 90. The only reliable explanation seems to be that the crack at the weld root, which normally initiates first, accelerates the crack initiation and crack growth at the weld toe in the vertical plate, causing this weld toe to have a low fatigue life. This phenomenon is a result of the crack at the weld root reducing the net section of the weld and thereby increasing the stress concentration at the weld toe in the vertical plate.

The reported FE analyses in some references are a bit dated. In some cases element sizes equal to the full plate thickness are used. In more recent references much finer meshes have been used. The application of finer element sizes often results in locally high stress peaks, for instance at the plate corners. This has not been encountered in the older references with coarser meshes. The influence of this on the hot-spot stress should be reduced because of the extrapolation method, but some effect might still be present. Some references, such as in Hanji et al. (2024) [18], only give a brief description of the model and boundary conditions. A model review cannot be performed satisfactory for such cases. The combination of all data in one regression resulted in a high scatter, both for the hot spot and the effective notch stress methods. At least a part of this scatter may be caused by differences in the FE analyses.

5.2 FAT values

Two different FAT values are used in the studied references for hot spot stress method assessments for as-welded conditions. In line with Chapter 2, Table 2.1, FAT 90 or FAT 100 was used for loaded fillet welds or other (full penetration or unloaded fillet) welds, respectively. However, Fricke & Doerk [9] used FAT 100 for specimens with loaded fillet welds. In accordance with Table 2.1, the current report used FAT 90 to evaluate the results of Fricke & Doerk [9].
The current report used the fatigue enhancement factor $f(R)$ for the stress relieved specimens, see Section 2.3.2. As most of these specimens have been tested with a stress ratio of $R \approx 0$, this enhancement factor $f(R) = 1.2$. However, the stress relieved specimens gave generally a *lower* fatigue resistance than the as-welded specimens, because of compression residual stresses at weld ends (see the next section). The fatigue enhancement factor hence creates an even larger difference between stress relieved and as-welded specimens. Nonetheless, the factor is applied according to the specifications in Hobbacher [3], because this is current practice.

5.3 Welding sequence & residual stresses

Doerk & Fricke [9], [12] have measured compressive residual stresses at the weld toe of the attachment or plate end for the welding sequences used in the manufacturing of their specimens. In the stress-relieved condition these compressive stresses are relaxed to values of approximately 10% of the original value. These residual stress conditions explain the obtained results in the current report that the fatigue life of the as-welded specimens is significantly higher than that of the same, but stress relieved specimens, as summarized in the Tables 3.32 and 3.33. This has a number of implications:

- The applied fatigue enhancement factor $f(R)$ for the FAT value for stress relieved specimens, although valid according to the recommendations, results in un-logical results for the weld toe of attachment or plate ends, see the previous section.
- The question emerges if other weld sequences can result in tensile residual stresses at the weld toe at attachment or plate ends? This would probably decrease fatigue life due to a faster crack initiation at the weld toe.
- All tests are conducted under constant amplitude loading. Relaxation of residual stresses may occur in practical, variable amplitude conditions with as-welded details. This is beneficial for tensile residual stresses, but detrimental for compressive residual stresses, as demonstrated by Doerk & Fricke [9] [12]. The stress relieved specimens tested in constant amplitude may be more representative for such conditions than the as-welded specimens tested in constant amplitude.

5.4 FAT values versus $\Delta\sigma_{C(m=3,p=5\%)}$

Hot spot stress Type “b” gives $\Delta\sigma_{hs,C(m=3,p_f=5\%)}/FAT$ ratios varying from 1.19 to 1.47 for the as-welded condition and from 0.85 to 1.05 for the stress-relieved condition, see Table 4.1. Thus, a conservative result for the as-welded condition. However, note the remarks given above in the previous section. The ratio is lower than unity for the full penetration and stress-relieved specimens. However, ignoring the applied fatigue enhancement factor $f(R)$ increases the ratios to 1.03 and 1.27, and thus also a conservative result. For practice, this implies that hot spot stress Type “b” can be used to assess the weld toe of attachment or plate ends, provided that the FAT is applied without fatigue enhancement factor $f(R)$.

For hot spot stress Type “a” only the as-welded condition is available and the ratios for this condition vary from 0.54 to 0.91, see Table 4.1. For this situation an unsafe result is found. As explained in bullet point 2) in Section 5.1 this can be a result of two crack initiations and crack growth close to each other, in this case at the weld toe and at the same time at the weld root, which results in an unsafe result when using the hot spot stress Type “a” method for the weld toe. It is recommended to not use this Type “a” method in assessments for details similar to the tested specimens.

The effective notch stress method gives $\Delta\sigma_{en,C(m=3,p_f=5\%)}/FAT$ = 1.42 for the as-welded condition and 0.96 for the stress-relieved condition. All data are above the FAT curve, see Table 4.2. Thus both conditions give safes results. This effective notch stress method can hence be used to assess the weld toe of attachment or plate ends, however, the scatter in fatigue life is very large.
When applied to the same specimens, the hot spot stress Type “b” method seems to give a somewhat lower $\Delta\sigma_{hs,C(m=3,p_f=5\%)}/FAT$ ratio than the ratio $\Delta\sigma_{en,C(m=3,p_f=5\%)}/FAT$ obtained with the effective notch stress method. This occurs for both conditions as-welded and stress-relieved.

5.5 Residual welding stresses & FAT values

5.5.1 Hot spot stress Type “b” method

The hot spot stress Type “b” stress ranges $\Delta\sigma_{hs,C,(m=3,p=5\%)}$ and FAT values are shown in Figure 5.1a/b as a function of the residual welding stresses at the weld toe, where Figure 5.1a applies to fillet welds and Figure 5.1b applies to full penetration welds. The hot spot stress ranges $\Delta\sigma_{hs,C,(m=3,p=5\%)}$ derived from the tests are indicated by orange dots and the FAT values according to the IIW recommendation for as-welded and stress relieved (using the same fatigue enhancement factor as in Section 2.3.2) by purple dots. The residual welding stresses at the weld toe have been measured by Doerk & Fricke [9], [12]. A simple extrapolation to the as-welded condition with tensile residual stresses is shown by the orange dashed line.

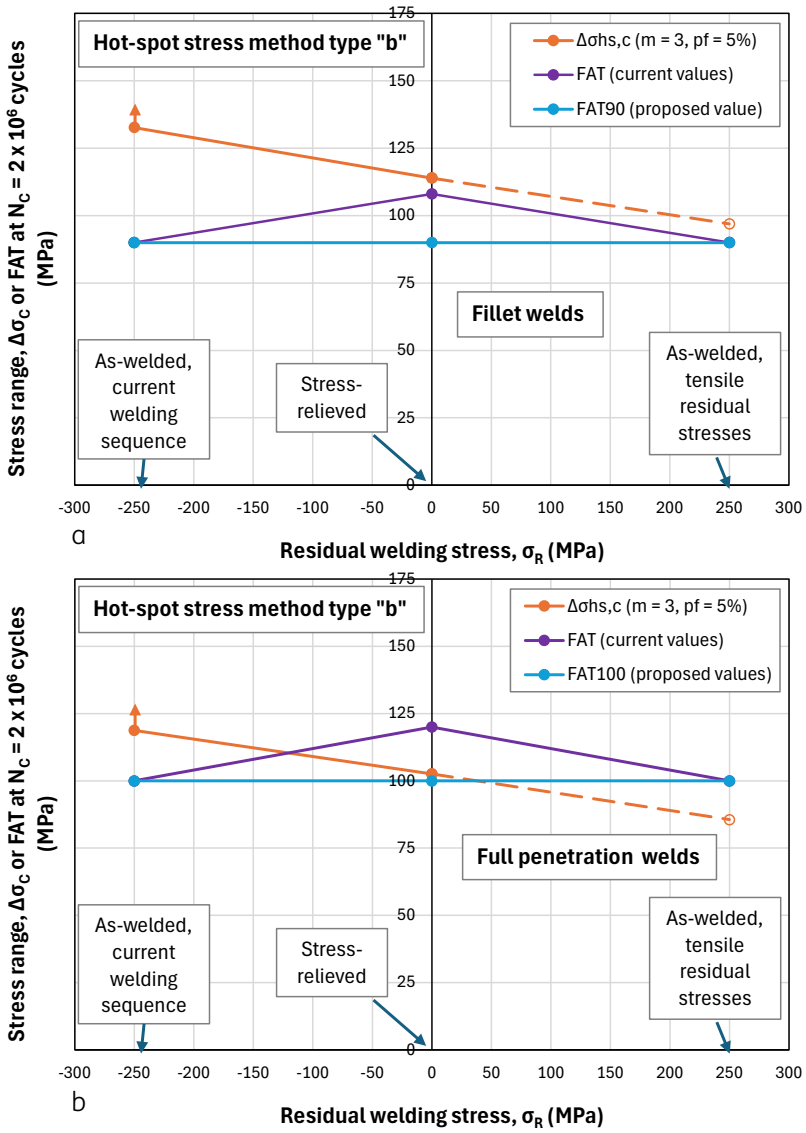

Figure 5.1a/b – The hot spot stress Type “b” S-N curves and FAT values as a function of the residual welding stresses at the weld toe. a) Fillet welds: $\Delta\sigma_{hs,C,(m=3,p=5\%)}$ values from Figures 4.1 and 4.2, b) Full penetration welds: $\Delta\sigma_{hs,C,(m=3,p=5\%)}$ values from Figures 4.3 and 4.4.

For the fillet welds both conditions, *stress relieved* and *as-welded with tensile residual stresses*, result in conservative predictions with the applied FAT values according to the current recommendations, see Sections 2.1 and 2.3. For the full penetration welds both conditions, *stress relieved* and *as-welded with tensile residual stresses*, result in unconservative predictions with the applied FAT values according to the current recommendations, see Sections 2.1 and 2.3.

However, as already mentioned above, ignoring the applied fatigue enhancement factor $f(R)$ gives a conservative result also for the stress relieved full penetration welds. This is indicated by the blue line in Figure 5.1a/b. For practice, this implies that hot spot stress Type "b", with the recommended FAT values [3],[4], for both fillet welds and full penetration welds, can be applied to assess the weld toe of attachments or plate ends. After all, initially *thermally stress relieved* structures are not present in steel bridges, and the condition of *tensile residual stresses* at weld ends due to welding or use seems to be quite un-logical. It is assumed that residual tensile stresses cannot arise in the critical area, not even by a compressive loading. However, no supporting literature for this assumption is available at this moment, thus a remark should be made that in situations with high *tensile residual stresses* which do not relax during use, this hot spot stress Type "b" assessment method can give un-conservative results.

5.5.2 Effective notch stress method

The same trend as a function of the residual welding stresses at the weld toe can be observed for the results of the effective notch stress method. These results are valid for both fillet welds and full penetration welds. Figure 5.2 shows the results. Also for the effective notch method, both conditions, *stress relieved* and *as-welded with tensile residual stresses*, results in unconservative predictions with the applied FAT values according to the current recommendations (see Sections 2.2 and 2.3).
However, in the same way as for the hot spot stress Type "b", ignoring the applied fatigue enhancement factor $f(R)$ gives also for the stress relieves situation a conservative result. This has been indicated by the blue line in Figure 5.2. For practice, this implies that the effective notch stress method, with the recommended FAT value [3],[5], can be used to assess the weld toe of attachments or plate ends. As mentioned above initially *thermally stress relieved* structures are not present in steel bridges, and the condition of *tensile residual stresses* due to welding or use seems to be quite un-logical. Thus also for this effective notch stress method a remark is made for situations with high *tensile residual stresses* which do not relax during use, that this assessment method can give un-conservative results.

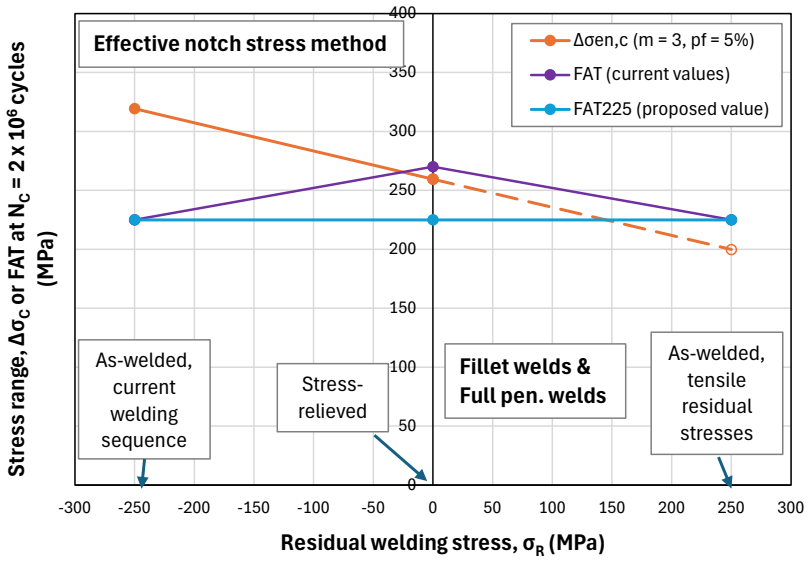

Figure 5.2 – The effective notch stress S-N curves and FAT values as a function of the residual welding stresses at the weld toe. $\Delta\sigma_{en,C,(m=3,p=5\%)}$ values from Figures 4.8 and 4.9.

5.6 Hot spot stress at plate corner

Fricke & Gao & Paetzold (2017) [17], see Section 3.3.2.1, calculated hot spot stresses at three locations, indicated by “plate edge”, “plate corner”, and “plate surface”, see Figure 3.28. For the plate corner they used extrapolation Type “a” (plate thickness dependent stress locations). Hanji et al. (2024) [18], see Section 3.4.2.1, calculated hot spot stresses by extrapolation along two paths: centre of the plate thickness and plate corner, see Figure 3.38. These hot spot stresses were calculated using Type “b” (plate thickness independent stress locations).

The stress distribution in the plate corner, when using a fine element mesh, seems to be mainly determined by the applied plate corner radius and only to a limited extent by the plate thickness.

According to the recommendations given by Hobbacher [3] and Niemi et al. [4] both extrapolation methods Type “a” and Type “b” are allowed to be used. At this moment no research results are available in literature which result in some preference for one extrapolation type for the plate corner.

5.7 Specimen width and thickness

In addition to the FE modelling of the fatigue specimens Hanji et al. (2024) [18] performed hot spot stress Type “b” and effective notch stress analyses to investigate the effects of the attachment width and/or thickness on the stresses at the weld toe of the attachment end. Compared to the fatigue specimens, these models consist of substantially larger specimens, with attachment widths up to 500 mm and plate thicknesses up to 75 mm. Appendix B gives a summary of their study. Hanji et al. observed that the stresses increase with increasing attachment width (W) and increasing attachment plate thickness (T). The highest stress peaks are observed at the corners of the attachments.

6 Conclusions

1) Two suitable fatigue life assessment methods to assess the weld toe of the attachment or plate ends are:
   - hot spot stress Type “b” (reference points at fixed locations),
   - effective notch stress method.

2) The evaluations show a large scatter if all test data of the different sources are combined. This applies to both the hot spot stress method and the effective notch stress method. At least a part of this scatter is caused by differences in the FE analyses, where some meshes were much coarser than others. Accurate modelling of geometry and boundary conditions appears essential for a proper assessment and a proper evaluation of test data.

3) In nearly all fatigue test programs summarized in this report the stress-relieved specimens show a significantly higher fatigue life than the as-welded specimens. Doerk & Fricke [9], [12] have demonstrated that a compressive stress state exists at the weld toe of the attachment or plate end in the as-welded condition for the applied welding sequences. This compressive stress is relaxed in the stress-relieved condition and thus explain the obtained fatigue life results.

4) According to the recommendations [3] a fatigue enhancement factor $f(R)$ for the FAT value for stress relieved specimens may be applied. However, in the case of weld toes of attachments or of plate ends, measured fatigue life shows the opposite trend. Use o the fatigue enhancement factor $f(R)$ can be unconservative for such geometries.

5) The hot spot stress extrapolation Type “b” gives $\Delta\sigma_{hs,C(m=3,p=5\%)}/FAT$ ratios varying from 1.19 to 1.47 for the as-welded condition, and 0.85 to 1.05 for the stress relieved condition including fatigue enhancement factor $f(R)$. However, ignoring the fatigue enhancement factor $f(R)$ for the stress relieved condition increases the ratio to between 1.03 and 1.27, hence conservative.

6) For hot spot stress extrapolation Type “a”, only test results in the as-welded condition are available and the $\Delta\sigma_{hs,C(m=3,p=5\%)}/FAT$ ratios for this condition vary from 0.54 to 0.91. For this situation an unconservative result is found.

7) The effective notch stress method gives $\Delta\sigma_{en,C(m=3,p=5\%)}/FAT = 1.42$ for the as-welded condition and 0.96 for the stress-relieved condition including fatigue enhancement factor $f(R)$. In the latter case, all datapoint are above the FAT curve. Thus the method is safe-sided for both conditions.

7 Recommendations

1) Eylmann & Paetzold (2004) [22] tested specimens with fillet welds around the attachment ends in bending and shear (three-point bending). Their hot spot stress extrapolation Type “a” analyses and fatigue tests resulted in an extremely low $\Delta\sigma_{hs,C(m=3,p=5\%)}$. Further analysis of this specimen geometry with FEM is recommended to clarify this result.

2) Doerk & Fricke [9], [12] have demonstrated that a compressive stress state exists at the weld toe of the attachment or plate end for the welding sequences used in their studies. This compressive stress relaxes in the stress-relieved condition. It explains the higher fatigue life of the as-welded specimens compared to the stress relieved specimens. Based on this observation it is recommended to not apply the fatigue enhancement factor $f(R)$ for the FAT value in assessments of the weld toe of attachment or plate ends for stress relieved specimens.

3) Welds at plate ends and corners in steel bridges are subject to variable amplitude loads, including overloads. This may relax residual (compressive or tensile) stresses. Initially stress relieved structures are not present in steel bridges and the condition of *tensile residual stresses* due to welding or use seems to be un-logical. Thus for practice, this implies that the hot spot stress method Type “b” and for the effective notch stress method, both with the recommended FAT values, can be used to assess the weld toe of attachments or plate ends. However a remark is made for situations with possible high *tensile residual stresses* which do not relax during use that these assessment methods can give un-conservative results.

4) In addition to the FE modelling of the fatigue specimens, Hanji et al. (2024) [18] performed hot spot stress extrapolation Type “b” and effective notch stress methods to study the effect of the attachment width up to 500 mm and/or thickness up to 75 mm on the stresses at the weld toe of the attachment end. They observed that all stresses increase with increasing attachment width (W) and increasing attachment plate thickness (T). The highest stresses are observed at the corners of the attachments. Because of the practical implications of these observed trends it is recommended to perform additional analyses to further quantify this observed attachment width and thickness effect.

8 References

[1] Fatigue assessment for weld roots and toes of weld ends, M.B.M. Haarman, G.J.A.M. Eumelen, TNO report: TNO 2024 R11105, June 2024.
[2] NEN-EN 1993-1-9+C2+NB, Eurocode 3: Design of steel structures - Fatigue, 2012.
[3] Hobbacher A.F., Recommendations for Fatigue Design of Welded Joints and Components, 2nd ed., Springer International Publishing, 2016.
[4] Niemi E., Fricke W., Maddox S.J., Structural Hot spot Stress Approach to Fatigue Analysis of Welded Components, Designer's Guide, 2nd Edition, IIW collection, Springer Nature Singapore Pte Ltd. 2018.
[5] Fricke W., IIW Recommendations for Fatigue Assessments of Welded Structures by Notch Stress Analysis, IIW-2006-09, Woodhead Publishing Limited, 2012.
[6] Fricke W., Bogdan R., Determination of Hot Spot Stress in Structural Members with In Plane Notches Using a Coarse Element Mesh, IIW-Doc. XIII-1870-01, International Institute of Welding, 2001.
[7] NEN-EN-ISO 5817:2014, Welding - Fusion-welded joints in steel, nickel, titanium and their alloys (beam welding excluded) - Quality levels for imperfections, 2014.
[8] Fricke W., Doerk O., Fatigue Analysis of Fillet Welds around Stiffener and Bracket Toes, Doc. XIII-2034-04 / XV-1170-04, May 2004.
[9] Fricke W., Doerk O., Simplified approach to fatigue strength assessment of fillet-welded attachment ends, International Journal of Fatigue 28, 2006, 141–150.
[10] Fricke W., Doerk O., Grünitz L., Fatigue strength investigation and assessment of Fillet Welds around Stiffener and Bracket Toes, Proceedings of OMAE-FPSO 2004 (ASME), Houston, USA 2004.
[11] Doerk O., Fricke W., Bruchmechanisches Konzept zur Bewertung der Schwingfestigkeit - Untersuchung von Kehlnähten an umschweißten Steifenenden, Materialpruefung/-Materials Testing, 2005, 47(10), 575–581.
[12] Doerk O., Bruchmechanische Bewertung räumlich ausgebildeter Nahtbrüche in schwingbeanspruchten Kehlnahtverbindungen, PhD-thesis, Bericht Nr. 632, Technische Universiteit Hamburg, 2005. ISBN-10-3892206325, ISBN-13-978-3892206323.
[13] Maddox S.J., Fatigue Strength of Welded Structures, 2e edition, Abington Publishing - Woodhead Publishing Ltd in association with The Welding Institute, Cambridge England, 1991.
[14] Andrews R.M., The effect of misalignment on the fatigue strength of welded cruciform joints, Fatigue & Fracture of Engineering Materials & Structures 19(6), 1996, 755-768.
[15] Fricke W., Fatigue Design and Structural Hot spot Stress Determination for Welded Joints 9th Portugese Conference on Fracture, 2004.
[16] Petershagen H., Das Strukturspannungskonzept - eine Fallstudie; Schiffbauforschung 39 (2000), H3, S.25-38.
[17] Fricke W., Gao L., Paetzold H., Fatigue assessment of local stresses at fillet welds around plate corners International Journal of Fatigue 101 (2017) 169–176.
[18] Hanji T., Tateishi K., Rabsel N., Shimizu M., Structural hot spot stress approach for toe cracking from plate edge of load-carrying welded attachment, Welding in the World 68 (2024) 1201–1209.
[19] Saito F., Anami K., Ikehara I., Shibuya A., Ono S., Fatigue strength improvement at attachment side boxer weld by low temperature transformation welding material, Journal of Structural Engineering 63A (2017) 681– 689 (in Japanese).

[20] Petershagen H., Cruciform joints and their optimisation for fatigue strength – a literature survey, Welding in the World 13 (1975) 143-154.
[21] Shingai K., Imamura K., Fatigue crack propagation in cruciform joints, IIW Doc. XIII-691-73, 1973.
[22] Eylmann S., Paetzold H., Schwing festigkeitsuntersuchungen an fertigungsgünstigen Details der Schiffskonstruktion, Report 625, Arbeits bereiche Schiffbau der TU Hamburg-Hamburg, 2004.

9 Signature

TNO › Mobility & Built Environment › Delft, 24 November 2025

Digitaal ondertekend door Dr.ing. H.M. Slot
op 2025-12-03 11:53:27

Dr.ing. H.M. Slot
Author

Digitaal ondertekend door Ir. L.M. Abspoel-Bukman
op 2025-12-03 13:31:36

Ir. L.M. Abspoel-Bukman
Project Manager

Digitaal ondertekend door Ir. M. van Roermund
op 2025-12-03 11:07:08

Ir. M. van Roermund
Research Manager
Reliable Structures

Appendix A

Statistical evaluation of fatigue data according to Eurocode 3

Introduction

In this report the statistical evaluations of the datasets of stress ranges ($\Delta\sigma_i$) and number of fatigue cycles to failure (N_i), with a number of tests (n), have been performed according to the Eurocode 3, see background document [A.1]. Other internationally accepted standards and recommendations, such as DNV, sometimes use other definitions or derivations for the characteristic S-N curve.

Starting points in Eurocode 3

The following starting point apply for the statistical evaluations of welded details according to the Eurocode 3:

1. The statistical evaluations are performed on logarithms of the main independent and the dependent variables ($\log \Delta\sigma_i$, $\log N_i$).
2. The S-N curve has a fixed slope of $m = 3$.
3. The detail category is calculated for a number of fatigue cycles $N_C = 2 \times 10^6$.
4. The prediction bound for 95 % survival was chosen to derive the design fatigue curve.

Evaluation of S-N curve

The S-N curve is given by:

$$\Delta\sigma^m N = C \tag{A.1}$$

And thus in logarithmic form this gives for the datapoints:

$$\log N_i = \log C - m \log \Delta\sigma_i$$

For the statistical evaluation x_i and y_i are used:

$$y_i = \log N_i \ \& \ x_i = \log \Delta\sigma_i$$

The analysis implies that there exists a linear relation between y_i and x_i as:

$$\hat{y}_i = a - m x_i \tag{A.2}$$

Where a ($= \log C$) is the parameter which must be estimated.
The residual e_i is now defined as:

$$e_i = y_i - \hat{y}_i$$

Evaluation of the characteristic strength at two million cycles

In the Eurocode 3 the characteristic strength $\Delta\sigma_C$ at two million cycles is noted as: $x_C = \log \Delta\sigma_c$ corresponding to $y_C = \log N_C$, with $N_C = 2 \times 10^6$.

In reality there is a difference between the estimated $\hat{y}_C$, as given by equation A.2, and y_C the real value. The difference $(\hat{y}_C - y_C)$ may be interpreted as a random variable following the standard normal distribution.

Very often in fatigue test analysis the sample size is small ($n \leq 30$) and the value of the estimation of the variance σ^2 fluctuates considerably from sample to sample. Taking into account this fact means:

1. The distribution of the residuals for a sample size $n \leq 30$ is assumed to follow the Student's t distribution.
2. The sample distribution of $(\hat{y}_C - y_C)$ can be obtained from the following estimation:

$$Mean: \quad \mathrm{E}(\hat{y}_C - y_C) = 0$$

$$Variance\ prediction: \quad \sigma^2(\hat{y}_C - y_C) = s^2\left[1 + \frac{1}{n} + \frac{x_c - \bar{x}}{S_{xx}}\right] = s^2|f| \qquad \text{A.3}$$

Using a fixed value of $m = 3$, this gives for the standard deviation:

$$s = \frac{\left(S_{yy} + mS_{xy}\right)}{(n-1)} \qquad \text{A.4}$$

$\bar{x}$ = mean of the x_i values in the dataset.

Where:

$$S_{xx} = \Sigma x_i^2 - \frac{(\Sigma x_i)^2}{n}$$

$$S_{yy} = \Sigma y_i^2 - \frac{(\Sigma y_i)^2}{n}$$

$$S_{xy} = \Sigma x_i y_i - \frac{\Sigma x_i \Sigma y_i}{n}$$

Evaluation of the characteristic S-N curve

In Eurocode 3 the characteristic S-N curve is based on the 5% lower prediction bound. Thus the probability $\alpha = 0.05$. With the derived standard deviation (s), the derived $|f|$–value and Student's t distribution $t(\alpha, n)$, the design fatigue curve, with $\left(\log \hat{N}_C - \log N_C\right) = (\hat{y}_C - y_C)$, is given as:

$$\log N_C = \log \hat{N}_C - t(\alpha, n)s\sqrt{f} \qquad \text{A.5}$$

And thus for the stress range at $N_C = 2 \times 10^6$ cycles

$$\log \Delta\sigma_C = \log \Delta\sigma_C - t(\alpha, n)\frac{s}{m}\sqrt{f} \qquad \text{A.6}$$

$\Delta\sigma_{c\_}$ = stress range of the characteristic S-N curve for a number of cycles $N_C = 2 \times 10^6$, a fixed slope of $m = 3$, and a probability $\alpha = 0.05$. Using equation A.1, the characteristic S-N curve is:

$$\Delta\sigma^m N = \Delta\sigma_C^m N_C$$

or

$$N = \left(\frac{\Delta\sigma_C}{\Delta\sigma}\right)^m N_C \qquad \text{A.7}$$

Reference

[A.1] J. Brozzeti, M.A. Hirt, I. Ryan, G. Sedlacek, I.F.C. Smith, Background information on Fatigue design rules – Statistical Evaluation, Chapter 9 – Document 9.01, Eurocode No. 3 - Design of Steel Structures – Background Documentation, first draft, University of Technology Aachen.

Appendix B

Large specimens – FE modelling – size effect

In addition to the fatigue tests and FE modelling results shown in Section 3.4, Hanji et al. (2024) [18] also performed hot spot stress and effective notch stress analyses to study the effect of the attachment width and thickness on these local stresses. Compared to their experiments, these models consisted of substantially larger specimens, using attachment widths up to 500 mm and plate thicknesses up to 75 mm.

The analyses were performed with a simplified version of the specimen used in their fatigue tests. Calculations were performed for different widths W = 80, 120, 160, 200, 300, and 500 mm and thicknesses T = 12, 18, 25, 50, and 75 mm of the load carrying attachment, see Figure B.1. Further, the bottom surface of the lower plate was fixed, and a load was applied to the end of the attachment. So basically symmetry boundary conditions seem to have been used for the bottom surface of the lower plate. This means that a specimen geometry of a cruciform joint with a mid-plate thickness of 90 mm has been simulated.
The weld was modelled with equal leg lengths of 6 mm, a toe radius of 1 mm, and a toe angle of 45°.

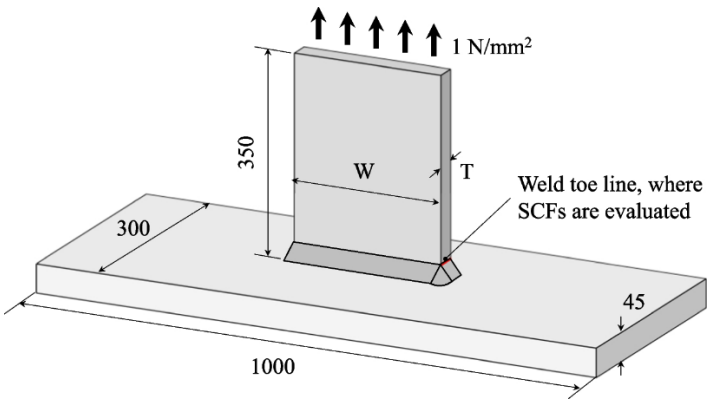

Figure B.1 – FE model of a simplified version of the specimen used in the fatigue tests, see section 3.4 (units: mm).

Figure B.2(a) and (b) show the stress concentration factors (SCF) for the effective notch stress and structural hot spot stress Type “b”, obtained with the 4, 8, and 12 mm reference points, as a function of (a) the attachment width (W) and (b) the attachment thickness (T). Both figures show the SCF’s as a function of the relative distance from the attachment centre (x/T).

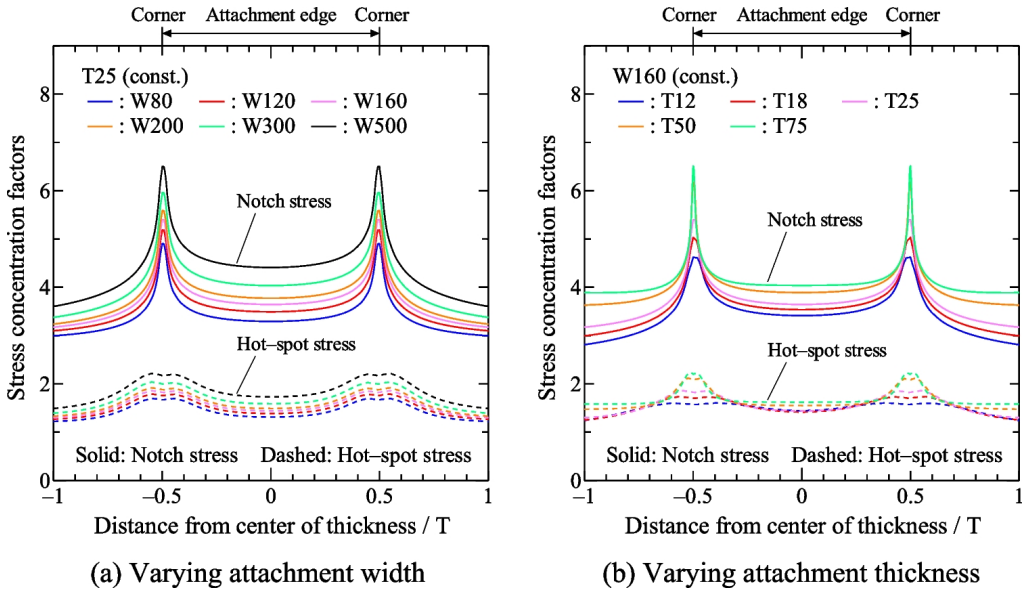

Figure B.2 - Stress concentration factors (SCF) for the effective notch stress and hot spot stress (4, 8, and 12 mm method), as a function of (a) the attachment width (W) and (b) the attachment thickness (T). Both figures show the SCF also as a function of the relative distance from the attachment centre (x/T).

The highest stress peaks are observed at the corners of the attachment. This corresponds with the crack initiation site observed in the experiments, see Section 3.4. These stresses increase with increasing attachment width (W) and increasing attachment plate thickness (T), see Figure B.3(a) and (b).

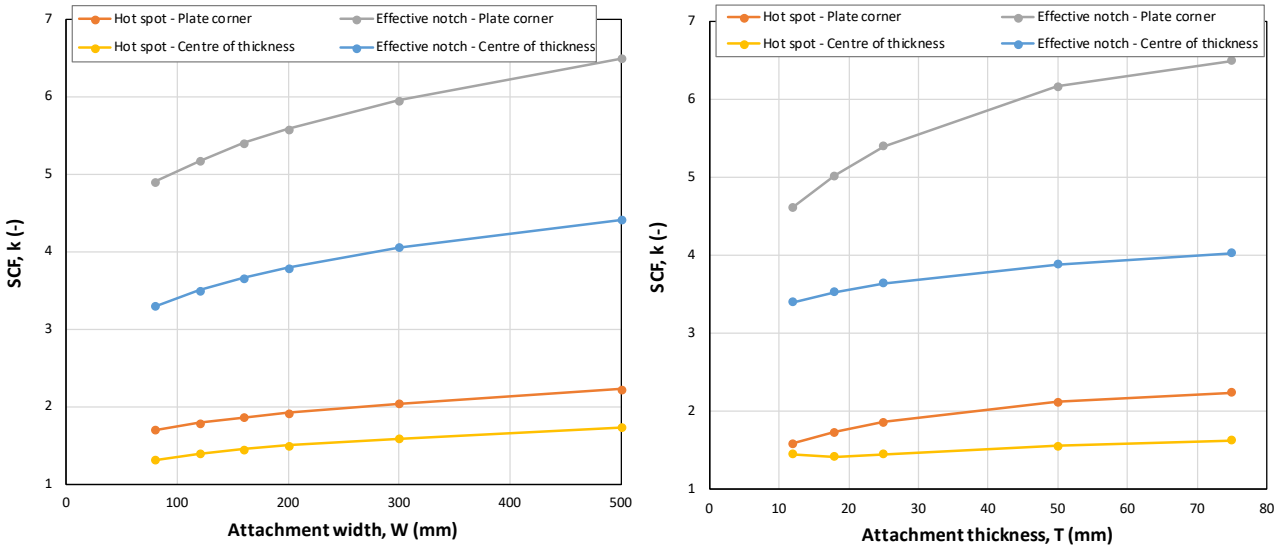

Figure B.3a/b – Stress concentration factors (SCF) for the effective notch stress (en) and hot spot stress Type “b” (hs) methods as a function of a) the attachment width (W), and b) the attachment thickness (T).

Figure B.4 shows the stress concentration factors (SCF) for the effective notch (K_{en}) as a function of the hot spot stress Type “b” (K_{hs}) SCF. Results are shown for the attachment plate corner and for the attachment centre of thickness at the plate edge.

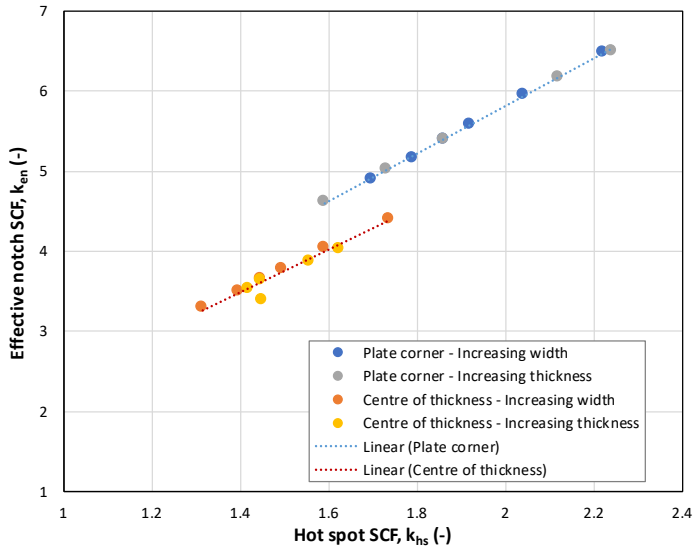

Figure B.4 - Stress concentration factors (SCF) for the effective notch (K_{en}) as a function of the hot spot (K_{hs}) SCF. Results are shown for the attachment plate corner and for the attachment centre of thickness.

Two clearly distinct lines between these effective notch SCF (K_{en}) and hot spot (K_{hs}) SCF, with nearly the same slope, are found for the plate corner and for the attachment centre of thickness. Figure B.4 shows that the structural hot spot stress Type “b”, determined by using the 4, 8, and 12 mm reference points, captures a size effect of similar magnitude as the effective notch stress method.

The FE analyses presented in this paper are only briefly described. A sub-modelling technique was used, in which the results of the large model (global model) are used as boundary conditions for a detailed model of the weld (local model). No information is given about the local model, with the exception of the element size. Hence, a review of the boundary conditions used in the local model is not possible.

These obtained results by Hanji et al. (2024) [18] are of interest for practical situations as it at least suggests that there is a specimen size effect in which the SCF’s increase with increasing plate width and plate thickness.

Mobility & Built Environment

Molengraaffsingel 8
2629 JD Delft
www.tno.nl

TNO innovation for life